Mojim roditeljima

Na izvoru, u tiho veče,
Sa vodom jedna riječ isteče
Žuboreć isto kao voda.
Tišina drugu riječ mi doda,
A treću vrba ili zova.
Poneku vjetar još mi dadne,
A neka bogzna otkud padne,
I govor mi je pun darova.

(Dobriša Cesarić)

The Tobacco Mosaic Virus (TMV) as Biological Template for Nanostructuring

DISSERTATION

zur Erlangung des Grades eines

Doktors der Naturwissenschaften (Dr. rer. nat.)

der Fakultät für Naturwissenschaften der Universität Ulm

2003

vorgelegt von

Mato Knez

aus Augsburg

Abstract

The Tobacco Mosaic Virus (TMV) as Biological Template for Nanostructuring

The Tobacco Mosaic Virus (TMV) is a very stable tubular complex of a helical RNA strand and 2130 coat proteins. The special shape makes this virus an interesting nanoobject, especially as template for reactions. In this thesis TMV is used as a chemically functionalized template for binding metal ions, either electrostatically or coordinatively. Chemical reduction or electroless metal deposition produces metal clusters of several nm diameter that are attached to the virus without destroying its structure. While gold clusters produced with an ascorbic acid bath bind to the outer surface as well as to the central cavity of the hollow tube, silver clusters grow with a formaldehyde protocol selectively on the outside. When TMV is first activated with Pd(II) or Pt(II), nickel and cobalt clusters and wires of up to 600 nm length and 3 nm diameter can be deposited selectively in the internal cavity. When TMV is activated with Au(I), nickel and cobalt can be deposited selectively on the outer surface.

The adsorption behavior and surface chemistry of the TMV on well-defined metal and insulator surfaces is studied, too. TMV serves as supramolecular model system with precisely known surface termination. The results show that if the surface chemistry of the substrate and the pH-dependent chemistry of the molecular surface match, e.g. by hydrogen bonding, a strong adsorption occurs, and lateral movement is impeded. Due to the adsorption the virion can be imaged by Atomic Force Microscopy (AFM) in contact mode. Self-assembled monolayers with an acyl chloride group are used in order to induce covalent bonding via ester formation. Structured adsorption of TMV on silicon wafer and mica surfaces is performed by soft-lithography.

Keywords: Tobacco Mosaic Virus, electroless deposition of metals, adsorption on inorganic substrates, microcontact printing;

iv

Contents

List of Figures

Chapter 1

Introduction

In the past decades, especially since scanning probe microscopy was developed, an interest in surface structuring with atoms, clusters, molecules or even larger entities increased steadily [105, 34, 40, 41, 55]. Apart from small molecules like silanes or thiol-terminated hydrocarbons [62, 63], biological molecules as large and functional molecular systems with several nanometres in size play an important role in nanoscale science [29, 99, 79, 81].

The use of biological molecules is advantageous from several points of view compared to the use of other organic molecules: Biological molecules are in most cases well defined in structure, easily reproducible in sufficient amounts and thus cheaper than organic molecules with similar sizes. Moreover, structure and chemical functionality can often be changed e.g. by altering the genetic code, if those molecules are reproduced in any kind of life-form. This method is well developed and it is usually much simpler to apply than selective organic chemistry in a small part of a complex organic molecule.

Apart from single amino acids, where conformational recognition on surfaces is an important topic in current research [28, 67], larger biological molecules like nucleic acids, protein tubes, viruses and even cells are often used as adsorbates or templates for structuring on the nanoscale [29, 99, 79, 81]. A very interesting candidate for this purpose is the tobacco mosaic virus (TMV), which is thoroughly characterized, since it became the key to a new discipline, virology, in the beginning of the past century. The size, physical and chemical stability, well-defined structure and easy reproducibility and thus cheapness of the TMV makes it a very interesting object for nanoscale science, especially since nearly all structural details are known [19, 125, 126].

TMV is a hollow tube with a length of 300 nm, an outer diameter of 18 nm and a

diameter of the central channel of 4 nm, comprised of helically arranged proteins around a single-strand RNA [65, 109, 125]. This special shape and the knowledge about the chemical functional groups of the outer surface and the surface of the inner channel of the virion increased the interest of scientists in TMV as a particle for structuring surfaces as well as a particle to be decorated with metals or semiconductors [30, 32, 35, 85, 106].

Decoration of TMV with inorganic molecules or metals is reported in a few cases [32, 66, 85, 106]. The detailed knowledge of the virion´s chemical structure and especially the difference between electrostatic charges on its outer surface and the surface of the inner channel at different pH values was advantageous: Simple wet chemical processes could be applied. First experiments with attachment of silver and gold to the virion were done already in the 1930s and 1940s [60, 94, 95]. In recent years decoration of TMV was achieved with PbS, CdS, Fe oxides and silica [106]. (Apart from those decorations of TMV from solution, decoration of TMV with Pt by evaporation was reported, which was done in order to make it highly conductive for STM experiments [52, 74, 108].)

TMV was adsorbed on inorganic surfaces (e.g. mica and graphite) in several cases [30, 35, 81, 118, 117]. It has even been proposed as a calibration standard for atomic force microscopes (AFMs) [113], which will be shown to be not feasible. Even scanning tunnelling microscopy (STM) on TMV has been reported in few cases and, although imaging of the pure TMV on a surface was very difficult, under certain circumstances (high humidity) an electric conductance in the TMV can be induced [45, 48]. (However, it is not yet clear whether this conductance is induced by ionic flow or water molecules (since high humidity is necessary) or other effects, like electron hopping through the backbone of the protein.)

The aim of this thesis is to employ TMV as a natural template or structure director for metallization. The basic idea is to understand the adsorption of TMV under various physicochemical conditions on various surfaces, applicable in nanoscale science and/or technology on the one hand, and to use the shape of the TMV as a template for production of metal wires and metal cluster arrangements on the other hand. Finding a proper wet chemical metallization procedure should lead - due to the well-defined template - to well-defined metal structures.

The first part of this project is focussing on the use of TMV as nanotemplate for metallization (see chapter 5). Since the particle is very small and routine contacting

for electrodeposition on this scale is very difficult (and since evaporation of metal from the gas phase onto the virion is not very selective), we decided to use the method of electroless deposition of metals (ELD) (see chapter 3.4). This method was continuously improved during the past 20-30 years. We show that this method, combined with the detailed knowledge of the biochemical structure of TMV, can advantageously be used for the metallization of TMV, resulting in arrays of metal clusters, linear chains and wires.

In the second part of this project the focus is on the adsorption of TMV on inorganic surfaces (see chapter 6). Although some experiments are already documented [30, 35], many results are unclear and even contradictive. In addition to a detailed reinvestigation of the adsorption process on mica and highly oriented pyrolytic graphite (HOPG), we explored the properties of adsorbed TMV on gold, silicon wafer and glass. Based on these results, surfaces were structured with TMV by soft lithography, in this particular case by micro contact printing (μCP) (see chapter 3.3).

Chapter 2

Tobacco Mosaic Virus

At the end of the 19th century Mayer [76] and Beijerinck [9] found that the mosaic desease of tobacco plants is caused by a non-bacterial pathogen. Investigations of this pathogen lead to the discovery of the first virus and thus to the establishment of virology as an essential topic in biology.

TMV can be isolated from most tobacco plants, which grow in natural environment (i.e. not in greenhouses), and thus it is present in almost every tobacco product which can be bought. A plant which has no natural resistance against TMV and is infected with the virion shows symptoms like a yellowish mosaic colour pattern at the leaves and hindered growth [51]. The infectivity of plants with TMV is not specific to tobacco plants: Tomato plants and others belonging to families like solanaceae or compositae can be attacked, too [87]. However, it is a plant virus and does not harm mammals, so it can easily be handled in a laboratory without precautions necessary for highly infective and mammal-harming bacteria, viruses or prions (e.g. influenza viruses or *bovine spongiform encephalopathy* (BSE) prions).

Ongoing research in the 20th century showed that the coat protein of TMV is coded in its RNA and that the infectivity of the virion is independent of the presence of the coat protein: The RNA alone can be used for infection [43]. But not only the coat protein is encoded in the RNA of the TMV. The nucleic acid contains coding for other proteins, too [124]. Today the genetic code of the coat protein is used for controlled modification of TMV. Several strains of TMV are known, and they are further modified in a very controlled way, mainly in order to understand the interactions between the amino acids building the coat protein. TMV is remarkably stable, and modifications in the coat protein can be used in order to find those sites that are responsible for the

stability. Specific exchanges of amino acids on those sites can then either stabilize or destabilize the virion, depending on the needs [25, 119].

2.1   Structure of TMV

First detailed information about the structure of TMV was obtained by x-ray diffraction [5]. In the following years the improvement in biological and biochemical analysis methods as well as rising possibilities in microscopy lead to increasing knowledge of the fine structure of TMV. The virus is a hollow tube with a length of 300 nm and an outer diameter of 18 nm, built up by 2132 identical proteins [65, 109]. These are arranged around a single strand RNA into a right-handed helix [120]. Each protein has a molecular mass of 17.5 kDa [47, 36]. In the interior of the particle a channel with a diameter of 4 nm was found by using the standard procedure of negative contrasting of biological material in transmission electron microscopy (TEM) [125, 65, 109]. The helix built by the RNA has a diameter of about 8 nm and is completely embedded in the protein sheath; three nucleotides bind to one protein unit. The RNA of TMV (*vulgare strain*) consists of 6395 nucleotides, which together with the 2132 proteins results in 131 turns and $16\frac{1}{3}$ proteins per turn, with a pitch of 2.3 nm per turn [20] (see figure 2.1).

The tertiary structure of TMV coat protein consists of four α-helices packed together in a barrel structure (see figure 2.2). Some hydrophobic side chains of the helices are buried inside this bundle; they make up the tightly packed hydrophobic core of the protein. The strand between the helices build a hairpin loop in order to be able to pack the helices together [109]. This building princile operates in many other proteins, too [17]. Calcium ions stabilize the loops in a protein by interaction with the carboxyl side chains from aspartic acid and glutamic acid, some main chain carbonyl groups and water molecules [38, 84]. The helices are arranged in an antiparallel fashion, where the interior hydrophobic side chains of the protein stabilize the structure with hydrophobic interactions, while most hydrophilic side chains are exposed to the outer surfaces of the protein, which are hydrophilic. The free space inside the protein and between two proteins after aggregation around the RNA is occupied by several water molecules, which are firmly bound to the protein [84, 125]. The proteins are arranged around a helical single strand RNA to build a helical hollow tube.

The effect of solvents on the structure of TMV might be important for the met-
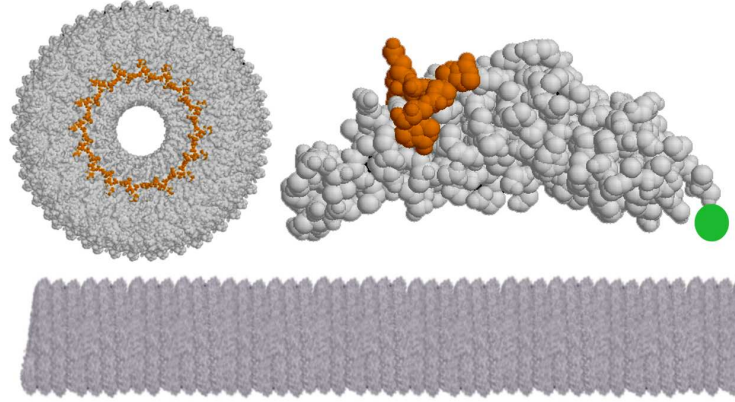
Figure 2.1: Models of a TMV generated with MDL[C] Chime [23] from protein database (pdb) files of TMV (*vulgare strain*) [125]. Upper left: The image shows the front view of the virion with the inner channel, which has a diameter of ca. 4 nm. The orange- coloured part shows the position of the RNA, which is embedded in the coat protein. One single turn consists of $16\frac{1}{3}$ coat proteins. Upper right: One single coat protein of TMV (*vulgare strain*). The orange-coloured part shows the position of the RNA. Bottom: Modelled part of TMV with ca. 45 loops (a complete TMV consists of 131 loops). The models are generated from a pdb-file, which does not contain the last four amino acids in the sequence (155-158) [10] and thus the models, especially at the terminal parts of the coat protein, are not exact. The green circle marks the position of the missing four amino acids.
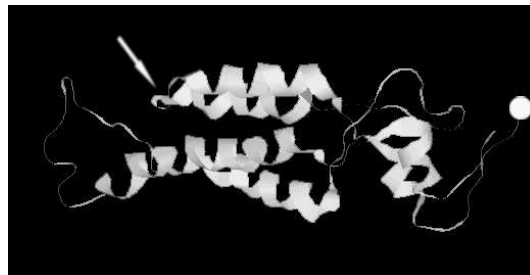
Figure 2.2: Model of the coat protein of TMV generated with MDL[C] Chime [23] from the protein database (pdb) file of TMV (*vulgare strain*) [125]. The ribbon model shows the four α-helices in a barrel structure and a hairpin loop (white arrow). The white circle shows the position of the four amino acids missing in this model (155-158) [10].

allization reactions in solution. The known amino acid sequence was detected from a 1D-oriented state (fibre). X-ray diffraction studies showed water molecules attached to the coat protein [38, 84]. Whether additional water induces changes to the structure is not yet known. A possibility to find the "real" structure of the coat protein of TMV (i.e. its structure in solution) would be the use of NMR spectroscopy as characterizing tool in solution, but the virus is a very large molecule and thus NMR spectroscopy becomes very difficult.

Another important point are electrostatic charges of the outer surface and the surface of the inner channel. In the inner channel amino acids with pK_a below 8 (aspartic acid and glutamic acid) are located, whereas the outer surface contains a number of amino acids with pK_a higher than 11 (Lys-53, Lys-68, Arg-61 and Arg-141). The question of accessibility of lysine and arginine is very difficult. While Arg-61 is located close to the outer viral surface, Lys-53 and Lys-68 are already deep inside the coat protein. In those areas where the coat proteins attach to each other, the outward extending gap between the proteins might make some additional amino acids accessible. Especially arginine (Arg-61) might be accessible. In those cases the electrostatic charge of the amino acid can play a role. The electrostatic charges of the outer surface and the surface of the inner cavity are in some pH regions opposite. The isoelectric point (pI) of TMV is around 3.5 [126]. Slightly below this point (pH around 3), the outer surface of the virion is positively charged, since it is protonated, while the surface of the inner channel is neutral [32].

2.2   Stability of TMV

The question of stability of TMV is crucial for any kind of manipulation of TMV. A large variety of methods for either adsorption or metallization of TMV could principally be applied, but many of them imply high basicity, acidity or temperature or even organic solvents. Others need to be investigated before applying a specific method. Some limitations of the stability are known, which will be discussed here.

TMV is compared to other bioorganic particles very stable. Ideally TMV should be handled at a pH value of 7-8.5. In this regime and at room temperature the virion remains as single, undestroyed particle. An increase of pH leads to disassembly of the particles and ends with a complete separation of RNA and proteins around pH 10.5 [24]. A decrease of pH to values lower than 7 makes the virion aggregate in both side-by-side

and head-to-tail fashion. Further increase of acidity leads again to disassembly and to complete separation of RNA and protein at pH 2.8-3 [20, 24]. Stability of biological matter in such a large pH range is not usual. Among the most stable molecules are DNA and prions (protein fibers), like BSE or scrapie. The scrapie prion for example does not denaturate between pH 2 and 10 [2], which is very similar to the range of TMV. Consequently, both DNA and prion-type proteins have been employed as templates or structure directors for metallization [18, 72, 100, 101, 78, 79, 103].

At neutral conditions the particle is largely deprotonated and has an overall negative charge. The isoelectric point of a TMV particle is around pH 3.5 [126]. Stronger acidity leads to a positively charged particle due to protonation of the amino acids, in particular their termini and side chains consisting of carboxylate groups and amines, and, because of weaker interaction ability of the coat proteins with each other, to lower stability. Within the coat protein, the protonation of amino acids like glutamic acid and aspartic acid can decrease the stability of the protein to a large extent. The loss of electrostatic charge of those amino acids weakens the interactions of the protein strand with the calcium ions [38, 84], which contribute to the integral stability of the coat protein. This leads to a rapid disaggregation of the virion if the pH is lower than about 3 [20].

Another very important point is the thermal stability of TMV. The decomposition or denaturation of the virion takes place at temperatures higher than 80-90°C. [126] This is again very similar to other very stable biomolecules, like DNA. Depending on the type of DNA, denaturation takes place between 80°C and 100°C [122]. Prions however can resist even higher temperatures: Even at 360°C BSE prions are not completely denaturated [2]. Handling of TMV at low temperatures is unproblematic. Infected leaves can be frozen for a longer time. An extraction of such leaves, even after several years, still yields virions intact in shape as well as intact biologically, since new plants can be infected with them. TMV itself can in dry form be stored at room temperature for extremely long times (at least 40 years) [83].

Besides the thermal stability, there is the question about chemical stability, especially the stability against solvents. It is known that TMV can resist DMSO (dimethylsulfoxide) dissolved in water up to a concentration of 70vol.% [86]. Higher concentrations lead to structural decomposition. Furthermore it is known that ethanol can be used to precipitate TMV from solution, but it does not affect the structure of the virion [126]. Whether the chemical composition of the particle is affected is not known. Tests

with TMV in combination with other chemical solvents have not yet been done and are part of this work (see chapter 6.1.4).

Mechanical stability [35] is for this particular work of less importance but it might be important for some future steps towards structuring of surfaces with TMV. In general it could be interesting in order to complete the knowledge about the stability of TMV. Therefore investigations on the mechanical stability of TMV will be part of the future work in this project.

The last part, which certainly can partially be assigned to mechanical stability, is the resistance against vacuum and high pressure. Most investigations on TMV have been done with a transmission electron microscope (TEM), which works under high vacuum conditions. Obviously the structural integrity of the virion is preserved under those conditions. However, the water molecules, bound to the proteins [125], might evaporate in high vacuum, which should lead to a structural decomposition due to decreasing stability of the virion. A possible explanation for the structural integrity is that the water is so tightly bound, that the vacuum conditions in a TEM do not allow for evaporation. In order to obtain detailed information about the behaviour of TMV in vacuum, experiments under vacuum conditions independent of TEM would be required. However, such experiments have not yet been done. Investigations in high pressure are generally of less interest for most biomaterials. Some work in this field has been done and it is known that TMV undergoes little dissociation at pressures up to 2.5 kbar. The combination of high pressure with low temperature increases the degree of dissociation of RNA and protein but without significant denaturation, i.e. the renaturation by reassembly of protein and RNA can take place if the conditions are changed again to physiological conditions. Urea is known to denaturate most proteins. With TMV the denaturation of the proteins with urea at room temperature is slow. Incubation with urea in addition with high pressure and low temperature leads to dissociation and denaturation of TMV [16].

2.3 Derivatization of TMV

Several approaches for obtaining derivatives of TMV, i.e. new chemical compounds, are documented. Basically, nature offers already some derivatives of TMV with different strains and mutants of TMV [124]. The differences in strains are limited to exchange of several amino acids in the protein sequence (and of bases in the RNA). Apart from that

some spontaneous mutations can be observed in nature, where at least one amino acid is replaced by a different one. The reproducibility of such mutants depends strongly on the stability of the mutant, i.e. on the amino acid exchanged. Such mutations can also be effected with biological methods in a controlled way [4, 25]. The coat protein of TMV is coded in the RNA, and thus it is very easy to replace parts of the code and to clone the mutant. But those are not the only derivatives known.

Apart from biological derivatization several approaches to chemical derivatization have been done. Already in 1960 Wittmann [124] has found that treatment of TMV with nitrous acid leads to replacement of 9 amino acids. Kausche *et al.* did several approaches to obtain chemically modified TMV in the 1930s [59, 61]. The basic idea was to treat the virion with different chemicals, determine the amount of attached molecules and then to calculate the number of molecules attached to a single virion or protein in order to find the exact number of basic and acidic groups in a single TMV. Among the chemicals used were dyes, like orange G or safranine T [61], diazo methane, and basic or acidic chemicals like acetyl chloride, benzoyl chloride, phenyl isocyanide etc [1]. Analyses were effected with accessible methods, like colorimetry in the case of dyes [61]. Other investigations with chemicals were done in order to examine the stabilization effects inside the virion. Nicolaïeff *et al.* treated TMV with dimethylsulfoxide (DMSO) and found that at concentrations close to 80 vol.% the coat protein is partially separated ("stripped") from the RNA [86]. Specific treatment like amidination and maleylation of lysine (Lys-68) and nitration of tyrosine (Tyr-139) were done in order to examine stabilization effects on the virion under alkaline conditions. In those cases amidination showed some additional stability of TMV, whereas maleylation and nitration destabilized the virion at pH 9-10 [123].

Other derivatizations of TMV are based on heavy metal compounds. Pfankuch *et al.* treated TMV with iron citrate and silver nitrate and found after polarography (iron) and potentiometry (silver) attachment of 20000 iron ions, respectively 3300 silver ions, to a single virion [94, 95]. Furthermore mineralization of TMV has been achieved with PbS, CdS, Fe(II)/Fe(III) and tetraethoxysilane (TEOS) [106] at the outer surface of TMV, and by attachment of immunogold labels either to the outer surface of the virion or to a specific end of the virion [114, 115].

Derivatization of TMV with mercury was done mainly in order to enhance the resolution of X-ray diffraction studies of TMV. Methyl mercury nitrate was used for attaching mercury to cysteine-27, which is located deep inside the coat protein [37].

Further investigations in this directions lead to treatment of TMV with phenyl isothiocyanate in order to react with lysine residues (position 53 and 63 in the *U2 strain*). These modifications lead to more attached mercury [39].

Chapter 3

Methods

In order to examine the possibilities of adsorption and metallization of TMV, it is necessary to take advantage of microscopy methods of different kinds. In this chapter the microscopy methods applied in this project are shortly described, as well as the methods for patterning the surfaces, and those for deposition of metal on the outer surface and inside the inner channel of TMV.

3.1   Scanning probe microscopy

Adsorption experiments of TMV on surfaces require a microscopy method which offers probing possibilities at high resolution (in the nm scale). Here two general methods come into play, since they are highly developed and since their use became routine during the last decade, namely the scanning or atomic force microscopy (AFM) [13] and the scanning tunnelling microscopy (STM) [11, 12, 8]. In the following, their principles and differences are shortly discussed.

3.1.1   Atomic force microscopy

The atomic force microscope was first developed in the 1980s [13] and was in the following years in the focus of scientists, both as tool for investigation of surfaces and as apparatus to be further developed. The principle mechanism is based on interactions of a very small tip, mounted on a cantilever, with a substrate [58]. Interactions are on the atomic scale and can be attractive and repulsive. An AFM tip consists usually of Si or Si_3N_4, but can sometimes be coated with a metal, e.g. gold. The tip and
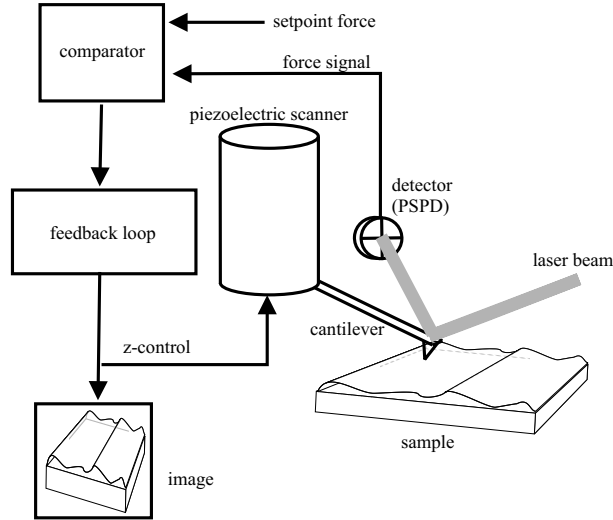
Figure 3.1: Principle of operation of an Atomic Force Microscope (AFM).

cantilever are often fabricated by controlled etching of a silicon wafer, yielding a chip (with mm sizes) with a small (μm size) "finger" (cantilever). At the apex of the cantilever the tip is mounted on the bottom side. In operational mode the chip is mounted onto a holder which is driven by a piezo crystal controlling the vertical force (or some related parameter) during scanning, approach to a surface or retraction from a surface. The information about the topography of a substrate is collected using e.g. a laser impinging on the top side of the cantilever. The reflection of the laser beam is registered by a photosensitive diode, consisting of four separate quadrants. While scanning a substrate, the tip follows the structure of the surface and the deflection of the laser beam induced by up and down movement of the tip (and thus the cantilever) is detected. A scan is done line by line, and the collected data is combined by the acquisition software into an image of the scanned area, where a colour code usually defines the differences in height.

However, this description is only valid for the so-called *topography mode imaging*. In contrast to this, very often the *error mode imaging* is used. Here the image represents a derivative of the topography in the scanning direction, where only the deflection of the tip compared to a nominal position is reflected in the image (e.g. by colour coding). In such images, irregularities on a surface compared to a nominal height value are represented with a brighter area where the tip moves upwards and a darker area for the opposite. The same objects, scanned in different directions, e.g. left-right and right-left, appear in such images in opposite colours. Note that the colour coding

contains no height information, but the images appear often more detailed.

While those modes extract the data from the vertical deflection direction, another very often used imaging method, the *lateral force mode* (LFM), is based on the deflection signal of the laser beam in lateral direction, which is due to twisting of the cantilever induced by friction forces. In this case additional information on the substrate can be obtained, since the friction forces are different for different chemical compounds [112]. High affinity of tip and sample and therefore high friction forces result in stronger twisting of the cantilever and hence in higher contrast in the image. The LFM mode imaging requires very sensitive detectors and careful settings of operational parameters. In most cases LFM is only applicable in *contact mode* imaging, since the frictional forces in this case are high enough to twist the cantilever and thus to be detected by the photosensitive diode. However, some AFM apparatus, e.g. the M5 from Thermomicroscopes^{TM} is capable of measuring LFM even in *non-contact mode*, although with very poor resolution.

The resolution of an AFM is determined by several factors. In vertical direction the limiting factor is the sensitivity of the photosensitive diode to light displacements, which is as small as 1 nm. The ratio of the path length between the cantilever and the detector to the length of the cantilever results in a mechanical amplification which enhances the the vertical resolution of the AFM to the atomic scale. The lateral resolution is mainly limited by the effective tip radius or the interaction area of tip and surface. The interaction area is strongly dependent on the effective tip radius, which can change during the scan, and on attached substances, either collected from the surface while scanning, or attached by purpose. Commercially available tips made of Si or Si_3N_4 nominally show a radius of curvature in the range of 10-50 nm, which leads to a corresponding broadening of small features. Objects closer than few nm to each other cannot be distinguished as individuals. Especially soft matter, like TMV, cannot be highly resolved, because of the forces applied to the molecules by the tip and because of the height of the molecules (> 10 nm). The fine structure, like the individual turns in the helix (see chapter 2.1) is not detected, because the tip penetrates into the virion and thus cannot "read" the information of the outer surface of the virion.

Generally the AFM imaging can be separated into two different methods, the so-called *contact mode* and the *non-contact mode*. For each one both topography and error mode imaging can be applied. The methods are completely different and require different kinds of tips, and even the microscopes are frequently not capable of both of them.
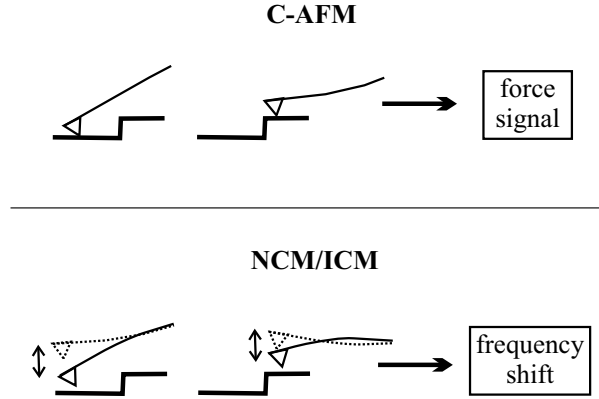
Figure 3.2: Principles of signal detection in contact mode AFM (C-AFM) and in non-contact mode or intermittent contact mode AFM (NCM/ICM).

Contact mode AFM (C-AFM)

With this method the AFM tip is constantly in contact with the sample and follows its topography during scanning. In this case one should be aware of strong (repulsive) interactions between tip and sample, which can be increased by increasing nominal force values ("set points"). This mode is used mainly with samples which are mechanically not very sensitive. Due to the steady contact with the substrate and the strong interactions, the tip can collect particles from the surface and/or can easily be flattened by loosing tip material, which results in loss of resolution.

Non-contact mode AFM (NCM)

Here the tip is not necessarily in contact with the surface, at most for a short time period (microseconds). The basic difference to contact mode AFM is that the tip is in permanent oscillation. The frequency is usually chosen close to the resonance frequency of the cantilever. A slightly higher frequency than the resonance frequency defines the "real" non-contact mode, where the tip is never in contact with the surface, whereas a slightly lower frequency defines the *intermittent-contact mode* (ICM), where tip and sample are very shortly in contact at the lower turning point of the oscillation.

Two important settings have to be done in NCM, namely the set point, which here is the nominal distance of the tip and the sample (at zero amplitude of the oscillation), and the drive, which is the strength of the oscillating force applied to the cantilever. Low set points as well as low drives lead to low interaction forces between tip and substrate, which is important for extremely sensitive substrates like soft materials.

3.1.2   Scanning tunnelling microscopy (STM)

Scanning tunnelling microscopy (STM) [11, 12] is in contrast to AFM dependent on an electric current flowing between sample and tip and requires therefore a conducting or at least semiconducting substrate. The basic principle is that the probability of an electron in a tip moving to a substrate, if a bias between both is applied, is low, but not zero. If a tip is brought sufficiently close enough to a surface and an appropriate bias is applied (which depends on the nature of the tip and the substrate), a current flow can be measured, the tunnelling current. The instruments nowadays are very sensitive and can measure tunnelling currents in the pA range for biases in the 1 V range. The higher the bias and the lower the tunnelling current, the larger the tip-surface distance. This certainly depends on the chemistry of the substrate; indeed inhomogeneous surfaces with varying local conductivity but flat topography can induce apparent height changes in STM scans.

In the mainly used mode (constant current mode) the tunnelling current is fixed to a certain value (nA to pA). While scanning, height variations of the surface induce variations of the tunnelling current. In order to keep the tip-sample distance constant, a piezo crystal, on which the tip is mounted, is contracted or expanded until the current reaches the set point again. The data for contracting or expanding the piezo is recorded and processed line by line into an image.

The vertical resolution of an STM is very high (less than 0.1 nm), at least on surfaces with high conductivity. Even molecules on surfaces can be resolved, if electrons are offered, which can be excited into a conducting energy state. Very often molecules with π-electron systems are used for investigations with STM. This works only for molecules with a low height. Since the probability of electrons to tunnel is a function of the distance of tip and surface, with molecules higher than few nm the critical distance is reached, where the tunnelling current is too low to be measured.

The lateral resolution, too, is very high (sub-nm range), if the surface is flat. Since the tip is not in mechanical contact with the surface, the tip convolution has less influence than in AFM. But still there is some influence, especially in those cases, where large and conductive particles are imaged on the surface. The electrons can tunnel between the side area of the tip and the particle. This leads again to a broadening of the particle (as with AFM).

3.2   Electron microscopy

Electron microscopy, in particular transmission electron microscopy (TEM) is used in this project in order to examine the metallization results on the virion. Conventional optical microscopy does not allow visualization of single TMV particles since its resolution is determined by the light source which is in this case usually in the visible wavelength spectrum. Depending on the light source, the resolution can reach several 100 nm. Using an electron beam instead of visible light opens the capability of higher resolution, even down to the Å range, depending on the energy of the electron beam. The basic principle of an optical microscope and a TEM are the same, just that the beam is in the latter case not focussed with optical, but with electric and magnetic lenses [116]. The electron beam is after proper adjustment guided through a substrate, which in our case is a copper grid (200-400 mesh/inch), covered by a thin (few nm) polymer film (Formvar or Pioloform) and a thin layer of carbon evaporated on the polymer [107]. The particles to be examined are deposited on this film. Due to interactions of the electron beam with the particles on the grid the electrons can be scattered or diffracted. The higher the atomic mass, the stronger the interactions. After passing through the sample, the electron beam is guided onto a fluorescent screen, where a magnified projection of the sample can be seen. Areas on the sample, where particles with higher atomic mass are deposited, appear darker, since more electrons can be scattered or diffracted, and places with low atomic mass appear brighter (only valid for standard, so-called bright field imaging). The opposite happens if the diffracted part of the electron beam is directed onto the fluorescent screen. Here only diffracted electrons are visible and appear bright, whereas all other areas appears dark (dark field imaging). The projection can be photographed either on a conventional photo negative or with an electronic camera, depending on the construction of the microscope.

Slightly different is the operation of a scanning transmission electron microscope (STEM). The electron beam in this case is focussed to a small spot (in normal operation 0.8 nm, but it can reach 0.22 nm). The beam is not static but it passes the sample line by line as in AFM or STM. Transmitted electrons produce an image which is recorded with a CCD camera to yield an image of the scanned area [26].

In addition to TEM imaging, an energy dispersive X-ray fluorescence analysis (EDX) can be done if the microscope offers the capability. In this method an electron beam is concentrated on the area to be examined in order to produce X-ray

fluorescence. The excited X-ray waves pass the detector and are assigned to the elements. The method is not very specific, since the electron beam is too large (several nm) for very small particles. The signal is therefore not only collected from the particle, but also from the surrounding area. In addition scattering of the electron beam from other parts of the sample takes place, in particular if heavy metals are present. Since the grids usually consist of copper, the EDX detector always shows copper in high concentration, independent of the area measured.

Another more specific method to examine the nature of the particles is the method of element mapping with energy-filtered TEM (EFTEM) [26] (see chapter 3.2.1).

Staining Methods for TEM

With biological samples standard TEM is routinely used. In order to visualize the biomolecules, in most cases staining with metal or metal salts is necessary, since the atomic weight of the building blocks of most biocompounds is very low [107] and thus the z-contrast. Attached metal clusters or metal ions to bioorganic molecules increase the z-contrast of those particular parts of the molecules and make them visible in the TEM. Uranyl acetate is mainly used for staining, since it is well dispersed, can easily be attached to biomolecules and has high atomic weight which offers a good contrast in TEM. Two methods of staining have to be distinguished: positive staining and negative staining. With negative staining, the molecules are incubated with uranyl acetate for a short time period (approx. 30 sec.), which results in an attachment of uranyl acetate at the contours of the biomolecule. This method offers only insight into the shape of the biomolecule, which in most cases is desired. For positive staining the incubation time is in the range of several minutes. The uranyl acetate in this case can penetrate the molecule and bind to very specific sites. In some cases the difference of positive and negative staining is not very obvious. For the case of TMV, positive staining enhances the contrast of the RNA (and some other sites), while negative staining enhances the contrast of the inner channel. Since the RNA is located close to the inner channel, the difference in the results is here very small.

3.2.1 Energy-filtered TEM (EFTEM)

With this method images of a sample sensitive to a particular element can be done. While passing the sample, the electron beam is inelastically scattered. The energy of

the electron beam is detected as E_0-ΔE, where E_0 corresponds to 120 keV with the microscope used in our case (Zeiss EM 912 Omega), and ΔE corresponds to the energy of the excited core shell electrons into unoccupied states, an element-specific process. In the resulting energy diagramme, the signal with the lowest energy loss (zero loss) corresponds to the signal of the unscattered incident beam (120 keV). The region with energy loss up to 100 eV (valence loss region) corresponds to the optical properties and the electronic structure of the elements exposed to the electron beam. In the region with higher energy loss (more than 100 eV, "core-loss region") the signals correspond to the energy of the excited core shell electrons of the elements. The detection window is limited to a narrow area around the element-specific signal ("edge"). The element-specific edge is detected as well as signals at slightly higher energy, which are used for subtraction of an average background intensity from the one at the element-specific edge. As a result an image of the distribution of the selected element on the sample can be obtained [26].

3.3   Micro contact printing

The method of micro contact printing (μCP) offers the possibility to pattern a substrate with molecules in a simple way. The principle is as easy as stamping a document, but operates on a smaller scale [63, 80]. First a master has to be produced. This is done by patterning a silicon wafer with standard lithography methods. Here the pattern width can reach the 100 nm scale, but the standard presently used has features in the range of 300-400 nm. After careful cleaning of the master, a liquid polymer is poured on top. The polymer used is usually poly(dimethylsiloxane) (PDMS), at least for pattern widths down to 300-400 nm. Smaller features require polymers with different chemical properties. After cross-linking, the rubber-like PDMS can be peeled off the master. It contains the inverted pattern. This stamp can now be inked with a solution of the molecules to be stamped, dried and then contacted with the substrate. Inking and stamping procedure take place in a time range of seconds to minutes, depending on the molecules to be stamped and the substrate to be stamped on. However, the diffusion of the molecules on the stamp causes problems in some cases. Due to diffusion, especially at the edges of the stamp, the pattern can be distorted. A possibility to avoid the diffusion is to add one step in this procedure: The inked stamp is used to transfer the pattern of molecules to another, flat stamp, which is then used to transfer the pattern
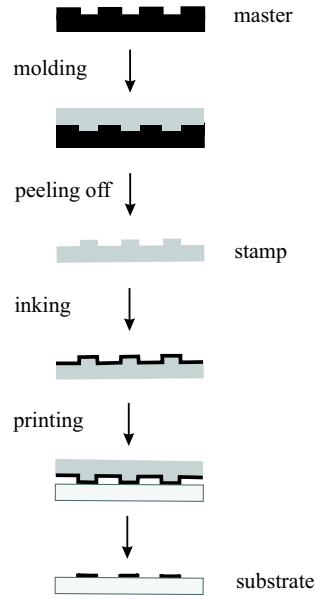
Figure 3.3: Schematic overview of the single steps in standard microcontact printing (μCP) procedure.

onto a substrate.

The polymers used, in particular PDMS, have a very hydrophobic nature. With some solutions this entails problems, since the use of water or ethanol as solvent becomes difficult. A method to avoid these problems is to pretreat the stamp prior to usage. A possibility is to use an oxygen plasma in order to oxidize the surface of the stamp. By this treatment hydroxyl groups are produced on the surface; they offer an affinity to hydrophilic solvents. Since the surface is mobile, the hydrophilized polymer chains can diffuse into the bulk, so the plasma treatment should be done shortly before use.

3.4 Electroless deposition of metals (ELD)

Electroless deposition of metals (ELD) is a simple method to metallize non-conductive materials. Whereas electrodeposition works only on conductive substrates, and the speed and amount of metal deposited on a substrate is controlled by applying a certain current, in ELD the deposition is controlled by the chemical redox potential of metal ions and the reducing agent [73, 91, 104]. The ELD differs from the method of first binding metal ions to a substrate and afterwards reducing them. The separate processes

can be written as follows (anodic stages for the case of alkaline media) [104]:

$$
\begin{array}{lll}
\text{1. Dehydrogenation} & : & RH \rightarrow R + H, \\
\text{2. Oxidation} & : & R + OH^- \rightarrow ROH + e^-, \\
\text{3. Recombination} & : & H + H \rightarrow H_2, \\
\text{4. Oxidation} & : & H + OH^- \rightarrow H_2O + e^-.
\end{array}
\tag{3.1}
$$
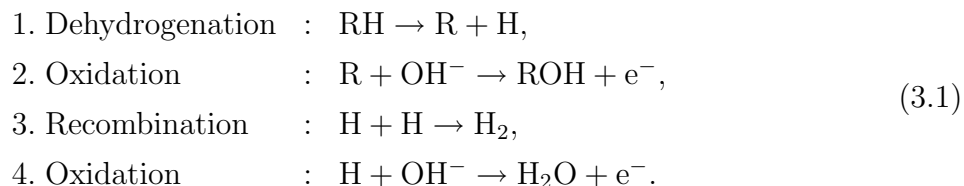
The cathodic stages in alkaline media can be written as:

$$
\begin{array}{lll}
\text{5. Metal deposition} & : & M^{+n} + ne^- \rightarrow M^0, \\
\text{6. Hydrogen evolution} & : & 2H_2O + 2e^- \rightarrow H_2 + 2OH^-.
\end{array}
\tag{3.2}
$$
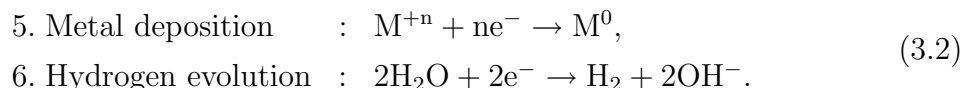
In acid media the stages 4 and 6 differ from the alkaline reaction and can be written as:

$$
\begin{array}{lll}
\text{4a. Oxidation} & : & H \rightarrow H^+ + e^-, \\
\text{6a. Hydrogen evolution} & : & 2H^+ + 2e^- \rightarrow H_2.
\end{array}
\tag{3.3}
$$
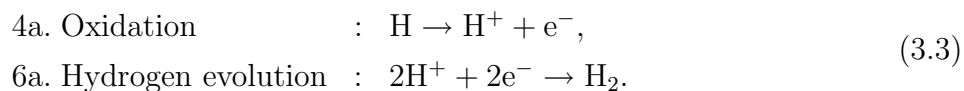
The reactions show that during the ELD hydrogen evolution takes place, independent of the acidity of the bath. Alkaline baths, however, often show faster reactions, which is due to suppressed reaction 6. Increased concentration of OH^- is offered in alkaline baths, which suppresses the hydrogen evolution and thus allows for increased metal deposition rate (reaction 5).

Electroless deposition is done from a bath containing both the metal complex and the reductant (one-step ELD). In some cases the substrate requires sensitation and is therefore pretreated with a solution of a very noble metal, not necessarily containing the reductant. If no reductant is offered, the reduction is done in the above mentioned bath which contains the metal to be deposited and the reductant (step-wise ELD or regular ELD) [91, 104].

In such cases the first step consists of attachment of noble metal ions from solution (usually Pd(II), Pt(II), Au(III), Au(I) or Ag(I)) to specific sites of the substrate [73]. The reducing agent (or light, like in the case of silver) reduces complexed ions and leads to growth of small metal clusters. High surface concentrations of metal can lead to coalescence of growing clusters. Proper conditions for sensitation (pH, ionic strength, temperature etc.) should produce metal clusters with sizes in the nm range or below. For the deposition of less noble metals those small clusters are used as initiation centres for further metallization.

The solution is replaced by a bath containing basically a metal complex of the metal to be deposited (Ni, Co, Cu etc.), a reducing agent and chemicals capable of complexing
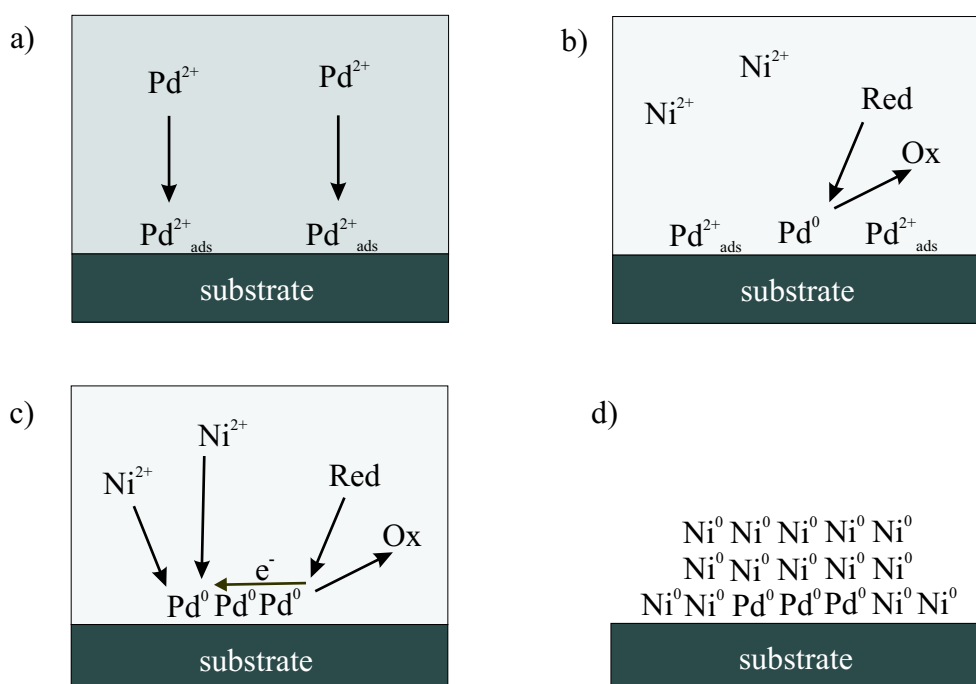
Figure 3.4: Schematic overview of ELD. a) Pd(II) attaches to a substrate from a Pd(II)-containing solution. b) The Pd(II)-activated sample is immersed in a Ni(II)- and a reductant-containing metallization bath. The reductant reduces the Pd(II) to Pd(0) and is oxidized. c) The reductant is oxidized at the Pd clusters, while Ni(II) is reduced to Ni(0) at the surface of the palladium clusters. The electrons for the redox-process are transferred through the palladium. d) The emersed sample contains attached nickel clusters with a palladium core.

the metal ion, which is necessary in order to avoid a too fast reduction of the metal ions or to provide solubility at high pH values. The speed of reduction can be directed by choosing a complexing agent with either high affinity to the metal ion (leads to slow reduction) or with a low affinity (leads to fast reduction). Of course the redox potential of the reducing agent and the metal ion is important for the choice of the complexing agents. Usually substances like dimethylamine-borane (DMAB), sodium hypophosphite (NaH_2PO_2), ascorbic acid or sodium tetrahydroboranate ($NaBH_4$) are used, but there are many other possibilities [91, 104]. One very important issue is the presence of an agent which can reduce the metal ions without interfering with the structure of the substrate. After replacement of the activation solution with the metallization bath the reducing agent is oxidized at the cluster surface and delivers electrons that can be transferred through the cluster to reduce the metal ion at any

place of the cluster surface [63]. The mechanism might be more complex, e.g. involving catalytic steps, but in any case a metal layer starts growing. The metal-ligand complex can loose a part of the ligand sphere while colliding with the metal particle, which makes the metal ion easier accessible for reduction. Therefore strong complexing agents may slow down or even completely block the reduction, which can be observed in experiments [33]. Another important point is the higher probability of a metal cation and a reducing agent to encounter a comparatively large cluster than the probability of them encountering in solution.

A running reaction is, compared to the case of electrodeposition, rather difficult to stop, especially when particles in solution or suspension are to be metallized. While in electrodeposition one can simply switch off the current, in ELD one needs to either change the pH to a value where the metallization cannot take place, or to dilute the bath in order to lower the probability for metal complex and reductant to encounter, which effectively does not stop the metallization, but slows it down, or one has to remove any essential component of the bath, e.g. the metal ions, by dialysis. One method which allows for a fast stop of a running reaction is the change of pH. Here another problem appears. The particles to be metallized need to be rather insensitive to large pH changes, which for TMV is the case in a pH window between 2.8 and 10.5 [20, 24]. Addition of concentrated acids or bases may destroy the particles, while slower addition of diluted acids or bases hinders an exact timing. In some cases adding substances (additives) that can stabilize the metal ions against reduction, and/or passivate the growing surface, slows down the reaction or even stops it completely [49, 70].

Chapter 4

Experimental Details

In all cases where water was used, it was purified from a Milipore^{TM} apparatus and showed a resistivity of at least 18 MΩcm.

4.1   Preparation of TMV

The preparation of TMV is done by infecting a tobacco plant, *nicotiana tabacum cv. samsun nn*, using sand paper or carborund to produce scratches on the leaves and afterwards treatment with a buffered TMV suspension. After 4 weeks the leaves show symptoms of infection, i.e. yellow mosaic patterns and smaller leaves, and are harvested.

The purification methods are standard methods used in the biology departments of the university of Hannover (CsCl method) and the university of Stuttgart (sucrose method).

4.1.1   Extraction with a CsCl gradient

For isolation the leaves are chopped with 0.1 M 4°C cold EDTA solution at pH 8 and afterwards pressed through gauze tissue in order to separate large particles from the filtrate. The latter is centrifuged at 5300 g for 15 min to sediment particles which passed the gauze. The supernatant liquid is removed and filtered through a 1 cm thick celite layer. Here phenolic components and plant dyes are removed from suspension. In the next step the suspension is incubated at 50°C for 90 min in order to denaturate dissolved proteins. TMV is stable at those conditions and will not be destroyed. To

remove the dissolved, denaturated proteins, centrifugation at 5300 g for 15 min is applied. The supernatant is removed and centrifuged at 117000 g for 90 min at 4°C. TMV sediments at these conditions, so the supernatant solution can be removed and the pellet containing the virion resuspended in buffer solution. Additional centrifugation for 10 min at 4800 g is applied in order to remove undissolved material after homogenization. The sedimented material is removed. The suspension, containing TMV particles as single particles, broken particles and aggregates, needs to be purified, ideally to a suspension of single and undestroyed virion. Therefore a density gradient method, the CsCl gradient method, is applied. The density of the suspension is adjusted by adding CsCl. Proper choice (33% weight) of the salt concentration makes a sedimentation of the virion after centrifugation possible; particles are distributed in the centrifugation tube according to their density. The centrifugation takes place at 100000 g overnight. A milky disc containing the particles can be removed from the tube using a syringe. The liquid is dialyzed against sodium-potassium phosphate buffer adjusted to pH 7.2 overnight and stored at 4°C.

4.1.2   Extraction with a sucrose gradient

The procedure is similar to above, but the gradient purification step is different. Instead of adjusting the density with CsCl, a mixture of sucrose and tri(hydroxymethyl)-methylamine (TRIS)-HCl buffer at pH 7.5 is prepared and frozen at -80°C. Before use the solution is slowly melted whereby a sucrose gradient builds up. The TMV-containing liquid is pipetted carefully on top and centrifuged at 25000 g and 10°C for 2.5 hours. In this procedure, the particles are separated according to their lengths (not their density). The proper fraction is separated [126], dialyzed against sodium-potassium phosphate buffer adjusted to pH 7.2, and stored at 4°C.

4.2   Adsorption of TMV

4.2.1   Apparatus

The AFM measurements of adsorbed TMV were performed using an Autoprobe M5 and Autoprobe CP by Thermomicroscopes (Atos, Germany; since 2002: Veeco) in combination with Ultralever tips, contact (UL0.6) and non-contact (UL2.0) (Atos, Germany), NTMDT tips, contact (CSC12) and non-contact (NSC11, NSC15) (Anfatec,

Germany) and Nanosensor tips, contact (NCHR) and non-contact (CONTR). Typical force constants for the mainly employed tips were 40 N/m for non-contact mode tips (NSC15) and 0.95 N/m for contact mode tips (CSC12).

STM measurements were performed using a Picoscan by Molecular Imaging (Witec, Germany; since 2003: L.O.T., Germany) with cut or etched tungsten tips. For *in-situ* measurements etched tungsten tips were covered with Apiezon wax (W type, Plano, Wetzlar) in order to reduce the electrochemical current, or commercially available wax-coated Pt/Ir tips (Witec, Germany) were used.

Image processing was done with the shareware WsXM4.0 (Nanotec, Spain). Ellipsometry was performed using an EL X-02C ellipsometer (DRE, Ratzeburg). The ellipticity of the HeNe laser beam (633 nm) was minimized with a λ /4 plate and the incidence angle was 70°. Infrared spectra were acquired at 80° incidence with a Bruker IFS 66 spectrometer equipped with a nitrogen-cooled MCT detector. The reference was gold, either flame-annealed or coated with a perdeuterothiolate.

4.2.2 Substrates

In almost all cases the TMV suspension was found to give reasonable coverage of the surface at a concentration of 0.1 mg/ml; it was diluted with water from stock suspension (10mg/ml) just before use. Stock suspensions were dialyzed against water for at least 15 min prior to dilution with "slide-a-lyzer" caps (14000 MWCO, Pierce).

Mica was purchased from Provac AG (Germany), cut into 15x15mm squares with a diamond saw and freshly cleaved with adhesive tape before use. In order to adsorb TMV, the surface had to be pretreated with a 0.1-1 M $MgCl_2$ solution (p.a., Fluka) for 5-15 minutes [30]. After removal of the Mg^{2+}-solution with an Ar stream, the surface was covered with $100\mu l$ virus suspension, incubated for 15 minutes, and the suspension was removed again with a weak Ar stream.

Silicon wafers (100 orientation, Crystal, Berlin) were cut into 10x10mm squares with a wafer saw and pretreated by the standard RCA procedure to obtain a termination by SiO_2 with hydroxyl groups, i.e. 15 minutes immersion into a 70-80°C hot 1:1:5 (vol.) mixture of 25% NH_4OH (VLSI Selectipur, Merck), 30% H_2O_2 (VLSI Selectipur, Merck) and water, followed by 15 minutes immersion into a 70-80°C hot 1:1:5 (vol.) mixture of 37% HCl (Suprapur, Merck), 30% H_2O_2 and water. Until use the wafers were stored in water. For adsorption the silicon was covered with $70\mu l$ virus suspension

for 15 minutes and afterwards blown dry with a weak Ar stream.

Glass substrates were obtained by cutting glass slides for microscopy into squares of approx. 10x10mm with a wafer saw, immersing them in Nochromix^{TM} (Godax inc., USA)/conc. H_2SO_4 solution for several hours and afterwards washing with water, acetone (p.a., Rotipuran, Roth) and ethanol (puriss., Rotipuran, Roth). The glass was covered with 70 μl virus suspension for 15 minutes and afterwards blown dry with a weak Ar stream.

Highly oriented pyrolytic graphite (HOPG) was purchased from NTMDT (ZYA quality, NTMDT, Moscow) and was freshly cleaved with adhesive tape before use.

Gold surfaces were either provided by evaporation of gold (300°C, 0.5 nm/s, 130 nm thickness) on preheated (300°C) mica at 10^{-6} mbar [71], or by a (111)-oriented single crystal (Mateck, Germany). The gold substrates were flame-annealed for several minutes (nearly invisible red glow) with a butane flame before immersion. Adsorption on gold was achieved from virus suspensions with increased acidity. Solutions were prepared using inorganic and organic acids, in particular HCl, H_2SO_4, $HClO_4$ and CH_3COOH of p.a. or Suprapur quality. The pH values of the virus suspensions were in the range of 2.8-4.

Self-assembled monolayers (SAMs) were obtained by immersion of a gold sample in an ethanolic solution of 16-mercapto-hexadecanoic acid (HS-$(CH_2)_{15}$COOH, 1mM) for 12 hours. The sample was emersed, rinsed with ethanol and water and dried in an Ar stream.

Chemically reactive SAMs were obtained by a chemical reaction at the solid-gas interface between the thiol-covered gold surface and $SOCl_2$ gas [31, 6]. For this, $SOCl_2$ (p.a., Fluka) was first purified by recondensation in an evacuated glass apparatus (0.01 mbar) into a cooled flask (-196°C). The purified $SOCl_2$ was heated again and evaporated in such a way that the vapour passed a chamber containing the gold sample. The procedure was done twice; the sample was then removed in an Ar-flooded chamber and immediately used.

Acid-catalyzed esterification was effected with an acidic TMV suspension (HCl, pH 4) on a SAM-covered gold surface. The reaction time was 2-4 hours.

4.3   Microcontact Printing of TMV

PDMS stamps (Sylgard 184, Dow Corning) were formed on patterned silicon wafer masters (IBM Zürich and Institut für Mikroelektronik Stuttgart, IMS). Before first use each master was rendered hydrophobic with fluoroalkyl-trichlorosilane vapour [14]. After polymerization, the stamp was peeled off the master and treated with an oxygen plasma at 1 mbar in several time scales between 2 and 30 sec in order to obtain different stages of hydrophilicity. The stamp was incubated with a 0.1 mg/ml suspension of TMV for 30-60 sec and - after removal of the supernatant with Ar - placed on a sample of mica or silicon wafer for several minutes.

4.4   Metallization of TMV

4.4.1   Apparatus

Metallized TMV was examined using transmission electron microscopes (TEMs) of following types: Zeiss EM10 operating at 60 kV, Philips CM200 operating at 200 kV, JEOL FX-4000 (equipped with an Oxford EDX analyzer) operating at 400 kV, and Zeiss EM912 Omega operating at 120 kV. For standard imaging mainly the Philips CM200 was used whereas element mapping was done with the Zeiss EM912.

Copper or nickel grids with 200-400 mesh/inch were used as samples for the TEM measurements. The grids were covered with a Pioloform or Formvar film and a thin carbon layer evaporated on top. Prior to usage the grids were treated with 20 μl of pure ethanol (Rotipuran, Roth) for 30 sec according to standard procedures in biology [107]. Afterwards small amounts of virion suspension (20 μl) were placed on the grid and kept there for 30-60 sec. The liquid was afterwards carefully removed with filter paper, and the grid was washed with a droplet of water. In all experiments the optimal concentration of TMV was found to be 0.1-0.2 mg/ml.

4.4.2   Metallization Baths

Adsorption of unstained and unmetallized virions was done from a dialyzed solution (15 min) by placing a droplet on top of a TEM grid. No further treatment except removing the remaining liquid by a filter paper was applied.

Staining of TMV with uranyl acetate was done with already adsorbed virions on

a TEM grid by adding a droplet of a mixture of 2% uranyl acetate and 1mg/ml baci-tracine solution in equal volumes on top of the grid and removal after 30 sec, according to standard procedures [107].

In order to metallize TMV with silver, a standard protocol for staining SDS-PAGE gels in biology was used. First a staining solution containing 4.1 μl 37% HCHO in 5 ml 0.2% $AgNO_3$ was added to the TMV suspension (10 mg/ml) in 10-fold excess. After 15 min the suspension was dialyzed against a mixture of 5 ml 6% Na_2CO_3, 2.7 μl 37% HCHO and 100 μl 0.02% $Na_2S_2O_3$ until a brown colour developed. For dialysis "slide-a-lyzer" caps with (14000 MWCO, Pierce) were used. The suspension was now dialyzed against water and afterwards against a mixture of 5 ml 99% methanol, 1 ml 99% acetic acid and 4 ml water. Aliquots for TEM imaging were taken and placed on a TEM grid for 30 sec, removed and the grid afterwards washed with a droplet of water.

Treatment of TMV with palladium or platinum was done by adding an equal volume of a 0.9 mM/l solution of Na_2PdCl_4 or K_2PtCl_4 (both p.a., Aldrich) in 1 M NaCl (p.a., Fluka), adjusted to pH 5-6 with 0.1 M/l HCl [77], to a dialyzed 0.1-0.2 mg/ml suspension of TMV. After an incubation time of 10 min the suspension was centrifuged at 14000 rpm for 10 min and the supernatant carefully removed. The pellet was resuspended in water and centrifuged again for 10 min at 14000 rpm in order to remove remaining palladium or platinum. This washing procedure was applied 2-3 times.

In the case of reduction of attached palladium using dimethylamine borane (DMAB), the washed suspension of TMV was treated with a 30 mM solution of DMAB (p.a., Aldrich) in water until gas evolved. 20 μl of the suspension were placed on a TEM grid for 30 sec and afterwards removed with filter paper. In the case of treatment with hypophosphite, NaH_2PO_2 (p.a., Fluka) was added to the palladium solution to obtain 30 mM. Here the suspension was not washed, but - immediately after gas evolution started - placed on a grid for 30 sec. The liquid was removed and the grid washed with a droplet of water.

For the deposition of gold a bath slightly modified from ref. [88] was used. The bath was composed of 10 mM $HAuCl_4$ (p.a., Aldrich), 0.1 mM NaSCN (p.a., Aldrich), 0.1 mM L-(+)-ascorbic acid (p.a., Fluka) and 60 mM Na_2SO_3 (purum, Fluka). The mixture was adjusted to pH 6 with 0.1 M NaOH. After addition of an equal volume to the virus suspension, the reaction vessel was heated to 60°C until gas evolution was observed. 20 μl were removed and placed on a TEM grid for 30 sec, afterwards removed with filter paper. The grid was washed with a droplet of water.

Nickel deposition with hypophosphite was performed from a bath containing 0.1 M $NiCl_2 \cdot 6H_2O$ (p.a., Fluka), 0.34 M $NaH_2PO_2 \cdot H_2O$ (p.a., Fluka), 0.3 M $Na_2B_4O_7$ (p.a., Aldrich) and 0.24 M glycine (purum, Aldrich) in water [97]. The pH was adjusted to 9 with 1 M NaOH. After pretreatment with the palladium or gold solution and washing, the virions were incubated in the nickel-containing bath until gas evolution was observed. The reaction was stopped by 10-fold dilution of the mixture with water. Aliquots of $20\mu l$ were removed and placed on TEM grids for 30 sec. After removal of the liquid with filter paper the grids were washed with water.

The deposition of nickel from a DMAB-containing bath was done in the same way. The difference was only the composition of the nickel bath. It was prepared from 0.18 M $Ni(CH_3COO)_2 \cdot 4H_2O$ (p.a., Fluka), 0.28 M lactic acid (85% in water, Fluka) and 34 mM DMAB in water. The pH was adjusted to 6-7 with 1 M NaOH solution [77].

Deposition of cobalt was from a bath containing 0.16 M $CoSO_4 \cdot H_2O$ (p.a., Fluka), 0.15 M sodium succinate (p.a., Fluka) and 7 mM DMAB in water. The bath was adjusted to pH 7-8 with 1 M NaOH [77]. The procedure was analoguous to the nickel deposition procedure.

Ruthenium deposition did not necessitate pretreatment with palladium, platinum or gold. The deposition bath contained 14 mM $RuCl_3 \cdot xH_2O$ (p.a., Aldrich), 70 mM ammonium oxalate (p.a., Fluka), 14 mM di-ammonium citrate (p.a., Fluka) and 0.27 M DMAB [22, 98]. The pH was adjusted to 8-9 using 1 M NaOH solution. After mixing equal volumes of the TMV and the ruthenium baths, the reaction vessel was heated to $70°C$ until gas evolution was observed. A sample of 20 μl was taken, placed on a TEM grid for 30 sec, removed with filter paper, and the grid was washed with water.

Chapter 5

Metallization of TMV

Using biological molecules as structure directors or templates for deposition or growth of metals or semiconductors has become very popular in recent years. Approaches to reasonable structures for possible applications in electronic devices focussed mainly on linear biomolecules like DNA [72, 100, 101, 79, 18], microtubuli (protein tubes) [77, 64, 99], bacteriophages (elongated virions that attack bacteria) [69], prions (protein fibers) [103] or TMV [32, 106]. Those molecules already offer a defined structure in 1D (e.g. tubular structures or DNA), 2D (e.g. TMV crystallites) and 3D. In order to use this "natural structure definition", it is necessary to understand the chemistry behind it, and to find a way to use it without destruction, or at least with controlled destruction of the biological molecule.

In this part of the project the focus is on controlled metal deposition and on cluster growth templated by TMV. Approaches to semiconductor growth have already been successful [106], and metal attachment to TMV (especially gold and silver) was already tested in the first half of the past century [94]. Silver is a metal routinely used in biology for tagging specific sites of proteins. First approaches showed that indeed a specific amount of silver can be attached to a virion. Since in this early stage of virology microscopic methods were not developed very well, the results of the silver deposition experiment were not visualized. Recent biomineralization experiments revived the interest in metallization of TMV with silver by applying not only routine biological methods but also modifying them, relying on the (in the meantime) large experience with methods like electroless deposition of metals (see chapter 3.4) [66, 32].

Experiments with attachment of gold to TMV have already been performed in 1939 [60] and showed that gold can easily be attached on TMV, but the distribution and

size of attached gold clusters is not uniform. (Some gold clusters grow without being templated by the virion itself, but probably on detached proteins or other impurities in the suspension.)

Another metal attachment method developed in biology, which promises to be useful for this project, is the use of specific markers, in the case of TMV antibodies with attached gold clusters. Those antibodies are very specific to the ends of the virion or to some parts of the outer surface, and the gold clusters are very small (5-10 nm) [114, 115]. The use of those clusters as catalysts for further metal deposition should be straightforward and well controllable. The fact that the gold is attached to a very specific part of the virion offers the possibility of a defined initiation area for metal deposition. This particular idea is a future part of this project and will not be further detailed in this work.

Apart from silver ions and gold clusters, biologists developed other methods to attach metal ions to biomolecules. Basically these are metals with high atomic mass and have the aim to contrast proteins for visualization in electron microscopy or enhancement of resolution in X-ray diffraction. This staining is usually done with salts of uranium, tungsten or complexes of mercury [107], platinum or palladium. The redox potentials for uranium and tungsten cations (to be reduced to metal) are very negative, therefore the use of those salts as catalysts for electroless deposition or even just the reduction of the cations in order to obtain metal needs very strong reductants [96]. But the use of strong reductants results in a destruction of the virion, so the implementation of uranium or tungsten staining methods in order to obtain metal growth templated by TMV becomes impossible. Mercury, however, could easily be reduced. The attachment of mercury to TMV is very specific with Cys-27, which is located deep inside the coat protein [39, 68]. The effective size of many mercury complexes in solution is small enough to allow for penetration of the coat protein. After attachment of mercury, it is buried deep inside the virion and thus not accessible for the comparatively large complexes of other metals, like nickel and cobalt, to act as an initiation centre for metal growth. From a technological point of view, but also scientifically, metals like uranium, tungsten or mercury anyway are of less interest in nanostructures, in contrast to platinum, palladium and gold.

An interesting candidate for nanoscale structuring is silver, since its capabilities for field enhancement promise a use as optical antenna, if silver can be grown in a linear shape. Other very interesting metals in nanoscale science are nickel and cobalt. First,

because the methods for electroless deposition of those metals are very well developed and second, because in certain alloys (e.g. with small amounts of phosphorus or boron) they show a quite large magnetic moment (depending on the second compound) [104, 91, 111]. The interesting point is here the magnetic behaviour of those compounds if the size is reduced to the nanometre scale, since it is not necessarily the same as in the bulk, or in the (sub-)micrometre scale [42].

The state of the art in electroless deposition methods is the growth of another metal under "mild conditions", i.e. in a pH and temperature range acceptable for TMV and with reductants which are not destructive for the virion: This metal is ruthenium (with only few reports in the literature) [22, 98]. Basically ruthenium is interesting because of its catalyzing capability for chemical reactions. While this capability is not subject of this project, a possibility for nanoscale structuring would be very interesting. In addition to that, a lot is already known about the metal-organic chemistry of ruthenium [75, 44]. This knowledge could be a big advantage in ruthenium deposition using TMV as template.

Another very important metal from a technological view would be copper. Here some problems occur if TMV should be used as template. Copper can easily be deposited applying the the method of electroless deposition and a lot of work has been done in this research area, but all the deposition methods work in a very basic milieu which is destructive for TMV. The mildest conditions for a copper deposition, which can be found in literature, work at pH 8-9 [56], which is already at the stability limit of TMV. A test of metallization with such metallization bath at lower pH would be possible, but first experiments did not yield metallized virions. The metallization of TMV with copper is part of the future work.

5.1 Results and Discussion

The attachment of metal ions to proteins in general is a process difficult to understand and to interpret. Already a combination of short peptides with metal ions that have strong affinity both to oxygen- and nitrogen-containing groups of amino acids leads very often to misinterpretations. The knowledge of the amino acid sequence of TMV in its genetically unmodified shape [125] (*vulgare strain*, *common strain* or U1) can help to understand the process of metal deposition.

The loop of the coat protein inside the inner channel of the virion is to a certain

extent flexible and thus offers enhanced accessibility of the amino acids situated not only at the surface of the inner channel, but also deeper inside the protein [10]. The amino acids in the protein loop and its vicinity offer a number of nitrogen-containing functional groups like amines and primary amides (Arg-90, 92 and 112; Asn-91, 98 and 101; Gln-99), alcohol (Thr-89, 103, 104, 107 and 111) and carboxylic acids (Asp-88 and 109; Glu-95, 97 and 106) [125]. At the opposite part (i.e. the outer surface of the virion) fewer amino acids are flexible [10]. The amino acid sequence of TMV (*vulgare strain*) shows that on the outer surface of the virion oxygen is predominantly present in form of carboxylic acid (or carboxylate) as terminus of the coat protein. In addition the amount of oxygen is increased by the alcoholic functional groups of accessible amino acids like threonine (Thr-153 and 158), serine (Ser-1, 3 and 154) and tyrosine (Tyr-2) (see figures 5.1 and 5.2) [125, 10]. The TMV clone used in the major part of this project contains an additional serine (Ser-155) in the coat protein, which replaces the glycine (Gly-155) in the sequence of the *vulgare strain*, else the amino acid sequence of both strains is identical. Presumably only the last 4-6 amino acids (152-158) can rotate, decreasing the amount of accessible polar groups [10]. The hydroxyl group of Tyr-2 is located inside the protein and is not accessible. The accessibility of the hydroxyl groups of Ser-1 and Ser-3 depends on the flexibility of the amino acids 152-158, since it is covered by them. In sum, the amino acids, positioned in the inner channel, offer more amine and primary amide functional groups than those on the outer surface of the virion (see figure 5.2).(Valid only for the *vulgare strain.*)

This is however only a glimpse into the chemistry of the viral coat protein. A very important question is whether the metal ions can not only diffuse through the channel, but also penetrate the viral coat, i.e. the integral arrangement of coat proteins. One confirmation for this scenario would be that upon negative staining of TMV with uranyl acetate the complete virion (the outer borders and the inner channel) is stained in a very short time (less than 30 sec). In no case a partial staining, resulting in a partial visualization of the inner channel by TEM, was observed. But the diffusion of the uranyl ions through the inner channel might be that fast, that the initial stage cannot be observed. A rough estimation of the diffusion time of a metal complex through the inner channel of the virion in water can be made with a simple formula. Assuming no interaction of the complex with the environment, e.g. interaction with the virion or other molecules, the following equation is valid [3]:

$$\sqrt{\langle x^2 \rangle} = \sqrt{2Dt}, \tag{5.1}$$
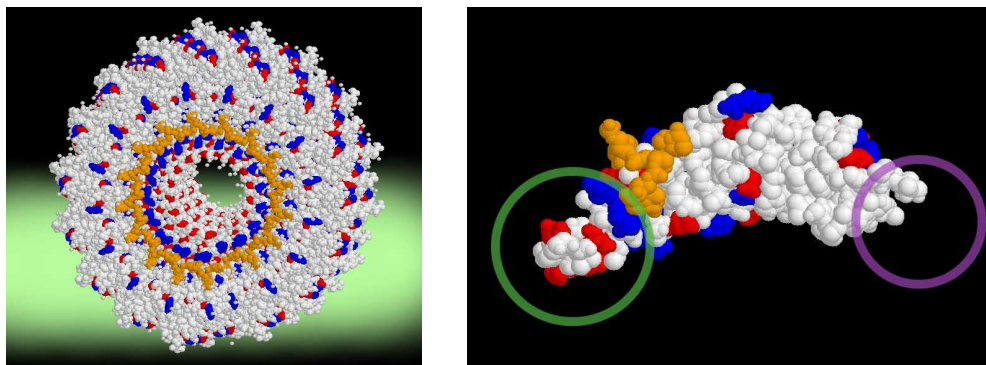
Figure 5.1: Left: Model of 49 helically arranged coat proteins of TMV (*vulgare strain*), generated with MDL© Chime [23] from [125]. The orange colour shows the RNA, the red colour the acidic amino acids and the blue colour the basic amino acids. Right: One single coat protein of TMV (*vulgare strain*) with the same colour coding as in the left image. The green circle shows the flexible loop of the coat protein. The purple circle shows the area where the last 4 amino acids should be found (Gly-155, Pro-156, Ala-157 and Thr-158 are missing in all the available models). Both images show an enhanced concentration of acidic amino acids in the central channel, while the outer surface shows acidic as well as basic amino acids.
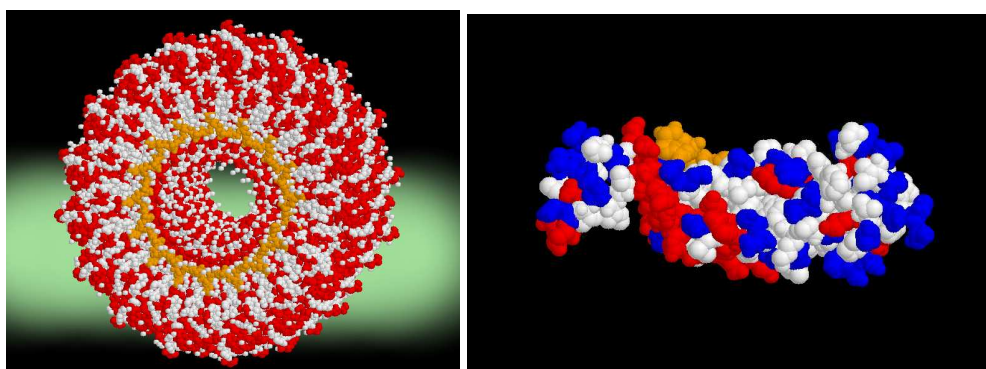
Figure 5.2: Left: Model of 49 helically arranged coat proteins of TMV (*vulgare strain*), generated with MDL© Chime [23] from [125]. The orange colour shows the RNA and the red colour the polar amino acids. Right: One single coat protein of TMV (*vulgare strain*). The orange colour shows the RNA. The blue colour shows amino acids containing hydroxyl groups. The red colour shows amino acids containing amine or primary amide groups. On the outer surface of the virion mainly hydroxyl groups are accessible, while the inner channel contains in addition amine and primary amide groups as well.

the average diffusion path of the molecule, which in our case is the length of the viral inner channel (300 nm). Diffusion coefficients in water for molecules of similar size and charge like the metal complexes in our case range from $1 \cdot 10^{-5}$ to $2 \cdot 10^{-5}$ cm^{2}s^{-1}. With an average of $1.5 \cdot 10^{-5}$ cm^{2}s^{-1} and the length of the virion (300 nm) the calculated time for diffusion of the complex through the inner channel of the virion is 30 μs. Of course this is just a rough estimation, but it provides the time scale for the diffusion of the complexes through the inner viral channel, hence it is not surprising that no initial (incomplete) stage of staining with uranyl acetate can be observed. Another indication for the diffusion of uranyl acetate through the channel and not through the coat protein becomes obvious in a recent publication by Dujardin *et al.* [32], where discrete silver particles were deposited inside the viral channel and the virions thereafter treated with uranyl acetate. Staining of the interior channel was only possible up to a silver particle and no further. The particle hinders a further diffusion of the uranyl ions through the channel.

The sizes of the complexes obviously play an essential role in the question whether a complex can diffuse through the channel or also penetrate the coat protein. But not only the size of complexes is important. As mentioned above, the coat protein offers flexible loops inside the channel [10], which leads to a locally varying effective radius of the inner channel. Still the diffusion of complexes through the inner channel should be practically always possible, since the diameter of the channel is 4 nm and thus large enough even for diffusion of complexes with large ligand spheres. The penetration of complexes into the coat protein is much more difficult. The complex needs to be very small in order to be able to penetrate the coat protein, which is rarely the case. The best example for this is the penetration of Hg(II) complexes into the protein [37]. Those complexes are small enough to penetrate the coat protein and reach the cystein inside. In addition they can have unpolar ligands, which allows for easier penetration of the coat protein in areas with higher concentration of unpolar amino acids.

For the diffusion of metal complexes into the channel as well as the diffusion through the channel the electrostatic charge plays a big role. The electrostatic charges of the outer surface of the virion and the surface of the inner channel may block the deposition of metal if the added metal complexes and the pH are not chosen properly (see chapter 2.1).

The following chapter will present the results of electroless deposition experiments with silver, palladium, gold, nickel, cobalt and ruthenium and discuss the physics and
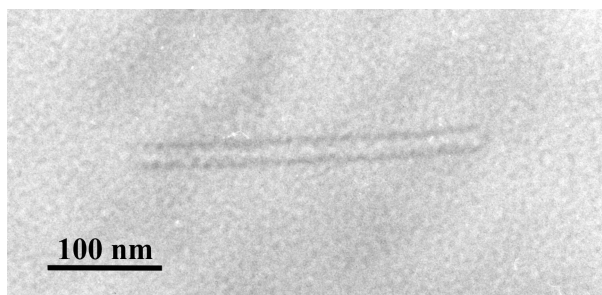
Figure 5.3: TEM (200 kV) micrograph of a single unstained TMV. The central channel is not visible and the outer borders are blurred. The inner part of the virion appears bright (i.e. like the background of the micrograph).
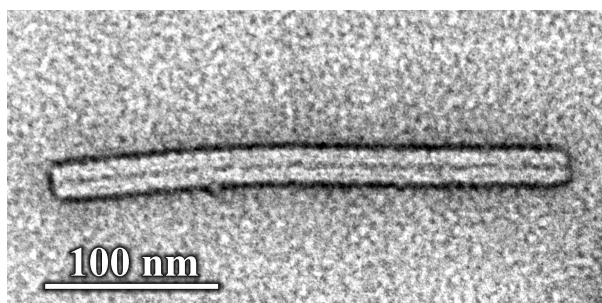
Figure 5.4: TEM (400 kV) micrograph of a single stained TMV with uranyl acetate. The central channel is clearly visible, and the outer borders are clearer than in the unstained case.

chemistry behind the attachment and growth of metal particles on or inside TMV. The metal particles can easily be seen in electron micrographs as dark spots or areas. As reference for those images, micrographs of unstained TMV, i.e. not pretreated at all, and stained with uranyl acetate (as standard staining method in biology) were taken. In the unstained case only a shade around a central bright line is visible, which can be assigned to the shape of a virion. No details can be seen (see figure 5.3). The bright inner part of the virion has a width of ca. 14 nm, while the distance of the outer borders (dark lines) is ca. 18 nm. The width of 18 nm is in agreement with the data from literature [126].

Treatment with uranyl acetate changes the appearance drastically. Here the borders of the virion shape are sharp, visible as dark areas and the central channel of the virion can be seen as a dark line (see figure 5.4). The closest distance of the dark lines is ca. 18 nm, while the distance of the outer borders of the lines is ca. 23 nm. The image shows a negatively stained TMV, where the uranyl acetate on the outer surface of the

virion does not penetrate the protein, but attaches to the surface of the virion.

In the following experiments no staining with uranyl acetate has been applied, in order to be able to identify the deposited metal without misinterpretation.

5.1.1   Deposition of Silver

The deposition of silver was investigated only for the sake of completeness. The images showed TMV with silver particles of very small sizes attached to the outer surface of the virion (see figure 5.5) [66]. The clusters had diameters in the range of 3-5 nm. In most cases clusters aggregated to larger cluster arrangements which grew perpendicularly to the viral rod. The reproducibility was very poor, i.e. only one in five experiments showed virions with attached silver. However, in these cases a coverage of the viral outer surface with silver clusters of up to 20% was observed, but no continuous coating of the outer viral surface. No silver clusters could be found in the inner channel of the virion.

First experiments attaching Ag(I) to TMV have already been done in 1942/43 [94]. Pfankuch *et.al.* have shown that ca. 3300 silver ions can be attached to a single TMV particle. With ca. 2300 coat proteins in one single TMV this means that only about 1.5 silver ions can be attached per protein. The metallization of the outer surface with silver (see chapter 5.1.1) could mean that Ag(I) has a special complexing capability with the outer surface of the TMV. This is however in contrast to the known coordination chemistry of silver [44]. While the outer surface of the virion offers mainly oxygen-containing possible ligands, the inner channel with primary amines and primary amides would be preferred by Ag(I). Therefore the chemical groups of the virion and their coordination chemistry with silver cannot act explanatory for this phenomenon, at least not in a simple way.

The virions used for the metallization with silver were not treated any further after purification. That means that the suspension was not dialyzed against water. In this case a small amount of sodium-potassium phosphate buffer was still present, due to the low concentration unable to act as buffer. A metallization of such virions with Pd activation and following Ni or Co metallization showed a metallization exclusively on the outer surface, too (see chapter 5.1.4 and 5.1.5). Here an assumption can be made, namely that the buffer plays an important role by complexing the metal ions. Indeed Ag(I) precipitates with $H_2PO_4^-$ as Ag_3PO_4 [44]. Dujardin *et.al.* [32] have proposed
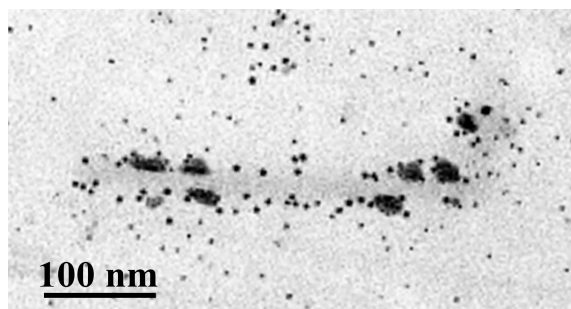
Figure 5.5: TEM (60 kV) micrograph of a single TMV metallized with silver. The outer surface is covered with silver clusters, while inside the central channel no silver particles are observed. The dark spots in the surrounding area are single silver clusters grown in solution and attached to the membrane of the TEM grid.

that for a treatment of the virions with metal the charge difference of the protein part inside the channel and on the outer surface cannot be neglected. At neutral conditions, where the positive electrostatic charge of the outer surface is reduced, and the negative electrostatic charge of the inner cavity is enhanced, they deposited several (4-10) silver clusters from a Ag(I) solution inside the inner channel, not with the method of electroless deposition, but with coordination of Ag(I) ions and subsequent reduction. The differences in charge are due to differences in the pKa of the outer and the inner part of the proteins. In the pH range (pH 4-7) this would mean that the inner channel is negatively charged and the outer surface is positively charged. In this pH regime the electrostatic attraction of the Ag(I) ions to the inner channel would be higher than to the outer surface, which would result in silver cluster growth inside the channel. However, the metallization bath used in our experiments shows significant differences in composition, which can explain the different results of both metallizations. As described (see chapter 4.4.2), our bath contained formaldehyde (HCHO) which diffuses through the inner channel of the virion. Due to its polar nature, it binds to polar groups and reacts with primary amines inside the inner channel, with the effect that on the one hand possible binding sites of the amino acids are blocked for the Ag(I) ions, and that on the other hand the electrostatic charge of the inner channel is even more negative. On the outer surface of the virion phosphate ions, which are negatively charged, can coordinate to the positively charged amino acids (e.g. lysine and arginine) and thus decrease the amount of positive charges on the outer surface even before HCHO is applied. An indication for this could be the fact that very small amounts of phosphate

buffer are evidently sufficient to change the general behaviour during metallization. The buffer concentration in the viral suspension is very low and during the metallization procedure it is diluted even more. The virion concentration is in this case lowered as well, so the ratio of the concentrations of the buffer and the virion remain the same. As a result, silver coordinates to accessible binding sites on the outer surface, which in this particular case are the coordinated phosphate ions, precipitates as Ag_3PO_4 and initiates the particle growth after the Ag(I) is reduced to the zerovalent state. The reduction of Ag(I) can be induced by three possible reductants: The formaldehyde in the solution, light, since the reaction vessel is exposed to light, and the virion itself.

The resulting silver clusters are loosely bound to the outer surface, which can be concluded from the resulting TEM images. The virion in the TEM image contains silver clusters attached exclusively to the side parts, but none is visible on top. The clusters can easily diffuse on the outer surface of the virion and are upon adsorption on top of a TEM grid stabilized by the virion and the grid surface. Basically the results show a negative staining of the TMV with rather large metal clusters, which are unable to diffuse through the inner channel. Remarkable is the weak interaction of the silver clusters with the virion. No silver clusters can be seen on top of the virion in the TEM images, which indicates a very loose bonding. Nanometre-sized silver particles are, like gold particles, commercially available. They are stabilized by a shell of organic or inorganic molecules (e.g. phosphate). One would expect that a silver particle can interact with the virion more strongly, but the results show that this is not the case. More likely is the stabilization of the silver clusters by other molecules from solution. The TEM image shows a narrow size distribution of the silver particles, which indicates such a stabilization, since usually a coalescence of the particles would be expected [33].

The specific metallization with silver does not seem to be directly connected to the coordination chemistry of Ag(I), but rather to secondary effects induced by additional chemicals in the solution and to the acidity of the solution.

5.1.2   Deposition of Palladium

With attachment of Pd(II), usually for activation of the virion in a step-wise ELD (see chapter 3.4), additional effects occur. The virion suspension was dialyzed against water prior to usage, in order to remove the phosphate buffer. The solution consisted only of $Na_2[PdCl_4]$ and excess NaCl. The latter is very important in order to avoid
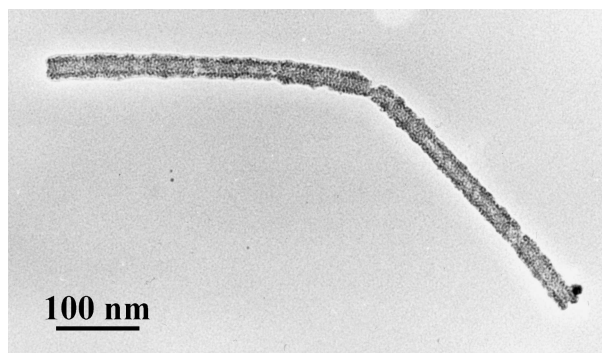
Figure 5.6: TEM (200 kV) micrograph of several head to tail-arranged TMVs metallized with Pd(II) and reduced with NaH_2PO_2. The outer surface is densely covered with palladium, while inside the central channel no palladium particles are observed.

the creation of palladium-oxo and -hydroxo complexes in water [63]. Those can form easily, especially if the pH is higher than 2 and the Cl^- concentration is low. The difficulties do not arise from those complexes themselves, but rather from oligo- and polycondensation to larger units. Depending on the pH, this process lasts hours (pH 5-7) or even days (pH 2-4), so a fast processing would be possible. However, during treatment with the bath several centrifugation steps need to be done, building up a concentration gradient of the Pd(II) complexes in the reaction vessel. The probability of oligomerization of those monomers becomes higher. Therefore the use of the native solution is not preferred. Since working at very low pH values is not possible due to instability of the virions [126], the other possibility to stabilize the monomers is used, the shift of the equilibrium towards the $[PdCl_4]^{2-}$ by adding Cl^-.

Palladium was deposited from an aqueous solution of $PdCl_4{}^{2-}$ (see chapter 4.4.2). The timing of the cluster formation in the TMV suspension and the amount of clusters depended on the reductant. Reduction of Pd(II) with hypophosphite in a single step ELD (see chapter 3.4) resulted in a dense outside coverage of the viral tube after a very slow reaction (more than 1 hr). Inside the channel no clusters could be observed (see figure 5.6).

With DMAB as reductant, a separate reduction step (see chapter 3.4) after incubation with Pd(II), yielded virions with a slightly darker colour than the unstained virion and some clusters of sizes up to 8 nm in diameter, attached exclusively to the outside of the virion (see figure 5.7). No clusters could be found in the inner channel. The reaction with DMAB as reductant was (compared to the reaction with hypophos-
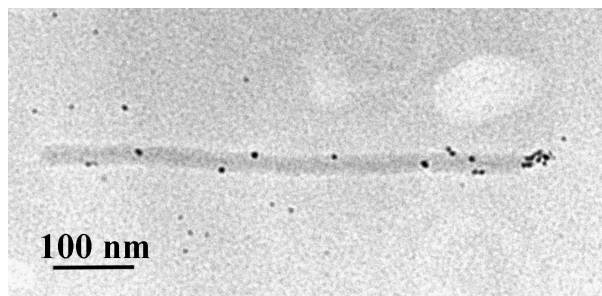
Figure 5.7: TEM (200 kV) micrograph of two head to tail-arranged TMVs met-
allized with Pd(II) and reduced with DMAB. The outer surface shows attached
palladium clusters, while inside the central channel no palladium particles are ob-
served. The dark spots in the surrounding area are palladium clusters grown in
solution and adsorbed on the membrane of the TEM grid.

phite) very fast (5-10 min), which could be judged by the gas evolution (H_2 in form of
bubbles) inside the reaction vessel (see chapter 3.4).

After treatment of TMV with palladium and DMAB, the results have shown that
the virion appears slightly darkened in the TEM, and that some larger clusters appear
at the outer surface of the virion (see figure 5.7). In clusters the density of Pd is
higher than in complexes or salts (some space is occupied by ligands or counter ions),
which leads to a stronger darkening of Pd clusters in the TEM compared to crystals
of e.g. Pd(II) salts or compounds containing unreduced Pd(II) complexes (compare
also staining with uranyl acetate). The channel of the virion cannot be seen. This
indicates that a very small amount of Pd(II) is complexed within the coat protein.
A further indication is that no EFTEM of palladium is possible (see chapter 5.1.4).
Palladium has a very high atomic mass (compared to the other elements building up
the coat protein). A higher concentration of palladium on the outer surface or in
the inner channel of the virion would result in a higher contrast of the sites where
Pd(II) is adsorbed. The image shows merely a few dark spots on the outer surface of
the viral coat. This can be explained as follows: In contrast to the single-step ELD
of palladium with hypophosphite as reductant, here TMV was exposed to a Pd(II)
containing solution, then washed and afterwards the Pd(II) was reduced with DMAB.
The effect of such a treatment is that the growth of Pd clusters is limited, since the
source, the Pd(II)-containing solution, is removed. Upon reduction some clusters can
grow, but the limiting factor for their size is the concentration of coordinated Pd(II)
and the capability of Pd atoms or small clusters to diffuse on the outer surface and on

the surface of the inner channel of the virion upon reduction of Pd(II). A diffusion of Pd(II) from solution to the outer surface and into the inner channel cannot take place, since no additional Pd(II) is provided.

Before removal of excess Pd(II), the amount of Pd(II) is by far more than needed to saturate the coordination sites of the coat protein. Although the affinity of Pd(II) to nitrogen-containing ligands is very high [44], the other binding sites, containing oxygen, can be saturated, too. Thermodynamically more stable are the complexes of Pd(II) with nitrogen-containing ligands, but kinetic effects can play a big role. Complexes of Pd(II) with oxygen-containing compounds are kinetically stable [44]. Since oxygen-containing groups are easily accessible on the outer surface of TMV, complexes with Pd(II) can form, too. During reduction from the ionic to the elemental state, Pd starts diffusing on the outer surface and coalescing with other Pd clusters. The clusters can grow until no more palladium is left. The palladium in the inner channel might also contribute to the cluster growth by diffusion through the channel to the opening of the virion. There the Pd atoms and small clusters can easily coalesce to larger, thermodynamically more stable clusters [33]. The effect of this scenario would be a few metallic clusters on the outside of the virion located close to the opening of the central channel. This is exactly what can be observed.

A scenario where Pd(II) is electrostatically bound to the virion is possible as well. The Pd(II) complex is negatively charged ($[PdCl_4]^{2-}$) and thus can be attracted by the positively charged outer surface of the virion at pH 5-6 (see chapter 4.4.2) [32]. The surface of the inner channel is in this pH regime predominantly negatively charged, which acts repulsive on the Pd(II)-complex. The result is an attachment of Pd(II) exclusively to the outer surface and thus, upon reduction to Pd, metallic clusters positioned at the outer surface. This, however, does not explain the concentration of metal clusters at the end of the virion, which was frequently observed. More likely is that there is a contribution of the inner channel to the cluster growth, which in this scenario is not the case. Most probably a mix of both scenarios (electrostatic interactions and complexing) leads to the attachment of Pd(II).

In another experiment, the reduction of Pd(II) coordinated to the outer viral surface was achieved with hypophosphite added to the Pd(II)-containing solution in a one-step ELD. With this procedure, metal growth takes place on the outer surface of the viral coat and continues until the major part of the viral surface is covered (see figure 5.6).

The difference in the results, i.e. discrete clusters on the one hand and almost

complete coverage on the other hand, can be assigned to two differences in the reaction vessel. First, different reductants were used. Second, the concentrations of the Pd(II) complex and its ligand (Cl$^-$) was different. While in the reaction with DMAB as reductant the amount of Pd(II) was limited to the amount coordinated to the coat protein, in the other case there was a continuous source. The differences in kinetics in those two reactions cannot be compared, since the reactions are not comparable. Basically the speed of an ELD depends on the mixed potential of the components and on the induction period, which is the time needed for the reaction to reach the mixed potential. The induction period is dependent on several factors, like temperature, pH, ligand concentration and reductant type and concentration [91, 104]. In our case the type of reductant as well as the concentration of the ligand and the pH were changed. However, the reaction started faster and had to be stopped earlier, which corresponds to a shorter induction period for the reaction with DMAB. Although the reactions are not comparable, the faster reaction corresponds to a more negative redox potential of DMAB as compared with hypophosphite, which indeed is the case [96]. The continuous source of Pd(II) in the hypophosphite bath leads to a more dense and uniform coverage of the viral outer surface. An analogous reaction with DMAB instead of hypophosphite was tried, but the reduction of palladium took already place upon adding DMAB to the Pd(II)-containing solution. In this case the mixed potential Pd(II) and DMAB is reached faster (the oxidation potential of DMAB is more negative than that of hypophosphite) [104], which decreases the induction period. In this particular case the induction period was very short and did not allow for attachment of Pd(II) to the virion, but the reduction of Pd(II) started already in solution. The reaction can be slowed down by cooling of the reaction vessel, but those possibilities were not further investigated, since attachment of Pd to the virion was basically done for activation purposes for further metal deposition (e.g. Co and Ni).

5.1.3 Deposition of Gold

The deposition of gold on the outer surface or in the inner channel of TMV works in a different way. The applied bath contains already the reductant, and also additives needed for stabilization of the gold ions in solution (single-step ELD) [88].

A treatment of the TMV suspension with the gold bath (see chapter 4.4.2) showed after a fast reaction (10-15 min) virions with no large clusters attached (like in the cases
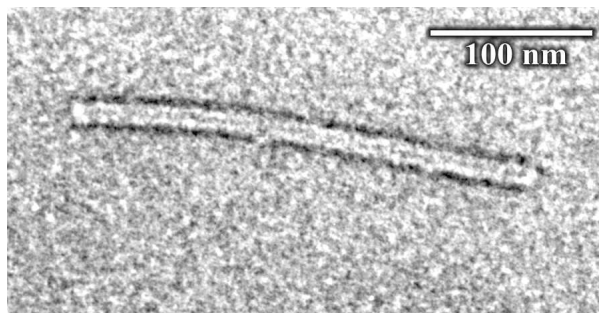
Figure 5.8: TEM (200 kV) micrograph of a single TMV metallized with gold (Au(I) reduced with ascorbic acid). The central channel and the outer surface appear stained.

mentioned above). But some structural details of the virions could be observed in the microscope. The resulting images showed a stained virion, where the outer border of the viral tube was clearly visible, and the inner channel as well. The images closely resemble those of TMV stained with uranyl acetate, but are a little weaker in contrast (see figure 5.8 compared with figure 5.4). The closest distance of the dark lines is ca. 15 nm, while the outer borders of the lines have a distance of ca. 20 nm. The closest distance (15 nm) shows that this staining cannot be exclusively negative since in this case the gold would attach to the outer surface of the virion and the distance would be 18 nm. The distance of the outer borders of the lines is 20 nm, and thus larger than the diameter of the virion. An exclusive positive staining is here not the case, too. Presumably the gold contributes to both, negative and positive staining.

The chemistry of the gold bath (containing $HAuCl_4$, NaSCN, Na_2SO_3 and ascorbic acid) is more complex and needs a closer look for better understanding. SO_3^{2-} reduces the Au(III) to Au(I) which is complexed by SCN^-. The resulting $Au(SCN)_2^-$ is stable in presence of excess SCN^- and can as such coordinate to amino acids and proteins [44]. In case of TMV it shows no large selectivity for certain sites. Once bound, Au(I) can easily be reduced even by ascorbic acid due to the high redox potential of gold. It is even likely that TMV itself can reduce Au(I). The rate of gold deposition can be increased by disproportionation of Au(I) into Au and Au(III) [104]. This, however, depends on the thermodynamic stability of the Au(I) complex. In order to increase the stability of such gold baths, many investigations aimed at suppressing the disproportionation. The $Au(SCN)_2^-$ appears to be sufficiently stable.

By treatment of TMV with such a metallization bath it is very unlikely that the

intermediate $Au(SCN)_2^-$ binds coordinatively to a specific site of the coat protein since this would require soft ligands which are not present in the amount needed. This is very much in analogy to the silver deposition. Here, gold can attach electrostatically (in analogy to uranyl acetate) to the TMV. The only possible attachment via complexation would in case of metallization with gold be a coordination with sulphur-containing amino acids. Indeed the coat protein contains such an amino acid, the cystein (Cys-27), but it is located deep inside the coat protein and is thus not accessible for the gold complex [125]. Methyl mercury nitrate, however, can obviously reach Cys-27, as shown by X-ray diffraction studies (see chapter 2.3) [37]. Presumably the effective size (i.e. the ligand sphere) of the complex plays an essential role. The mercury complex is hydrophobic and small enough to penetrate the coat protein (i.e. not only the central channel, but also the protein itself), while the gold complex is too large. The fact that the gold complex cannot penetrate the protein is confirmed by the TEM images, since no increased concentration of metal can be found between the central channel and the outer surface of the virion.

The increased contrast of the outer surface and the inner channel of the TMV in the TEM images confirms an attachment of gold in general. Such gold attachment to proteins is well known from the immunogold labelling by gold clusters attached to antibodies [114, 115]. The use of the applied gold bath is compared to the immunogold labelling a much simpler method for attachment of gold clusters on TMV although its selectivity for particular parts of the coat protein is lower. Concerning the cluster size, the dark spots on the outer surface could not be resolved further. The gold clusters in this case are smaller than 2 nm. Even longer metallization with gold did not enlarge the clusters. It appears that by reaching a certain cluster size, the maximum stability of the attached cluster is reached and further growth is stopped. Very small gold clusters show increased stability with discrete numbers of atoms. For example Au_{55} is a stable cluster and can be commercially obtained (although with a stabilizing shell, like citrate), while Au_{54} or Au_{56} are not available. A continuing growth of the clusters would detach the gold from the protein, since the ratio of the surface area of the cluster to the number of binding sites shared with the protein increases, and due to the convection inside the reaction vessel increasing forces act on the cluster. Examination of the solution in TEM showed loose gold particles in solution, which were by far larger in size (several tens of nm) than the clusters attached to the coat protein. This is an indirect proof of the scenario, i.e. unbound Au clusters can continue to grow.

The inner channel of the TMV after gold deposition does not show distinct clusters, but the channel itself is clearly visible. Here one can assume that those clusters are even smaller than the ones deposited outside. The coalescence seems hindered, which is probably either due to hindered diffusion of gold atoms on the surface of the inner channel or due to lower stability of binding sites of this part of the protein with larger gold clusters, which would suppress the cluster growth. The nature of this particular stabilization effect is not yet known, so this particular chemistry cannot be described in detail.

Fact is that this method of metal attachment can act as alternative to the standard staining methods in biology, avoiding uranyl acetate. The staining should correspond to negative staining, since the gold complex attaches electrostatically to the outer surface and the surface of the inner channel of the virion [107]. If the binding was more specific, e.g. to Cys-27, the staining would be positive. But gold ELD is also a simple and effective way to synthesize metal/bioorganic composites, where the metal is in the form of small clusters.

5.1.4 Deposition of Nickel

Nickel could not be deposited in a single step. An activation step prior to nickel deposition was necessary in any case (step-wise ELD). The main difference to the metal deposition methods discussed above is that the focus is no longer on the chemically active sites of the virion, but on the accessibility for catalyst clusters of palladium, platinum or gold, since the metal growth takes place exactly at those clusters [104, 63]. Therefore the places where nickel can grow are limited to those places, where a catalyst for the growth can be attached.

The deposition of nickel was effected in several ways, therefore several cases need to be clearly distinguished.

First the deposition of nickel was performed from a palladium-pretreated virion suspension with hypophosphite as reductant (step-wise ELD, see chapter 3.4) [97]. The reaction took place in 10-20 min. TMV treated in this way yielded virions containing metal clusters with diameters of 3-4 nm in the interior channel (see figure 5.9 (b)) [66]. In some cases short rods with widths of 3-4 nm and lengths of 10-50 nm could be seen in the direction of the viral tube (see figure 5.9 (a)). Clusters attached to the outer surface of the virion could be observed only rarely. The yield of virions
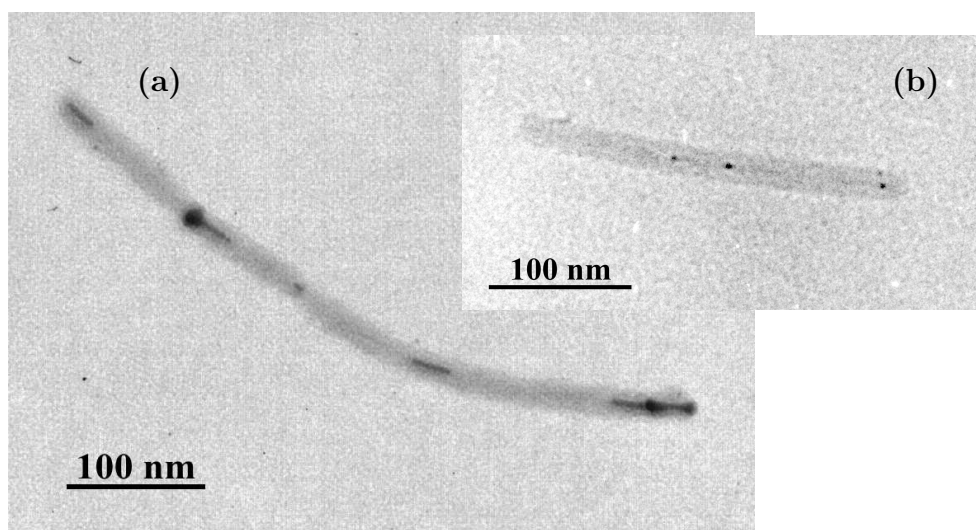
Figure 5.9: TEM micrographs of TMV activated with palladium and metallized with nickel (Ni(II) reduced with NaH_2PO_2). (a) TEM (400 kV) image showing short metal rods exclusively situated in the inner channel of two virions. The rods have diameters of 3-4 nm and lengths of 10-50 nm. (b) TEM (200 kV) image showing spherical clusters inside the viral channel of a single TMV. The clusters have diameters of 3-4 nm.

containing metal clusters differed from experiment to experiment, and in no case the amount was higher than 40%. The assumption that the clusters inside the virion start growing on discrete places (due to some possible irregularities in the protein or RNA structure) inside the channel could not been confirmed: The cluster distribution inside the channels of different virions was random [110].

The nickel deposition was also performed with palladium-pretreated virions and DMAB as reductant. Here the reaction was faster than with hypophosphite. Once started (the initiation time was in the range of 1-2 min), the metallization took place within seconds. The resulting images showed virions with their channels partially filled with metal. The deposited metal had the shape of a wire. The diameter was 3-4 nm and the lengths ranged from 50-600 nm (see figure 5.10). In some cases the metal was deposited without gaps in channels of head to tail-aggregated virions, thus surpassing 300 nm length (see figure 5.10 (b)). In most cases the yield of virions containing metal was 30-50%. Whether the linear features consist of aggregated clusters or show linearly grown metal, could not be distinguished by TEM. The metal was not exclusively found inside the virion: In some cases metal could be found on the outer surface. In very few
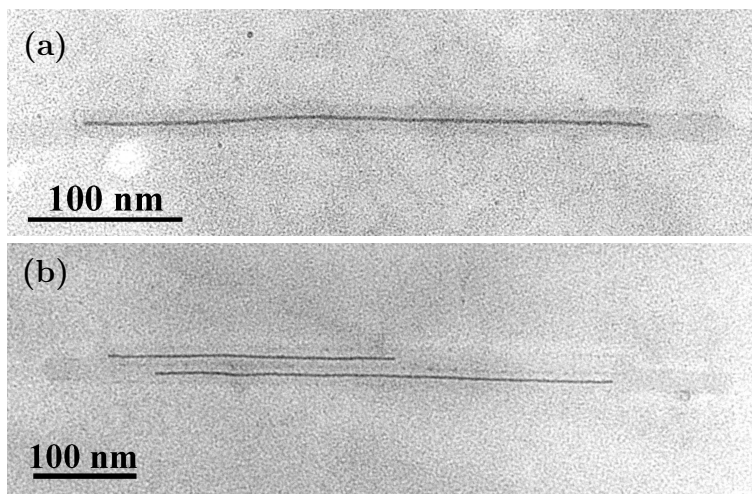
Figure 5.10: TEM micrographs of TMV activated with palladium and metallized with nickel (Ni(II) with DMAB as reductant). (a) TEM (200 kV) image showing TMV continuously metallized inside the channel. The length of the metallized part reaches 350 nm with a diameter of 3-4 nm. (b) TEM (200 kV) image showing several virions aligned head to tail and side by side with metallized channels (diameter 3-4 nm). The length of the metallized part of the channels can reach 600 nm.

cases metal both in the inner channel and on the outer surface was observed (see figure 5.11). The replacement of palladium with platinum gave very similar results, therefore in the following palladium and platinum pretreatment are not discussed separately. In order to proof that the obtained wire consists of nickel, EFTEM (see chapter 3.2.1) and EDX (see chapter 3.2) were performed. The images confirmed that the wire consists of nickel (see figure 5.12). A mapping of palladium was not effective. Presumably the concentration of palladium was too small to be detected either by EFTEM or by EDX.

A replacement of palladium by gold (further procedures as above) (see chapter 4.4.2) resulted in small metal clusters attached to the outer viral surface. A comparison with the images of gold-pretreated TMV (fig 5.8) shows additional clusters of nickel on the outer surface of the virion. The reaction was slightly slower than for the palladium pretreatment and took 5-10 min. If the reaction was stopped in a very early stage, very few small clusters could be observed on the outer surface of the TMV in addition to the staining observed after gold treatment (see figure 5.13(a)). A stop of the reaction in a later stage showed a continuing growth of nickel on the outer surface of the virion covering additional surface, but also growing perpendicularly to the virion axis (see
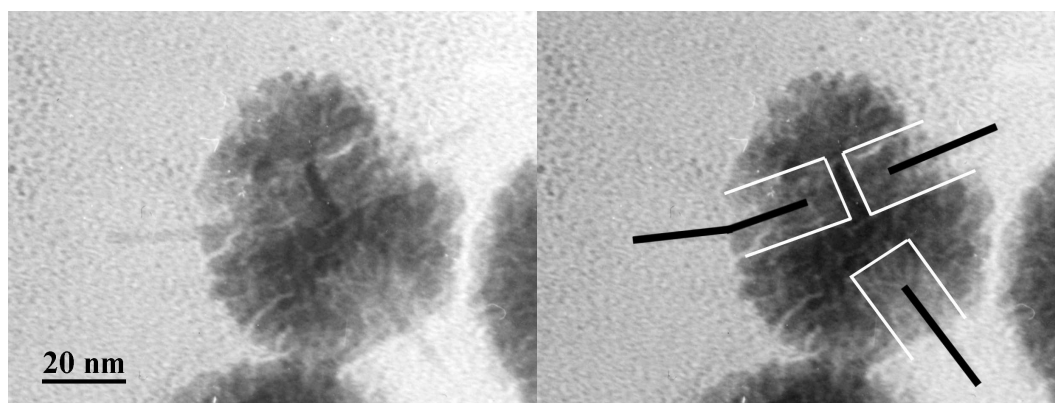
Figure 5.11: TEM (200 kV) micrograph of TMV metallized with nickel/DMAB after activation with platinum. The virions show short metal rods inside the channel and are metallized on the outer surface with nickel. Left: Original image of metallized TMV. Right: Same image with marked areas: White lines show the outer borders of the virions, black lines show the metallized inner channel.

figure 5.13(b)). About 50-60% of the virions contained metal. A smooth coverage of the viral surface could not be achieved.

Another approach to a coverage of the outer viral surface with metal was performed again with the method of palladium or platinum pretreatment and deposition of nickel from a DMAB-containing bath, but without dialyzing the TMV suspension before usage. This suspension contained in a small amount sodium-potassium phosphate buffer. In this case metal could not be found in the interior channel of the virion, but exclusively on the outer surface (see figure 5.14). Different stages of metallization could be observed. Once the outer viral surface was covered with metal, the growth continued perpendicularly to the orientation of the virion. The yield of metal-containing virions was very high (70-80%).

In the first case, palladium was chosen as catalyst and nickel was deposited from a solution which contains hypophosphite as reductant. The results showed discrete clusters in the central channel of the virion (see figure 5.9). TMV treated with palladium only, and afterwards reduced with hypophosphite, primarily showed opposite results: Palladium was deposited on the outer surface of the virion (see figure 5.6). Here a closer look at the growing clusters themselves is required. While on the outer surface the growth of the clusters is not space-limited, in the channel it is. The growth of attached clusters can only take place until a stability limit is reached, similar to
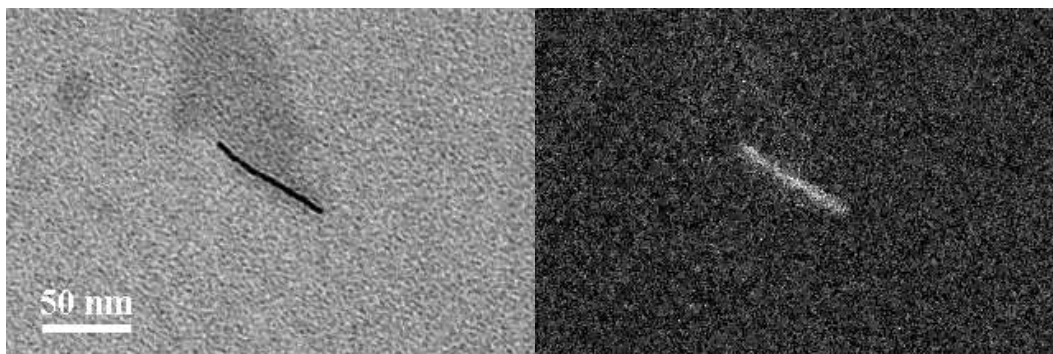
Figure 5.12: TEM (120 kV) micrographs of TMV activated with palladium and metallized with nickel (DMAB as reductant). Left: STEM (120 kV) image showing the metal wire inside a viral channel. The virion itself is not visible due to lack of contrast using this method. Right: Ni-selective EFTEM of the same region.

the growth of gold clusters. During the reaction hydrogen evolves (see chapter 3.4), in particular at the surface of the growing clusters 3.4 [104]. The hydrogen forms bubbles, which tend to move to the surface of the bath, since their density is lower than the density of water. During the movement of the bubbles, forces act on the metal clusters, pulling them away from the virion. A detachment of the cluster from the surface of the virion becomes possible, because the forces acting on the cluster, induced by the hydrogen bubbles, rise due to increased surface of the cluster, while the interactions with the virion become comparatively weaker. This is in contrast to the scenario with Au(I) sensitation, because gold interacts stronger with the proteins and therefore the forces induced by hydrogen bubbles are not strong enough to detach the gold clusters. Once the clusters are detached, the only remaining active sites for metal deposition, i.e. palladium clusters, are in the central channel, since they are encapsuled by the surrounding coat proteins. The detached clusters in solution can of course grow further, too, but they have no influence on the metallization of the virion itself any more. In this way it is possible to obtain TMV with discrete clusters inside the channel, which are in some cases even elongated to short wires, without metal attached to the outer surface. In a certain way, this is a selective metal deposition inside the virion, although the growth itself is not selective.

Very similar results are obtained if DMAB is used instead of hypophosphite under else same conditions, namely palladium or platinum as catalyst. The only visible difference is that longer wires inside the virion can be obtained (see figure 5.10). The
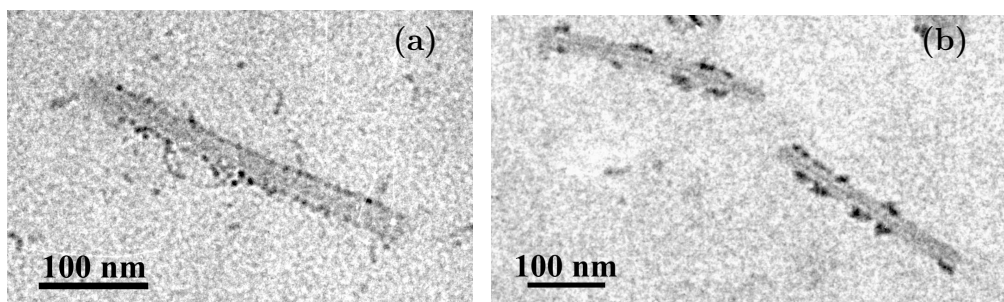
Figure 5.13: TEM (200 kV) micrographs of TMV metallized with nickel/NaH$_2$PO$_2$ after activation with gold. (a) Metallization of TMV stopped in an early stage showing few metal clusters attached to the outer surface of the virion. (b) Two virions showing larger metal clusters on the outer surface after continued metallization.
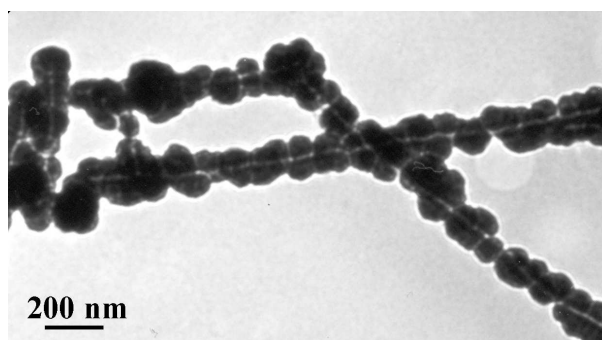
Figure 5.14: TEM (200 kV) micrographs of undialyzed TMV metallized with nickel/DMAB after activation with platinum. The surface of the virions is densely covered with nickel.

largest difference in chemistry in comparing those two cases is the speed of the reaction. As in the case with metallized palladium, the induction period for reaching the mixed potential is shorter with DMAB than with hypophosphite [104]. Again the reactions cannot be directly compared from a kinetic point of view, since the metal complexes contain different ligands and the reductants are different and have different concentrations (see chapter 4.4.2). Obviously the kinetics of our particular DMAB-containing bath is faster than in our hypophosphite bath. The slower reaction needs longer time, and thus thermodynamics plays a comparatively larger role. The growth of already existing clusters, i.e. clusters in solution detached from the outer surface of the virion, is forced due to higher thermodynamical stability. This effect can be explained as follows: In a fast reaction, more nucleation centres (initial metal clusters) are formed in solution in a shorter time. The probability of coalescence or coagulation

of such clusters increases, since it is directly proportional to the concentration of the clusters in solution. A larger number of coalescence or coagulation events in the same time leads to a larger number of (smaller) clusters. For slower reactions the opposite is the case [33]. Decreased concentration of small clusters, i.e. initial metal clusters, forces the growth of larger clusters, since the probability of coalescence events of small clusters with large clusters becomes higher.

In the experiments more clusters, which were larger in size, could be found in solution, detached from the virion. The faster reaction (i.e. the reaction with DMAB as reductant) forces the kinetic growth, i.e. the growth of initial clusters and the growth of small clusters as well. Those are the clusters situated inside the channel, which have only one possible direction to grow, namely the 1D direction along the channel orientation. The mechanism of this metal growth is not yet clear, but TEM snapshots from different time scales during growth suggest the following scenario: First nickel starts growing around small palladium clusters, reduced by the DMAB in the nickel solution. In the TEM image (figure 5.15) a pale gray channel becomes visible (see black arrows in figure 5.15). A concerted growth and coalescence of clusters results in closing the channel at a certain place. Images show that the pale gray colour does not cover the whole length of the channel (see white arrows in figure 5.15), an indication for the coalescence of the growing clusters. From then on the cluster can grow to both sides, becoming a metal nanowire, except for the case when the viral channel is closed on the other side by another cluster and the diffusion through the channel hindered. In this case the growth is slowed down, since it can only take place in one direction. In some cases virions with more than one cluster inside the channel were found and in all such cases the particles were comparatively short.

Metallization of TMV on the outer surface is performed in two ways. First gold instead of palladium (or platinum) was used as catalyst. Here the higher stability of gold clusters attached to a protein comes into play 5.1.3. The larger clusters are situated on the outer surface (see figure 5.13) and offer higher accessibility for the nickel ions and the reductant as well as the opportunity to grow in 3D, which is preferable for the cluster growth [33]. The effect is that large that no considerable metal growth in the channel takes place. The further the reaction proceeds, the lower is the tendency for the nickel to grow inside the channel. Remarkable is the stability of the attached metal on the exterior surface. In contrast to the palladium (or platinum) activated ones, they do not detach from the proteins. The stability of attached gold nanoparticles to
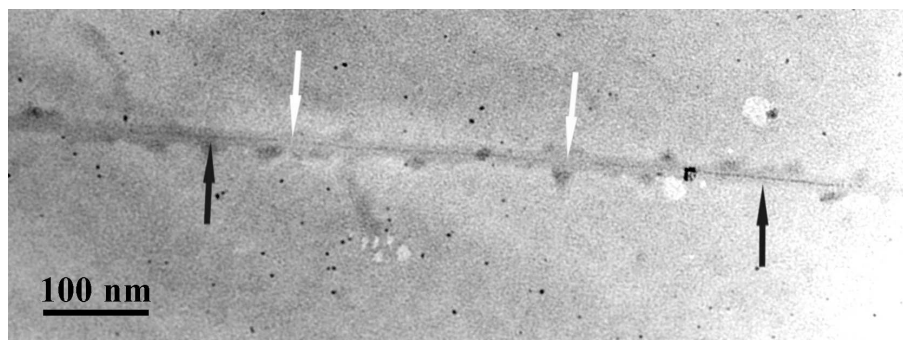
Figure 5.15: TEM (200 kV) micrograph of TMV metallized with nickel after palladium activation. The reductant was DMAB. The pale grey lines (black arrows) indicate the starting of the growth of a wire. Some parts of the virion do not show metal in the interior channel (white arrows). The image is done in the initial stage of the metallization reaction.

organic molecules is well known from immunogold labels or Au_{55} clusters stabilized by phosphate or citrate, while such compounds with palladium or platinum are not known [114, 115]. The continued growth of such nanoparticles leads to coalescence and continued 3D growth [33].

The other method to decorate the outer surface of the virion with metal is to contact palladium-pretreated TMV with Ni(II) and DMAB, but without dialysis prior to the palladium treatment (see figure 5.14). Here some questions about the mechanism appear. Since the metallization solutions are exactly the same in both cases (the metallization inside the channel and the metallization on the outer surface) the difference can be assigned to the existence or concentration of the phosphate from the sodium-potassium phosphate buffer. While on the one hand the buffer was almost completely removed from the virion suspension by dialysis, on the other hand the suspension still contained some phosphate. First of all the question arises, whether the centrifugation and washing steps (see chapter 4.4.2) during the procedure can remove the phosphate from the suspension. During dialysis the concentration difference of phosphate between the virion suspension and the pure water forces the phosphate to diffuse through the dialysis membrane until an equilibrium is reached. The larger the amount of water or the number of dialysis steps, the lower is the concentration of phosphate in the virion suspension. Of course time plays an important role. In order to remove the buffer (almost) completely, the dialysis was done for at least 15 min (see chapter 4.4.2). Hence the equilibrium concentration was reached in both the viral suspension and the water.

In contrast, the centrifugation steps do not remove significant amounts of phosphate from the suspension. The phosphate, electrostatically attached to the outer surface of the virion, concentrates together with the TMV during centrifugation. The question in this context is, how the phosphate interferes with the metallization reaction.

The phosphate is present in the virion suspension and is electrostatically attached mainly to the viral outer surface. In the pH regime to which the metallization baths are adjusted, the phosphate is unlikely present as PO_4^{3-}, but rather as coexistent HPO_4^{2-} and $H_2PO_4^{-}$ [44]. Since those are negatively charged, they can electrostatically interact with the positively charged amino acids at the outer viral surface. In this pH regime this is basically Arg-61 (see chapter 2.1). Addition of Pd(II)- or Pt(II)-containing solution leads to a competition of negatively charged HPO_4^{2-} or $H_2PO_4^{-}$ with $[PdCl_4]^{2-}$ or $[PtCl_4]^{2-}$ for the positively charged binding sites at the viral surface. But the Pd(II) or Pt(II) complexes may also bind coordinatively to the coat protein. As long as the Pd(II) or Pt(II) are in the native solution, i.e. in 1 M NaCl solution, the high concentration of Cl^- shifts the equilibrium

$$[PdCl_4]^{2-} + H_2O \rightleftharpoons [PdCl_3(H_2O)]^- + Cl^-, \qquad (5.2)$$

towards $[PdCl_4]^{2-}$, which is certainly only the first step in hydrolysis of the complex. After centrifugation and washing, the excess Cl^- is removed, which shifts the above mentioned equilibrium towards the right side [63]. The complexed water molecule can now be replaced by a hydroxyl group from an accessible amino acid at the outer surface of the virion, e.g. Ser-155 or Ser-154. Both the electrostatic and the coordinative attachment of the Pd(II) or Pt(II) complex lead to a coexistence of Pd(II) and phosphate at the outer surface of the virion. With these facts, still the exclusive metallization of the outer surface of the virion cannot be explained.

If the metallization is forced by the phosphate, it is not due to the chemistry of it with Pd(II) or Pt(II): Although a Pt(II) complex with phosphate as ligand ($[PtCl_3(PO_4)]^{4-}$) was proposed to exist in excess of PO_4^{3-}, it was never proven [15, 92, 93]. Moreover, despite considerable interest in the preparation of Pt(II)-protein compounds for X-ray diffraction of proteins in phosphate buffers, very little coordination chemistry of Pd(II) or Pt(II) with phosphates is known, most probably because those compounds are unstable in aqueous solvents. Few complexes of Pt(II) or Pt(II) with phosphates have been reported, but those are mainly binuclear pyrophosphate complexes. The formation of those takes place photochemically or under harsher con-

ditions (higher temperatures) than in the metallization experiments [21]. A possible
explanation would be a photochemical reaction of the coordinated Pd(II) or Pt(II) with
the attached phosphate, since the metallizations were done in daylight. However, if the
energy of the light, passing the reaction vessel, was high enough to induce a reaction
of phosphate with the Pd(II) or Pt(II), a certain amount of the metal ions would be
reduced to the metal and coalesce to small clusters. Such clusters would be visible with
TEM. Examination of TMV treated with Pd(II) in daylight did not give evidence of
such a reaction. A possible explanation for the forced metallization at the outer surface
of the virion, induced by phosphate, follows from the further experimental procedure:
The phosphate and Pd(II)- (or Pt(II)) containing TMV is treated with the Ni(II)- or
Co(II)-containing metallization bath. We checked that Ni(II) and Co(II) precipitate
in presence of PO_4^{3-} in aqueous solutions (the same nickel and cobalt baths as for the
metallization of TMV were used, and the pH was adjusted to similar values). Imme-
diately upon addition of phosphate (in form of dissolved Na_2HPO_4 and KH_2PO_4 in
water) precipitation of presumably $Ni_3(PO_4)_2 \cdot xH_2O$ or $Co_3(PO_4)_2 \cdot xH_2O$ was visible.
A treatment of a virion, which contains attached phosphate on its outer surface, with
the nickel or cobalt bath would then lead to a analogous precipitation on the viral
outer surface. This leads to enhanced concentration of Ni(II) or Co(II) on the outer
surface and thus to forced metal deposition at this place. A proof of this model requires
additional experiments, especially on the coordination chemistry of Pd(II) and Pt(II)
with the virion, with and without presence of phosphate.

5.1.5   Deposition of Cobalt

The deposition of cobalt on the outer surface or inside the channel of the virion works in
the same way as the deposition of nickel except for one difference. It is not possible to
deposit cobalt on or inside TMV from a metallization bath containing hypophosphite
as reductant. The redox potential of hypophosphite is not low enough to reduce cobalt
in a reasonable time scale on small clusters of palladium, platinum or gold. Since
metal deposition of cobalt using hypophosphite is known from literature [111], the
only possible explanation is that the activity of the cobalt bath is too low in the pH
range applied. The case is very similar to copper. Metallization works only in a very
basic medium. If the pH is lower, the reduction of the metal ions slows down or even
stops [104]. In most cases, if metallization baths are applied which are too stable, and
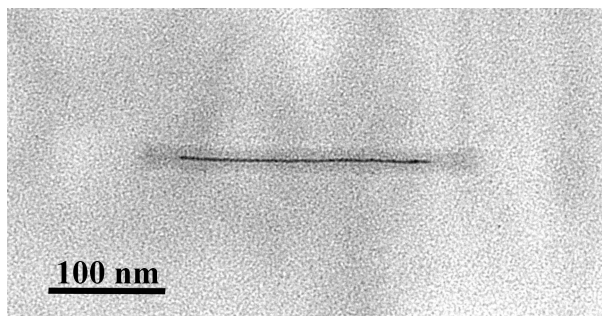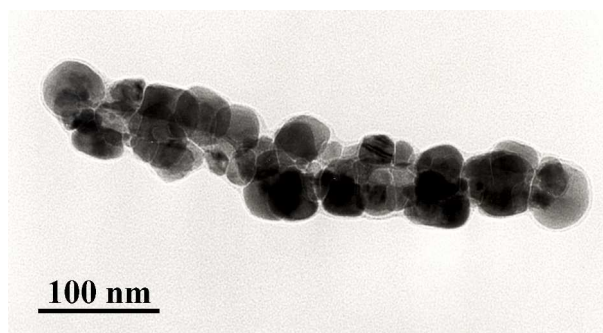
Figure 5.16: TEM (200 kV) micrograph of TMV metallized with cobalt/DMAB after activation with palladium. The metallized inner part reaches a length of 250 nm with a diameter of 3-4 nm.

if metallization does not start, the bath can be slightly destabilized by deaeration. In this case dissolved oxygen, which is a stabilizer for the metallization bath, and carbon dioxide, which is a (weak) destabilizer for the bath, can be removed from the solution by bubbling with e.g. argon for several minutes [91]. In cases like metallization with gold, the reaction after such a treatment runs out of control, whilst in the case of cobalt there is no effect. Other cobalt baths from literature [111, 90] as well as a mixed bath of cobalt and nickel were applied in order to force a cobalt deposition with hypophosphite as reductant [54, 57], but with none of them a metallization could be observed. Deposition of cobalt could only be observed when DMAB was used as reductant.

In analogy to nickel, the cobalt deposition was performed in a step-wise ELD with palladium- or platinum-pretreated TMV (both yielded the same results). After treatment of the activated virion suspension with a cobalt bath containing DMAB (see chapter 4.4.2), metal deposition in the inner channel of the virion could be observed. The results appear similar to those with nickel, but the length of the deposited metal line was shorter. The lengths varied from 50 nm to a maximum of 250 nm (see figure 5.16). The amount of virions adsorbed on the TEM grid containing metal was, like in the case of nickel, 50-60%. The metallization reaction was fast and took after an initiation time of 1-2 min only seconds, after which metal deposition became obvious in the reaction vessel.

A coverage of the virion on the outer surface was approached in the same way as with nickel: Instead of a palladium or platinum pretreatment, gold was used for activation (see chapter 4.4.2). Again the results were similar to the nickel deposition on the outer surface of the TMV (see figure 5.17). A growth of cobalt could be observed on the outer

Figure 5.17: TEM (200 kV) micrograph of TMV metallized with cobalt/DMAB after activation with gold. The virion is densely covered with cobalt.
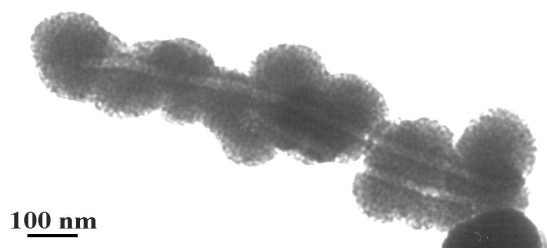
Figure 5.18: TEM (200 kV) micrograph of undialyzed TMV metallized with cobalt/DMAB after activation with platinum. The virion is densely covered with cobalt.

surface of the virion, extending perpendicularly to the virion axis. A smooth coverage of the viral surface could again not be obtained. The amount of virion containing metal was 50-60%. The metallization reaction took around 5 min.

The approach to deposit cobalt on the outer surface of a palladium- or platinum-pretreated virion with a small amount of sodium-potassium phosphate buffer (i.e. not dialyzed TMV) was done, too. Again the results could be compared to those where nickel was deposited: Most of the virions (70-80%) were decorated with cobalt, and no metal particles inside the channel could be observed (see figure 5.18).

A change to metallization baths containing DMAB yielded in all cases the same results as with DMAB-containing nickel baths. The mechanisms of deposition in all the different cases should be the same as with nickel.

5.1.6 Deposition of Ruthenium

The last metal used for decoration of TMV was ruthenium. As Ru(II) or Ru(III) it can coordinate to a large variety of organic ligands [75]. Since TMV offers several different active groups, deposition of ruthenium was very promising both on the outer surface and in the interior channel. The procedure known in literature is done at slightly harsher conditions than allowed for the work with TMV, i.e. pH around 9 and temperatures around 90°C [22, 98]. In order to avoid those conditions, the bath was modified with DMAB as reductant and slightly lower basicity (pH 8) and temperatures (75°C), below the critical ones for the stability of the virion. (A similar procedure will be tried with the copper bath mentioned before (see chapter 5) [56].)

The employed ruthenium deposition is a single step procedure (substrates to be metallized do not need to be activated with palladium, platinum or gold before (see chapter 3.4). The TEM image (figure 5.19) shows a shading around the outer viral surface and inside the channel. No discrete clusters of metal could be observed. Pretreatment of TMV with palladium and platinum before ruthenium deposition was tried, but yielded identical results.

As seen in the TEM image, the virion is surrounded by a dark haze, and the inner channel is darkened, too. The reaction gave macroscopically no evidence that a reduction of the ruthenium ions did take place. Since the metal gives enhanced contrast also in its ionic form in the TEM (like staining with uranyl acetate), it is possible that no reduction took place at all, but that the enhanced contrast arises from accumulated Ru(III) ions at the outer surface and the inner channel of the virion. Ru(III) is not easily reduced; it shows a variety of different complexes which are very stable. A reduction of Ru(III) to Ru(II) can be done e.g. with Ti^{3+}. But the bivalent state is known as good oxidant. If a reductant is used, which is too weak, Ru(III) might be reduced to Ru(II) instead of Ru(0). Ru(II) can easily on air, but also in water, be oxidized again to Ru(III) [50]. In order to obtain metal, presumably more rigorous methods need to be applied, and since work with higher pH and/or higher temperatures is not possible, the only way would be to try different reductants. Here a problem with the structural integrity arises. While mineralization of TMV with platinum, gold and silver, reduced with hydrazine, was reported, we observed in some cases partial stripping of TMV after treatment with DMAB. The observations were made with virions aged in water. Presumably our particular clone had a difference
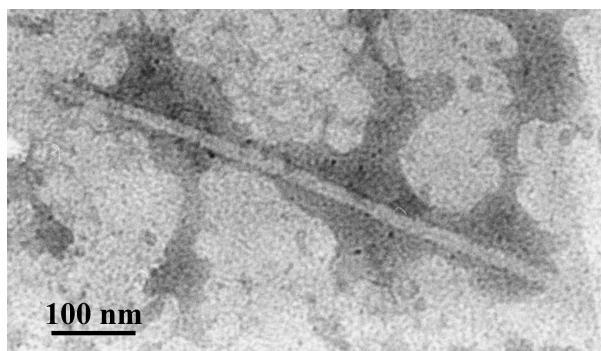
Figure 5.19: TEM (200 kV) micrograph of TMV treated with a self-activating ruthenium bath. The inner channel of the virion as well as a shading of the outer surface can be seen.

of one single amino acid in its amino acid sequence compared with the sequenced clone which remained unaffected after treatment with DMAB, but the first was never sequenced, so that the real amino acid sequence is not known. The difference of one single amino acid is unlikely the reason for a destabilization of the virion to such extent. The other destabilization possibility could arise from changes in the viral biochemistry during aging. Whether one of those facts is responsible for the instability of the virion is not yet known, but it is conceivable that small changes in the protein interactions, possibly induced by contaminations of water (e.g. with RNAses), can have enormous effects.

In the case of ruthenium deposition, future experiments will show whether different reductants like hydrazine or even borohydrides are applicable without destroying the viral integrity. If this is not possible, the shown results promise another good staining method after the virion is washed in order to remove the dark haze around it.

5.2   Summary

The summary of the obtained results is given in table 5.1. The choice of metallization bath, and thus the type of metal and the reductant, determined the metal deposition rate, i.e. the length of the metal wire, deposited in the inner channel (summarized in table 5.2), or the coverage of the outer surface of the virion with metal (summarized in table 5.3) and the size of the metal particles deposited there.

The results in chapter 5.1 show, that metallization of TMV is possible inside the inner channel as well as on the outer surface. Depending on the applied metallization

deposited metal//activation//reductant	buffer	in./out.
Ag//no//HCHO; light	yes	clusters out. (staining)
Pd//no//NaH$_2$PO$_2$	no	clusters out.
Pd//no//DMAB	no	clusters out.
Au//no//ascorbic acid	no	in. and out. (staining)
Ni//Pd(II); Pt(II)//NaH$_2$PO$_2$	no	clusters/wires in.
Ni//Pd(II); Pt(II)//DMAB	no	wires in.
Ni//Pd(II); Pt(II)//DMAB	yes	coating out.
Ni//Au(III)//DMAB	no	coating out.
Co//Pd(II); Pt(II)//NaH$_2$PO$_2$	no	no metallization
Co//Pd(II); Pt(II)//DMAB	no	wires in.
Co//Pd(II); Pt(II)//DMAB	yes	coating out.
Co//Au(III)//DMAB	no	coating out.
Ru//Pd(II); Pt(II)//NaH$_2$PO$_2$ or DMAB	no	in. and out. (staining)
Ru//no//NaH$_2$PO$_2$ or DMAB	no	in. and out. (staining)

Table 5.1: Tabular overview of the results of metallization of TMV. The applied metallization baths contained chemicals as described in chapter 4.4.2. The column "buffer" indicates, whether the virion suspension was dialyzed prior to metallization (no buffer present) or not (buffer present). The column "in./out." indicates whether the metal deposition took place inside the inner channel (in.) of the virion or at the outer surface (out.) of the virion.

procedure and the deposited metal, the metallization is selectively inside the inner channel or on the outer surface of the virion.

The electrostatic charge of the proteins of the TMV in various pH regimes as well as the coordination chemistry of the metal ions or complexes with the proteins play an essential role for a controlled metallization. Additives (e.g. buffers) can strongly influence the metallization by directing it to specific parts of the protein, and altering the deposition rate.

deposited metal//activation//reductant	met. virions [%]	length [nm]
Au//no//ascorbic acid	100	cont. (staining)
Ni//Pd(II); Pt(II)//NaH$_2$PO$_2$	40	50
Ni//Pd(II); Pt(II)//DMAB	50	600
Co//Pd(II); Pt(II)//DMAB	60	250
Ru//Pd(II); Pt(II)//NaH$_2$PO$_2$ or DMAB	100	cont. (staining)
Ru//no//NaH$_2$PO$_2$ or DMAB	no	cont. (staining)

Table 5.2: Tabular summary of the results of the metallization of the inner channel of TMV. The applied metallization baths contained chemicals as described in chapter 4.4.2. The column "met. virions [%]" indicates the max. percentage of virions containing metal inside the inner channel. The column "length [nm]" indicates the maximum length of the deposited metal along its axis. "cont. (staining)" indicates that in those cases staining was achieved, which was continuous.

deposited metal//activation//reductant	met. virions [%]	coverage [%]
Ag//no//HCHO; light	20	20 (staining)
Pd//no//NaH$_2$PO$_2$	80	90
Pd//no//DMAB	80	<5
Au//no//ascorbic acid	100	100 (staining)
Ni//Pd(II); Pt(II)//DMAB	80	100
Ni//Au(III)//DMAB	60	100
Co//Pd(II); Pt(II)//DMAB	80	100
Co//Au(III)//DMAB	60	100
Ru//Pd(II); Pt(II)//NaH$_2$PO$_2$ or DMAB	100	100 (staining)
Ru//no//NaH$_2$PO$_2$ or DMAB	100	100 (staining)

Table 5.3: Tabular summary of the results of the metallization of the outer surface of TMV. The applied metallization baths contained chemicals as described in chapter 4.4.2. The column "met. virions [%]" indicates the max. percentage of virions containing metal on the outer surface. The column "coverage [%]" indicates the approx. percentage of surface of a virion covered with metal.

Chapter 6

Adsorption of TMV

In order to structure a substrate with molecule it is important to understand which interactions of the molecule with the surface play an important role. For structuring of a surface with TMV, first it is necessary to understand which forces act between the virion and the substrate and in which way it is possible to improve those interactions. Second it is necessary to examine whether the virion shows interactions with chemicals, which need to be applied for additional technological steps like lithographic structuring. Third the structuring or ordering of TMV on substrates needs to be done in a controlled way. For this particular step soft lithography [80] appears to be the method of choice. Only the understanding of those three challenges and the ability to use results emerging from them can lead to a possible application by optimization of procedures. In this work the focus is however not set on applications but on understanding the chemical and physical processes (fundamental research).

As a basis for further tests, interactions of TMV with different substrates need to be examined. Such substrates are ideally as defined as possible to be able to generalize the bonding properties between those particular biomolecules and the substrate. As representative substrates a number of different substrates, conductive and non-conductive, technical and natural, crystalline and amorphous, were investigated. In particular mica, glass, Si wafer, graphite and gold were chosen. The latter evaporated on mica and as single crystal, bare and with a self-assembled thiol monolayer. This choice opens different aspects in bonding properties, since the substrates represent a wide variety. On the other hand investigations with different microscopy methods like atomic force microscopy (AFM) and scanning tunnelling microscopy (STM) can be done, since - apart from non-conductive substrates -, conductive substrates are employed, too. The

results are classified in relation to the bonding strength of the virion with the substrate, qualitatively measured using an AFM, which is capable of measuring in contact mode (C-AFM) as well as in non-contact mode (NC-AFM).

6.1   Results and Discussion

Before the adsorption results can be an interpreted, a closer look into the capsid protein of the virus [125] is required. First, we define an "outermost surface" made up from those amino acids, which are located at extreme distances from the inner channel of the virion. Diffraction studies show that this outermost surface consists predominantly of alkyl, hydroxyl, amide and carboxylate (C-termini) groups ($-COO^-$, $-COOH$ and $-OH$ groups on the outermost surface of the virion from the amino acids Thr-153, Thr-158, Ser-154 and Ser-155 and the water molecules bound to the protein). The surface accessible by molecules (e.g. water) is much larger and offers amines as well, but it should not have large influence in the interactions during adsorption. Therefore the focus for the major part of the interactions with the substrates can be on the above-mentioned groups. In addition one should also include water: In biology, water is the natural environment. Biomolecules are perfectly adapted to water and most of them even contain water. TMV has some water molecules tightly bound to the coat protein, and they can be detected with X-ray diffraction [37]. The water molecules can even be seen as structural part of the coat protein. Water has a huge influence on the stability of the virion and on the interaction capability of TMV with hydrophilic molecules or surfaces, since hydrogen bridges, dipole-dipole interactions or induced dipole-dipole interactions can be built [53]. The experiments have shown that TMV can be adsorbed on a variety of substrates, which are either hydrophilic or hydrophobic. The performed tests under various conditions should lead to an understanding of the bonding properties and to new possibilities to improve the interactions between TMV and a particular substrate.

The results of the adsorption experiments lead to a classification into three categories depending on the bonding strength between the virion and the substrate, namely *weak bonding*, *strong bonding* and *covalent bonding*. Indications for the bonding types can be obtained by estimation of the coverage of a substrate with virions and by application of different forces to an AFM tip. The coverage of the substrate is only in those cases an indicator for the bonding strength where kinetics do not play an essen-

tial role [81, 82, 53]. The DLVO (Derjaguin, Landau, Verwey, Overbeek) force theory describes the interaction forces of colloidal particles when they approach each other or a substrate. Most biological molecules, and thus TMV, are charged in aqueous environment, which results in a charge cloud around the particle (electrical double layer, EDL). Counter ions from solution are attracted and they balance the charge. If two charged clouds approach each other, the EDLs of both start to overlap. Depending on the electrolyte concentration this overlap can result in repulsive forces at certain intermolecular distances (larger than ca. 1 nm). In order to overcome this repulsive regime and to reach the attractive regime, the particles have to come closer than this value. During adsorption of TMV from solution the virions have to reach virion-substrate distances of less than 1 nm. If an energetic barrier in the DLVO potential is present and sufficiently large, the virions prefer to remain suspended rather than to approach the surface. In some cases this could block the adsorption of the virion, although the adsorbed state would be the energetic minimum [81, 82, 53]. Thus, the higher the coverage of a substrate, the higher is the bond strength between virion and substrate, but only in absence of kinetic effects.

For estimation of the coverage of the substrate, it is necessary to compare samples produced in the same way and to measure them with an AFM in a mode with the lowest possible tip-substrate interaction. Of course this method strongly depends on tip quality and on the interaction strengths virion-substrate and virion-tip. Since especially the tip shapes and their quality vary, those measurements have only a qualitative nature. Nevertheless, in absence of kinetic effects the density of virions on a substrate is directly connected with the bonding strength and with the number of bonding sites, with one exception: If the concentration of TMV in the used suspension is too high, the substrates can be covered with a network of virions. The interactions between virions are quite strong, and they can stabilize themselves on a substrate even in absence of strong interactions with the substrate. Here the case of overlapping charge clouds from DLVO interpretation due to increased concentration of virions is effected. The distance between the virions is close and the repulsion turns into attraction.

By application of different forces to the AFM tip, some more reliable data for the bonding strength can be obtained. On a surface on which one can easily observe virions with an AFM, the *set point* of the tip (i.e. the tip-sample interaction strength) can be varied. The set point can be increased in a controlled way, until the virus is destroyed or removed from the sample [89, 35]. In this case even quantitative data can

be obtained, but this requires an exact calibration of the apparatus and the reliability to image one single and complete virion on a substrate. In the following experiments no exact calibration of the set point has been done. In addition, due to the tip shape one can never completely rely on the width and length information obtained from an AFM measurement, since the tip convolution (see chapter 3.1.1) makes the virion always wider and longer than it actually is. For this reason our measurements are of qualitative nature.

Another important indication for the bonding strength can be obtained by measuring the height of the particles on a substrate using AFM. Since the tip-virion interaction strength differs from that between the tip and an inorganic substrate, the resulting effective heights in a measurement do not reflect the geometrical height of the particle. In this particular case, the AFM tip can penetrate the virion, since proteins are, in comparison to inorganic particles, rather soft matter. The higher the set point, the deeper can the tip penetrate into the virion and thus deform it [102]. For this reason the experiments where heights of the virion adsorbed on different substrates are compared are done with the lowest possible interaction forces. Still an exact comparison cannot be done, since the experiments were performed with different tips and on different days (small differences in temperature, humidity etc. can play a role, too). In order to keep the results comparable, the environmental conditions were controlled to some extent (e.g. air-conditioned room, controlled humidity etc.); The tips for the comparative studies were at least of the same type and manufacturer, operating at similar oscillation frequencies (in the case of NCM measurements), if they were not the same (measurements with the same tip were not always possible, since an AFM tip has a certain lifetime for reasonable measurements until the the reliability is lost due to increasing dullness of the tip). For those reasons, the obtained results are still comparable, at least if a certain error is considered, which is presumably not higher than 5%.

6.1.1   Weak bonding

A coverage of HOPG with TMV can be obtained by either covering the substrate with a droplet of TMV suspension and drying, or by covering the substrate with a virion suspension containing 40% dimethylsulfoxide (DMSO) [30, 35].

In the first case one obtains (depending on the concentration of virions in suspen-
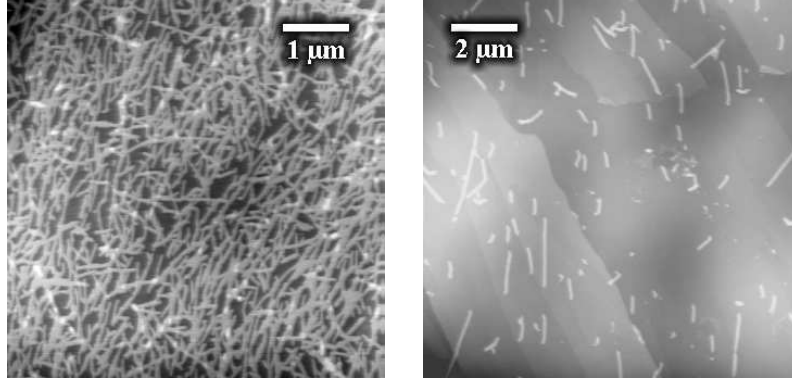
Figure 6.1: AFM (NCM) images of TMV adsorbed on HOPG (topography mode). Left: Adsorption after drying of a droplet of TMV suspension, without DMSO. Right: Adsorption from a suspension containing 40 vol.% DMSO in water.

sion) a surface covered with a large amount of virions as a network of rods, with strong interparticle interactions (see figure 6.1). In this case a measurement with an AFM even in *contact mode* (see chapter 3.1.1) is possible. Reduced virion concentration in order to avoid aggregation of particles on the substrates does not yield the expected result, since the interaction of the virions with the solvent is so strong that upon evaporation the particles concentrate in the shrinking droplet. The result is again a high coverage, but in a smaller area of the sample.

Another possibility to adsorb TMV on graphite is to add DMSO in concentrations up to 40vol.% to the suspension, in order to hinder the aggregation of TMV [30, 35]. The adsorption requires now at least 30 min. Good results are obtained after 1-2 hours adsorption time. Due to the slow adsorption process, it is important to hinder the evaporation of the solvent by keeping the substrate in a humid chamber. Afterwards the solvent can be removed by soaking a piece of filter paper or with a very weak Ar stream. Figure 6.1 (right image) shows TMV particles distributed on a graphite surface. Several lines, where bright and dark areas meet, crossing the image from the upper left to the lower right show multiatomic steps of graphite. Several linear aggregates of TMV (e.g. in the lower right of the image) can be seen, which exceed lengths of 1 μm. Such aggregation is frequently observed in all adsorption experiments. Some particles with lengths less than 300 nm (length of a single TMV) can be observed as well (upper right of the image), which arise from broken or disassembled virion particles.

This procedure yields well-distributed TMV or linear TMV aggregates on a HOPG surface with very little side-by-side aggregation. Single virions can be imaged by AFM,

but the interactions with the substrate are so weak that imaging in *contact mode* becomes impossible. Even the tip-substrate interactions in intermittent contact mode (ICM) (see chapter 3.1.1) are too strong. In this case the virions can be imaged, but a displacement, presumably induced by the tip, can occur, leading to a distorted image. Only the *non-contact mode* (see chapter 3.1.1) results in nice images of TMV deposited on the substrate. Of high importance are proper settings for the *set point* and/or *drive* to obtain useful images. The settings with low tip-substrate interactions, i.e. low *drive* and low *set point*, are preferred for obtaining undistorted images of TMV on HOPG.

The measured TMV show in these images an average height of 17 to 18 nm, which is in good agreement with the width obtained by TEM (see figure 6.2). The AFM width of the particles is by far too large; this is due to the tip convolution, which is again strongly dependent on the tip quality. Commercially available tips made of Si or Si_3N_4 nominally show a radius of curvature in the range of 10-50 nm. In our line scan a width of ca. 80 nm (full width at half maximum (FWHM)) indicates a tip convolution of about 30-35 nm, which corresponds to the values of the tip manufacturers [113]. The error in measured length of TMV induced by the tip convolution is lower due to the length-to-width ratio of the virion, while the tip convolution remains the same. The length of a single virion in such an AFM image is 370-380 nm and thus 70-80 nm too large. In the image (6.2) again multiatomic steps of graphite can be seen, crossing the image from the upper left to the lower right. The image shows a smaller scan area of the image 6.1. Linear aggregates of TMV exceeding 1 μm as well as particles shorter than 300 nm can be seen. In some cases small particles attached to a virion aggregate can be seen, which look like a bent TMV. These particles are presumably smaller protein aggregates attached to the tip and deposited at the virion during scanning. Although this particular image shows an orientation of the TMV in vertical direction, the virions are randomly oriented on the substrate, which can be seen in the overview image (figure 6.1 (left image)).

The results of the adsorption experiments on HOPG show that this particular substrate is quite difficult to employ. The interactions of the virion with the substrate are very weak, and imaging with the AFM yields only good results in *non-contact* mode.

A freshly cleaved graphite surface offers no hydrophilic chemical groups. Existing interactions can only be of hydrophobic nature, which are indeed very weak [82]. Such interactions consist mainly of van-der-Waals forces and an enhanced mobility of TMV
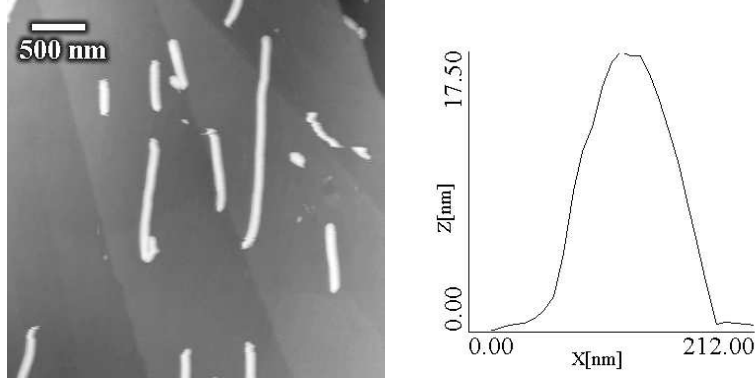
Figure 6.2: Left: AFM (NCM) image of TMV adsorbed on HOPG with 40 vol.% DMSO in water (topography mode). Right: Height profile of TMV on HOPG showing ca. 18 nm height and ca. 80 nm width (FWHM). The image shows a smaller scan area of the image 6.1.

on such substrates could be expected. Van-der-Waals forces are dispersion forces between molecules. The molecules can be polar or unpolar, but in the latter case they need to be polarizable. Interactions of such molecules can be based on dipole-dipole, dipole-induced dipole or induced induced dipole-dipole interactions (here impossible since the HOPG has an extremely small dipole moment). The van-der-Waals interaction free energy can be estimated with the Hamaker summation method [53]:

$$E_{vdW} = \frac{AL}{12\sqrt{2}D^{\frac{3}{2}}}\sqrt{R},$$ (6.1)

where L is the length of the virion (300 nm), R is the radius of the virion (9 nm), D is the contact surface of the virion with the substrate (0.3 nm^2) and A is the Hamaker constant (ca. $1.5 \cdot 10^{-19}$ J [82]). The resulting energy is $4 \cdot 10^{-17}$ J. The thermal energy can be calculated as:

$$E_T = kT,$$ (6.2)

where k is the Boltzmann constant and T is the temperature. With a temperature of 300 K the thermal energy is $4 \cdot 10^{-21}$ J, which is three orders of magnitude lower than E_{vdW}. The van-der-Waals free energy is high enough to overcome the thermal energy at room temperatures and thus adsorption of TMV on graphite is expected in this model when kinetic effects are absent (DLVO barrier). But AFM imaging of TMV adsorbed on HOPG is difficult. Imaging has to be done with lowest possible tip-virion interactions in order to obtain reasonable images.

The difficulties in imaging of the virion with higher *set points* can be explained with stronger interactions of the virion with the tip than with graphite. An AFM tip usually consists of Si or Si_3N_4. Storage in ambient conditions can oxidize the terminal surface, yielding a hydrophilic surface of the tip [121]. Hydrophilic interactions are stronger than dispersion forces. The kinetics in this case are of no importance, since the tip moves towards the virion and the (sometimes) repulsive double-layer force (i.e. the force resulting from the approaching charged surfaces when their charge clouds begin to overlap) is overcome by the forced approach of the tip to the virion [82, 53]. The hydrophilic interaction forces of the tip and the virion are stronger than the van-der-Waals forces and may result in detachment of the virion, induced by the AFM tip. The strength of those forces depends on the tip-virion distance. The lower the *set-point*, i.e. the larger the tip-virion distance, the weaker are the hydrophilic interactions. The distance between tip and virion can be controlled by optimizing the scanning parameters. In *contact mode* imaging the tip is in permanent contact with the substrate and thus with the adsorbed virion, resulting in strong interaction forces between tip and virion.

But also the lateral forces acting on the virion are important [35]. A very rough estimate of the surface diffusion barrier of TMV, which provides "protection" against lateral forces, is several 10 % of E_{vdW} (this is still well above E_T, so no surface diffusion should be observed) [7]. Since the AFM tip in *contact mode* does not oscillate as in *non-contact mode* (see chapter 3.1.1), but is in permanent contact with the substrate, lateral forces, induced by the tip, act on the virion, whenever the tip encounters a virion. This leads to enhanced mobility of the virion (vertical forces acting on the virion, e.g. by the AFM tip in *non-contact mode* or *intermittent contact mode*, do not enhance the lateral mobility of the virion). Virions are moved out of the scanning area or simply remain stuck to the tip. In such cases the result is an image of an apparently uncovered graphite surface. In *non-contact mode* AFM the tip is not in permanent contact with the substrate. Due to the oscillation of the cantilever, the tip-virion distance varies and the interaction time at the point with the closest distance is only microseconds. However, the critical tip-substrate distance for developing interactions is not only limited to the closest distance (lower turning point of the cantilever oscillation), but also shortly before and after, depending on the nature of interactions (e.g. long-range interactions like dipole-dipole interactions; see also chapter 3.1.1. Therefore it is necessary not only to image in *non-contact mode*, but also to increase the nominal distance of tip

and substrate by choosing a low *set point* and decreasing the oscillation amplitude by applying a low *drive*. Such settings lead to lowest possible interactions of the tip and the virion and thus to imaging of TMV adsorbed on graphite (see figure 6.1 and 6.2).

In such images the virion shows heights that are comparable with the diameters obtained from TEM images. A TEM grid has properties similar to graphite, since its surface consists of evaporated carbon. Adsorption of TMV on a TEM grid requires a coverage of the grid with a thin layer of ethanol in advance. The interaction forces of the virion and a TEM grid are indeed rather weak. Similar to graphite, tests with imaging of TMV on a TEM grid yielded only results with *non-contact mode* AFM. Due to weak interactions with the substrate, the morphology of the virion should be preserved. Indeed the diameter of a TMV is in all publications declared as 18 nm, which corresponds to the results from TEM and X-ray diffraction studies [37, 126, 68]. The undistorted shape of the virion, evident from the correct height in the AFM image, confirms the weak interaction with the substrate. There is no driving force for deformation of the virion in order to enhance the interaction with this particular substrate.

The tendency of the particles towards aggregation on the substrate (see figure 6.2) can again be assigned to the weak interactions with the substrate. The intermolecular interactions are larger than the interactions with the substrate. A possibility for the virions to diffuse (e.g. in water during the adsorption process) may lead to aggregation already in the water droplet, since there are no interaction forces that are strong enough to act instantaneously on the particle and fix it to the substrate. The repulsive energy barrier is too high [81]. The use of DMSO in low concentrations offers the possibility for adsorption of TMV on graphite [30, 35]. Presumably the aggregation of the particles is hindered by attachment of DMSO molecules to the outer surface of the virion with their oxygen atoms pointing towards hydrophilic groups of the coat protein, and the methylene groups pointing away from the surface of the virion, resulting in lower interaction forces between the particles. The interactions of TMV with HOPG are in this case enhanced, since the accessible hydrophilic groups of the viral outer surface are shielded by DMSO and the number of hydrophobic groups on the outer surface becomes larger due to the methylene groups. The overlap of the EDLs becomes easier (see chapter 6.1) [81].

Generally one could say, that the interactions of TMV with a hydrophobic substrate are very weak and the adsorption of TMV on such substrates is not simple. Microscopy

becomes difficult, even in *non-contact mode* AFM. A characterization of the bonding type with AFM is only possible if DMSO is added to the virion suspension, which should alter the virion to some extent since DMSO obviously interferes with the chemistry of the virion [86, 30].

6.1.2   Hydrophilic bonding

Stronger bonding of TMV with a substrate is obtained with substrates which contain hydrophilic groups [81, 118, 117]. As representatives of such substrates mica, glass, silicon wafer (with natural oxide termination) and gold (covered by a thin water layer from laboratory air) surfaces were used.

Adsorption of TMV on mica was achieved after pretreatment of the substrate with $MgCl_2$ solution for 5-15 min. and adsorption of the virions from a suspension [81]. The adsorption time was 15 min., resulting in a high coverage with TMV and good dispersion of the virion at the substrate. In some cases aggregation was observed, but not in extended areas, if the concentration of TMV was kept around 0.1 mg/ml. Imaging was possible in both *contact mode* and *non-contact mode*. The imaged virion particles show heights of 10-14 nm, independent of the measuring method (see figure 6.3). Similar to the images on graphite, linear aggregates in the μm range and particles smaller than 300 nm can be observed. Several virions with correct lengths (300-400 nm) can be observed in the image (e.g. near the scale bar).

Adsorption of TMV on mica was also tried with acidic TMV suspension (pH 3, adjusted with HCl) on a freshly cleaved mica surface, which was not pretreated with $MgCl_2$. The adsorption time was 10 min. Imaging in *contact mode* was possible. The virions on images both in *contact mode* and *non-contact mode* appear distorted, which is an indication for a starting decomposition of TMV due to the treatment with acids. In such images the TMV shows several protrusions along its axis, with height differences of 3-4 nm. The width of the virion differs in the single line scans, which indicates attachment of loose particles (e.g. protein aggregates) to the tip, which are deposited again next to the virion [127].

Adsorption of TMV on a glass surface did not require a pretreatment with $MgCl_2$. The adsorption time was only few minutes of from a neutral TMV suspension with a concentration of 0.1 mg/ml. The coverage of the glass surface appeared similar to the coverage of the $MgCl_2$-pretreated mica surface. As on mica, imaging was possible in
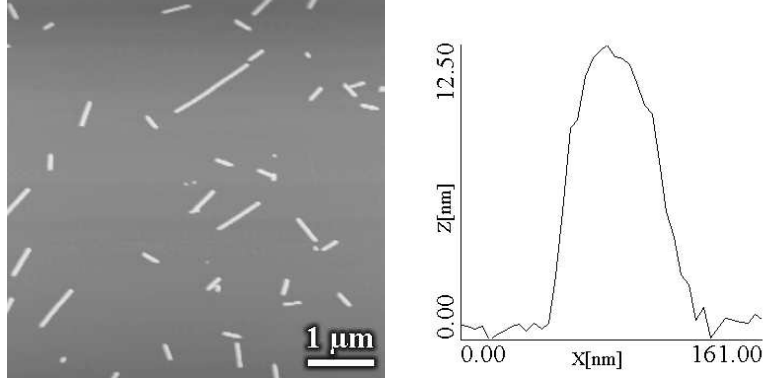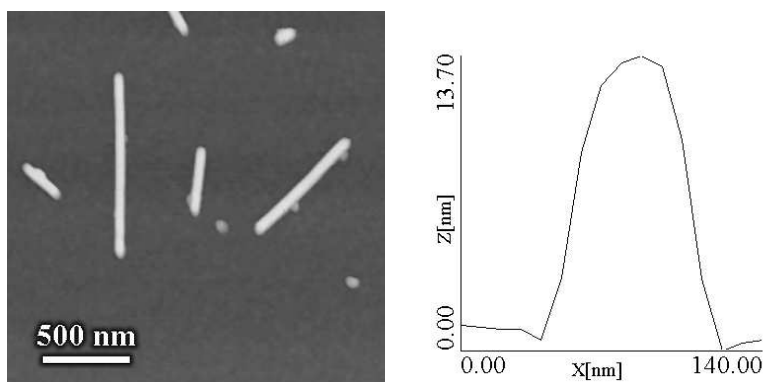
Figure 6.3: Left: AFM (NCM) image of TMV adsorbed on Mg(II)-pretreated mica (topography mode). Right: Height profile of TMV on mica showing ca. 13 nm height and ca. 80 nm width (FWHM).
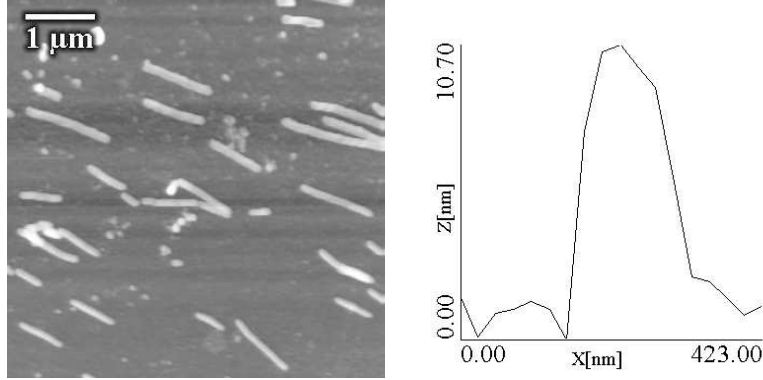
Figure 6.4: Left: AFM (NCM) image of TMV adsorbed on glass (topography mode). Right: Height profile of TMV on glass showing ca. 11 nm height and ca. 120 nm width (FWHM).

both *contact mode* and *non-contact mode*. A pretreatment of the substrate with $MgCl_2$ had no influence on the coverage of the substrate with the virions. The measured height of the virions was 10-14 nm and was the same on glass, both pretreated and not pretreated with $MgCl_2$ (see figure 6.4). In the image several linear aggregates of TMV as well as small particles can be seen. The latter are presumably protein aggregates and broken or disassembled virions. The orientation of the virions in this case is random, although this particular image shows some ordering. In several experiments this ordering could not be reproduced.

A similar behaviour of the particles could be found on silicon wafers. Here again adsorption was possible both with and without pretreatment of the substrate with

Figure 6.5: Left: AFM (NCM) image of TMV adsorbed on silicon wafer (topography mode). Right: Height profile of TMV on silicon wafer showing ca. 14 nm height and ca. 70 nm width (FWHM).

$MgCl_2$. A pretreatment of the substrate with $MgCl_2$ yielded a slightly higher coverage of the substrate with virions. The average height was again 10-14 nm and imaging was possible in *contact mode* AFM (see figure 6.5). In the image linear aggregates of TMV and smaller particles (protein aggregates and decomposed parts of TMV) can be seen. The virion in the centre of the image is a single TMV, since the length (360 nm) fits to the length of a single TMV with additional length contributed by the tip convolution. TMV adsorbed on a $MgCl_2$-pretreated substrate did not show differences in height and shape in the AFM micrographs.

As a representative of conductive substrates, adsorption studies on gold (111) surfaces were done both on a single crystal and on gold evaporated on mica [71]. Adsorption was performed from an acidic suspension of TMV, adjusted with $HClO_4$ to the pH values 1.1, 2.5, 4.0 and 4.4. Treatment with a variety of organic and mineral acids (acetic acid, sulphuric acid and hydrochloric acid) instead of perchloric acid yielded identical results. For the sake of completeness, adsorption was tried from a neutral suspension (pH 6.8) and a basic suspension (pH 8.8, adjusted with NaOH). The adsorption time was 10 min. AFM imaging was performed in *contact mode*. The images show that adsorption of TMV on gold was possible in a pH range between 2.5 and 4.0. From more acidic (pH 1.1) or more basic (pH 4.4, 6.8, 8.8) suspensions no adsorption was observed (see figure 6.6). The images show in most cases bright spots, which exceed the height of the virions. Those spots are partially due to large gold grains, which grow during evaporation of gold onto mica [71]. Some of the spots are
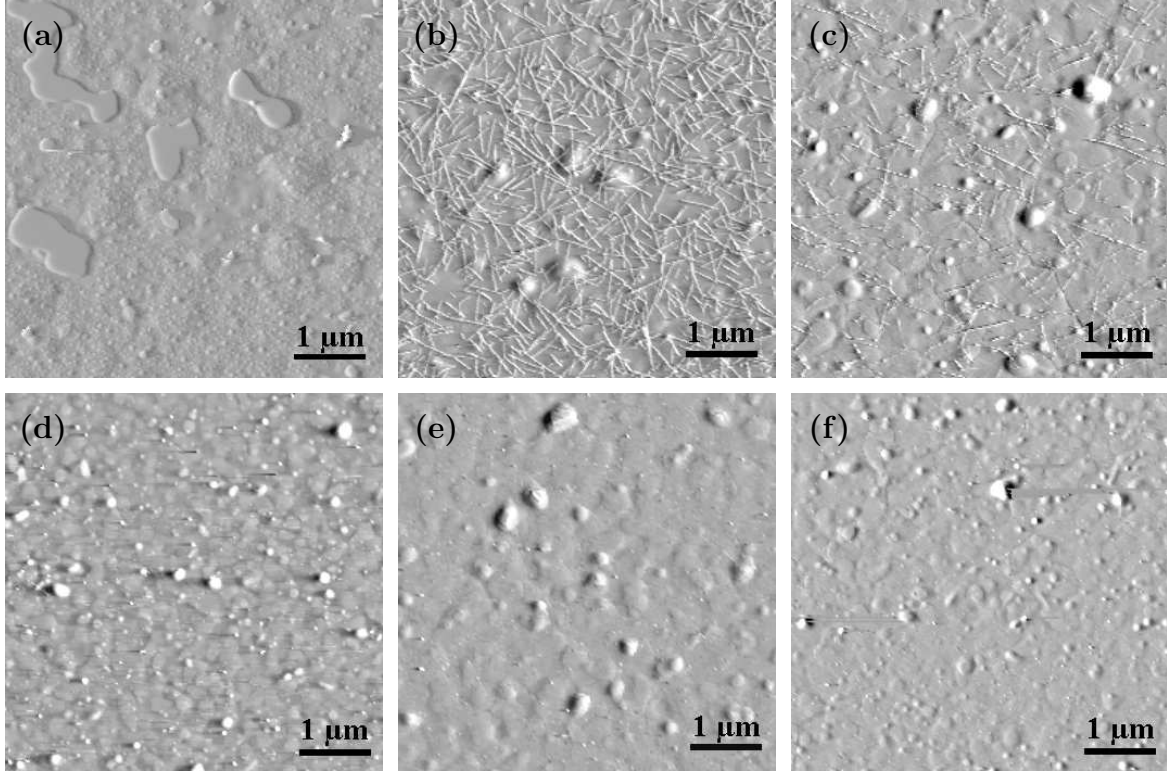
Figure 6.6: AFM (C-AFM) images of adsorption studies of TMV on gold at different pH values (error mode). (a): TMV with $HClO_4$ adjusted to pH 1.1. (b) TMV with $HClO_4$ adjusted to pH 2.45. (c) TMV with $HClO_4$ adjusted to pH 4.0. (d) TMV with $HClO_4$ adjusted to pH 4.36. (e) TMV in water with pH 6.8. (f) TMV with NaOH adjusted to pH 8.8. The bright spots in the images are due to dust deposited from laboratory air and gold grains from the gold deposition procedure [71].

due to dust deposited from laboratory air. *Contact mode* AFM scans were performed on such substrates, followed by *non-contact mode* scans of the same area and adjacent areas. The images showed that some of those bright particles could be moved by the tip in *contact mode* (dust particles). They were moved to the borders of the scanned area. Other particles could not be moved (gold grains). None of those particles or grains could be removed by rinsing with solvents (ethanol, methanol, toluene, acetone etc.) or by flame annealing prior to adsorption of TMV.

The results show that stronger bonding is achieved after adsorption of TMV on mica, glass, silicon wafer and gold surfaces. Here we can differentiate between adsorption resulting from electrostatic interactions and adsorption resulting from hy-

drophilic interactions [82, 53]. The electrostatic interactions are Coulomb interactions between charged molecules or ions. Hydrophilic interactions are based on the polarity of molecules. Such hydrophilic molecules tend to contact water molecules; however, the molecules repel each other. The tendency to displace water molecules defines the strength of the hydrophilic interactions.

In order to adsorb TMV on mica at neutral pH values it is necessary to pretreat the surface with Mg(II) [81, 118, 117, 35]. The same procedure is possible with silicon wafer and glass, too, but it is not necessary. The number of OH groups on a mica surface is compared to glass and silicon wafer surfaces (after standard RCA treatment, see chapter 4.2.2) low. The interactions in the case of mica can be, at least to a certain extent, assigned to the charge of Mg(II) [81]. The solution species $[Mg(H_2O)_6]^{2+}$ can form complexes at the surface, presumably with the hydroxyl termini of the mica surface. Water molecules, forming the remaining half shell of ligands of the cation, can now easily be substituted with the hydroxyl and carboxylate groups on the outer surface or even with the water molecules tightly bound to the coat protein of the virion [125]. In this case a kind of salt bridge between the virion and the mica, silicon or glass surface is built. Here electrostatic interactions are proposed, since Mg(II) can replace K(I) or Na(I) on the surface (in particular mica) and charge the surface positively (freshly cleaved mica surfaces show negative surplus charge) [81]. Since the pI of TMV is around 3.5 [126], in neutral conditions TMV is negatively charged (at least to a certain extent) due to deprotonation of the protein. However, there are some factors which are not considered in this scenario. First, the Mg(II) is added as $MgCl_2$ to the substrate. This solution contains the counterions (Cl^-), which of course influence the surface charge of the substrate. The surplus charge on the surface is not very likely. Cl^- cannot attach to the mica surface due to the negative charge of the mica surface, but it can build ion pairs with Mg(II). Second, the Mg(II) on the surface is not available as Mg^{2+}, but as the corresponding aquo- and hydroxo-complexes [50]. The ligand sphere and counter ions in water shield the charge of the cation and thus decrease the electrostatic attraction on objects approaching from solution. More likely is however that a part of the ligand sphere of the Mg(II) is replaced by the previously mentioned groups of the viral coat protein. Hence the interactions have an ion-dipole character. In addition, hydrogen bridges between the hydrophilic groups on the outer surface of the virion (and the water molecules bound to the protein) and hydrophilic groups on the mica surface (in particular water, which is always present as a thin film)

can increase in number, thereby increasing the bonding strength of the virion with the substrate. The interaction forces are compared to those of the virion with HOPG very strong, which is obvious from the resulting AFM images.

As a first result, it becomes possible to image the virions in *contact mode* AFM. Here the interaction forces between the AFM tip and the virion are higher than in *non-contact mode* AFM (as described in the previous chapter). Although AFM was performed in *contact mode*, no movement of the particles was visible during the scans. Another indication for higher interaction forces of the virion with the substrate is the lower height, measured with AFM. While on HOPG the height of the virion fits very well to the height obtained from TEM, AFM imaging with similar conditions in this case results in lower heights of the virions (10-15 nm) (see figure 6.3). This can be assigned to a deformation of the virion. Since TMV consists of proteins which are up to a certain degree flexible [10], the tube, which under regular conditions has a circular cross-section, can be flattened in order to present more interaction sites with the substrate. Several other factors might also contribute to the difference in measured height to the expected value of 18 nm. Additionally, the AFM tip can penetrate the virion [102], since the matter is very soft. This depends on the forces and thus on the *set point*. Since the conditions were similar to those used for imaging TMV on HOPG, and the virion showed the correct height in this case (see figure 6.2), it is unlikely that this particular contribution is very high.

However, there is another important point that cannot be neglected. The substrates were in several steps of the experiment contacted with aqueous solutions. Even without those steps, the substrates would be covered with a thin film of water molecules from laboratory air, which is not removable, at least not in ambient conditions [27]. Depending on the type of substrate (hydrophilic or hydrophobic) this film can reach several monolayers. On a freshly cleaved mica surface, or on the corresponding silicon wafer or glass surfaces, especially after treatment with water, this film can reach 1 nm (depending on the humidity of the environment). The forces acting here on an AFM tip are different from those on a graphite surface (which is hydrophobic). Capillary forces act between the hydrophilic AFM tip and the substrate [113, 27]. Such interactions artificially modify the height information of an AFM scan. This leads to even lower heights of the virions. The contribution of those capillary forces is difficult to estimate, since it depends on several factors, like the hydrophilicity of the tip, the humidity of the environment, the tip-substrate distance and the frequency of the oscillation (if

measured in *non-contact mode*). Still one should be aware that the capillary forces are contributing to the height information.

In our case all of those problems surely occur. Most probably there is a small contribution of all three effects, resulting in the height difference of 3-8 nm as compared to the measurements on graphite.

An adsorption of TMV on mica without pretreatment of the surface with Mg(II), but from an acidic virion suspension, yielded adsorbed virions as well. Since the incubation of TMV in an acidic solution for long times (more than 10 min.) destroys the virions [20, 24], the shape of the adsorbed virions in the images is already distorted (see figure 6.3). The fact that TMV can be adsorbed (although partially destroyed) can be assigned to the protonation grade of the outer surface of the virion. Especially the carboxylate termini of the coat protein play an important role. Below the isoelectric point (pI) most of them are protonated and thus offer the capability for hydrogen bridging with oxygen (from Si-O and Si-O-Si groups) on the surface of mica and with the water film on top of it (with partial replacement of water molecules).

Similar results are obtained by adsorption of TMV on glass (see figure 6.4) and silicon wafer surfaces (see figure 6.5) without pretreatment with $MgCl_2$. The substrates offer sufficient accessible hydroxyl groups and are capable for hydrogen bridging with the $-COO^-$, -COOH and -OH groups on the outermost surface of the virion (from the amino acids Thr-153, Thr-158, Ser-154 and Ser-155 and the water molecules bound to the protein) [121, 81, 50]. The measured particles show a lower height than expected from TEM measurements, which can again be assigned, like in the case of mica, to a strong interaction of TMV with the substrate. In contrast to mica in this case the interactions are exclusively based on the interactions of the hydrophilic groups of the virion and the substrate, since no additional bivalent cations are offered. The affinity of the natural oxide on the silicon surface to the accessible groups on the outer virion surface is strong enough to bind the particle tightly to the substrate. The fact that the coverage is slightly increased after $MgCl_2$ pretreatment indicates that additional binding sites on the substrate can be produced using bivalent cations. Since no difference in the height and shape of adsorbed TMV is visible, an assumption could be that the two adsorption possibilities (with and without Mg(II)) result in similar interaction strengths with the substrate and in a similar thickness of the water film covering the substrate.

Adsorption on gold, apart from using thiol monolayers (see next chapter), can be

achieved from an acidic suspension of TMV. The bonding of the virion with the substrate can be described as a replacement of water molecules on top of the gold surface with terminal carboxylic acids (protonated carboxylates at low pH values) or hydroxyl groups of the proteins which is in analogy to the adsorption of uncharged molecules on a gold surface [46]. A deprotonated TMV particle can presumably not adsorb on a gold surface, since only those anions can adsorb, which can be fully or partially discharged on the gold surface. This is reflected in the adsorption experiments at slightly decreased pH values (see figure 6.6). Adsorption already takes place at pH 4, but the number of adsorbed virions is low and the bonding is not very strong, as seen from the poor resolution of the images. Here kinetic and thermodynamic effects play a role [53, 81]. In this pH regime the partial protonation of the virion enables the approach of some virions to the surface. The energetic barrier is small enough for the virions to overcome the repulsive regime (if present). But the bonding strength between substrate and virion is not very high. Presumably the number of protonated carboxylates is not high enough to develop enough bonding sites with the substrate. Increasing acidity enhances the bonding strength, because additional protonated carboxylates are now accessible for interaction with the gold surface, resulting in an increased stability as seen in the AFM image. Further decrease of pH yields again gold surfaces without adsorbed virions, due to destruction of the virion at such low pH values [20, 24].

6.1.3   Covalent bonding

To obtain covalent bonding of the virion, an Au (111) surface was first covered with a self-assembled monolayer (SAM) of 16-mercapto-hexadecanoic acid (HS-$(CH_2)_{15}$-COOH) [117]. The monolayers were treated with $SOCl_2$ gas (see 4.2.2) [31, 6] and afterwards with a TMV suspension in a (dry) Ar environment, resulting in a substrate covered with virions. The adsorption time was 5-10 min. Imaging with AFM was possible in *non-contact* mode as well as in *contact mode* without differences (see figure 6.7).

In addition, ester bonding was obtained by an acid-catalyzed esterification. In this case an acidic (pH 3-5) TMV suspension was placed on top of a SAM- (HS-$(CH_2)_{15}$-COOH) covered gold surface and kept there for several hours, yielding a similar distribution of the coverage of the substrate (see figure 6.7). The obtained particles show heights of 10-14 nm.
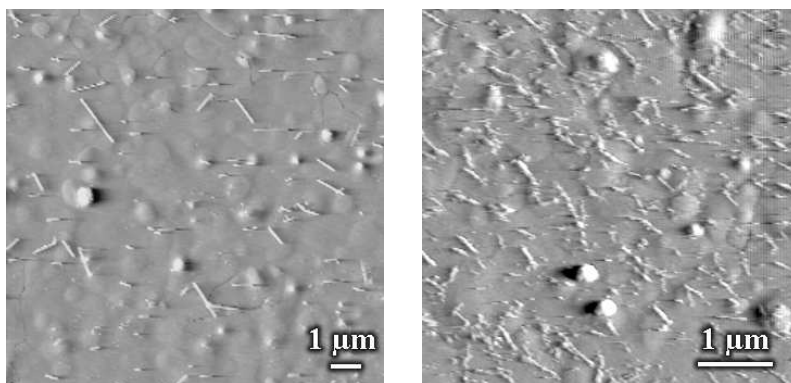
Figure 6.7: Left: AFM (C-AFM) image of TMV adsorbed on gold (error mode) after activation of the monolayer with $SOCl_2$ [31, 6]. Right: AFM (C-AFM) image of TMV adsorbed on gold (error mode) after acid-catalyzed esterification. The bright spots on the surfaces are due to dust deposited from laboratory air and gold grains from the evaporation of gold onto mica.

An esterification is well known from organic chemistry and can easily be achieved, either via the reaction of an alcoholic functional group with an acyl chloride, which is the faster way, or via an equilibrium reaction of a carboxylic functional group with an alcoholic functional group catalyzed by acid or base, which is the slower way. Both ways yield the same results, namely adsorbed TMV on a gold surface covered by a thiolate with an acyl chloride end group. In the case of the acid-catalyzed esterification, the images showed partially destroyed virions (see figure 6.7, right image), which is a result of the immersion of TMV in acidic solvents for a long time, so the reaction via the acyl chloride [31, 6] was preferred in the experiments. A direct proof for the esterification could not be obtained, since infrared or Raman spectroscopy on a surface with such small number of ester molecules is difficult to perform. However, an indirect proof could be obtained. From neutral virion suspensions no virions were attached to the monolayer, even after several hours immersion time. The esterification requires an acid to shift the equilibrium towards the ester, which is a slow reaction. Indeed the adsorption from acidic solution required several hours.

Adsorption of TMV on gold in absence of the monolayer was faster. This indicates that the monolayer is not removed from the gold surface. The esterification was very fast if the carboxylic acid was treated with $SOCl_2$ prior to the esterification. The employed alkanethiol (16-mercapto-hexadecanoic acid) offers a terminal carboxylic functional group which is capable for an esterification. After treatment with thionyl

chloride, which reacts with the carboxylic functional group to the corresponding acyl chloride, the surface was covered with an aqueous suspension of TMV. The reaction of the acyl chloride terminal group of the monolayer on gold with the alcoholic functional groups of the coat protein surely competes with a reaction of water molecules with the carboxylic group, which can react with the acyl chloride back to the carboxylic acid. Still the the number of built covalent bondings is high enough to bind the whole virion tightly to the monolayer. AFM becomes easily possible in *contact mode* AFM (see figure 6.7). With weaker bonding strength or only few covalent bonding sites, one would expect the virion to be removed from the substrate upon applying higher *set points*. Experiments with increasing forces show that this is not the case. The number of covalent bondings is sufficiently high and they are distributed over the whole contact area of virion and gold surface, hence movement of either a part of the virion or the whole virion is impossible.

The bonding strength of the virions adsorbed via $SOCl_2$ was examined by increasing the force between tip and substrate during a scan until destruction of the virions. At set point values of 30 nN (nominal value of the apparatus, not calibrated) the images showed a degradation of the virion. Additional features in the slow scan direction, i.e. "scan up" or "scan down" (whereas the fast scan directions were "left-right" and "right-left"), appeared close to the virion. Increased set point values showed continuing degradation until a value of ca. 50 nN, where no traces of the virion could be found. The disappearance of the virion was proven by decreasing the set point to the initial value and scanning the same region, which did not change the image any further (see figure 6.8). The test was done several times with similar results.

The images show that upon increasing the *set point* the structural breakdown of the virion is preferred rather than breaking all of the ester bonds with the thiolate (see figure 6.8). The result is a stepwise decomposition of the virion, i.e. cutting off proteins or even bundles of proteins from the top part of the virion, until no trace is left. The last image, where the *set point* is reset to the initial value, shows that the virion indeed disappeared and that the disappearance is not an effect of the tip scanning the gold surface by penetrating the TMV completely at increased forces.

Since gold surfaces are conductive, scanning tunnelling microscopy (STM) of adsorbed TMV on gold was tried. The same samples as above were used. At ambient conditions (20-25°C, <40% rel. humidity, 1 atm.) the virion particles on the gold surface could not be imaged. The substrate appeared to be a pure Au (111) surface.
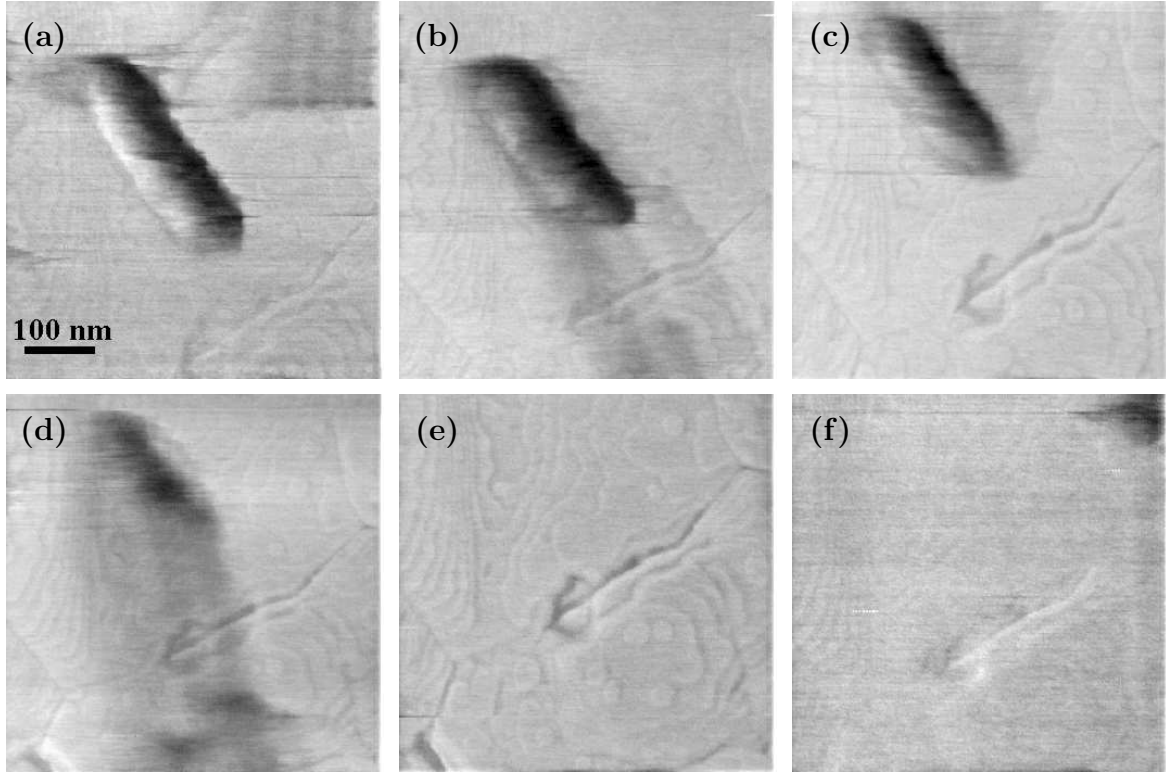
Figure 6.8: AFM (C-AFM) images of examination of bonding strength of TMV adsorbed on gold (lateral force mode). (a) through (e) Increasing *set point* (10, 30, 50, 80, 100 nN) leads to continuous removal of TMV from the gold surface (f) Resetting of the *set point* to the initial value (10 nN) proves that there are no remains of the virion. Step edges of the Au single crystal are visible as dark lines especially in the lower right part. All images show a linear defect extending from the middle to the middle right part. The substrate is not imaged at exactly the same spot, hence all features shift slightly from image to image.
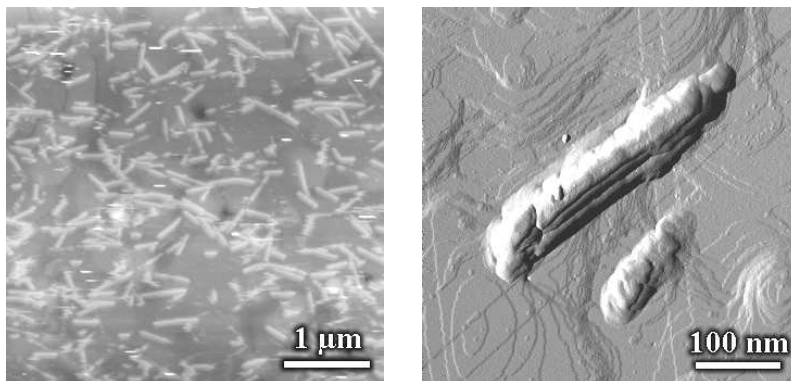
Figure 6.9: Left: STM image of TMV covalently adsorbed on gold. Right: STM image (derivative in x-direction) of TMV covalently adsorbed on gold. The gold below the virion shows terraces with monoatomic heights (thin bright or dark lines) of the Au (111) surface with correct step heights (0.24 nm). Tunnelling tip parameters were in both cases -0.3 V and 100 pA.

Increased humidity (40% and more) resulted in virion particles in the image, but the resolution was poor. Resulting heights of the virion in the line scan showed 10 nm and less, and no details of the virion could be seen. Reduction of tunnelling parameters down to 1.4 pA at 10 V (tunnelling impedance $7 \cdot 10^{12}$ Ω) did not improve the results. *In-situ* STM imaging of TMV on gold, i.e. scanning of a substrate covered with an electrolyte (in this particular case water or diluted $HClO_4$ at pH 4) yielded images with higher resolution than in humid air, but the reproducibility was poor and no significant additional data about the structure of the virion could be obtained (see figure 6.9).

Several approaches have already been tested in order to obtain STM images of TMV. Apart from the approaches where metal was deposited on top of TMV [52, 74, 108], Guckenberger *et.al.* have shown that STM imaging is possible with native TMV as well [45, 48]. A special technique was used for this purpose, the so-called hydration STM, where the mica surface is made conductive by water from a humid environment. For adsorbed TMV on gold, no increased humidity is needed in order to make the substrate conductive, but the adsorbed virions cannot be imaged if the humidity is less than 40%. Water molecules from the humid air induce a certain conductivity, but whether this conductivity is an effect of ions in or on the virion or of the charged nature of the particle itself, is not clear. Although imaging of TMV in humid air is possible, the images have a poor resolution and can only testify that virions are indeed present on the surface (see figure 6.9).

6.1.4   Solvent Effects

The resistance of the virion against various, especially organic solvents was apparently not investigated before this thesis. However, some hints can be found in the literature. It is well known that TMV precipitates from ethanol [126] and that DMSO in concentrations of up to 40% in water can be used to disassemble TMV on graphite surfaces [30, 35], while concentrations of 80% DMSO can be used for partial and complete stripping of the coat proteins from the RNA [86].

We focussed on that particular question, because the behaviour of TMV in contact with different solvents might be very important from the technological point of view. As an example N-methylpyrrolidone and acetone were used in the lift-off technique for removal of polymer resists from carbon nanotubes. This was necessary in order to expose tubes as well as contact wires, thus enabling electron transport measurements. Before a contacting of TMV can be done, it is necessary to know whether TMV is resistant against the chemicals which should be used.

In order to examine the resistance of TMV against the most common solvents, adsorbed virions on either mica or silicon wafer surfaces were treated with a variety of organic solvents. The experiments were done by AFM: Images of the virions before and after treatment with the solvent were compared. The tested solvents were acetone, alcohols (methanol, ethanol and isopropanol), N-methylpyrrolidone, which is used for the so-called *lift-off* technique (which is useful for lithographical production of electric contacts to nanoobjects), dimethylsulfoxide (DMSO), tetrahydrofurane (THF) and toluene. Since the experiments are performed with an AFM, only substantial changes, effecting the structure of the virion (towards loss of structural integrity), could be seen. Changes on the molecular level, which should not always lead to structural decomposition of TMV, could not be examined. Therefore, even if the virion remained unchanged after the treatment, the solvent might have affected the chemistry of the virion.

An important solvent which kept TMV unaffected even after long time immersion is acetone. After 3 h immersion in pure acetone the images before and after treatment are comparable. Substantial changes in coverage of the substrate and shape of the virions were not observed (see figure 6.10). In both images (left and right) μm long linear aggregates of virions and small (less than 100 nm long) particles (broken or decomposed parts of TMV) can be seen. The right image appears a little "fuzzy". The slight loss in resolution is due to small particles (proteins or protein aggregates), which
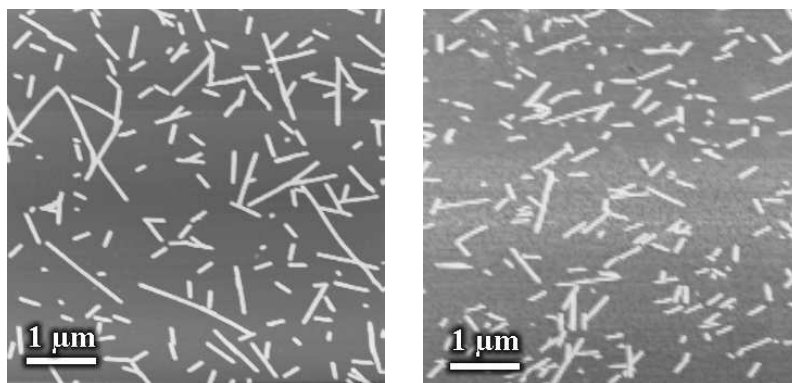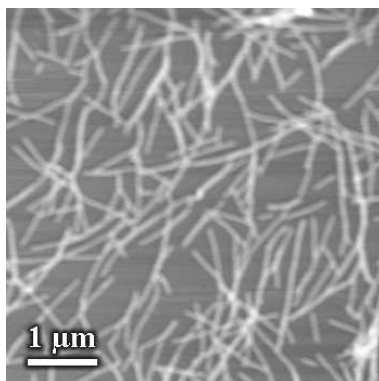
Figure 6.10: Left: AFM (NCM) image of TMV adsorbed on a silicon wafer prior to incubation with acetone (topography mode). Right: AFM (NCM) image of TMV adsorbed on a silicon wafer after incubation with acetone for 3 h (topography mode).

in this particular case were collected from the substrate by the tip.

Methanol, ethanol and isopropanol in high concentrations ($> 99\%$) did not change the appearance of TMV attached to the substrate either. Since those alcohols are most commonly used for nanoscale structuring processes, no other alcohols were tried. The immersion time was 10 min.

Immersion in N-methylpyrrolidone for 10 min. did not result in structural changes (length, width) and number of the adsorbed virions on the substrate (see figure 6.11). In contrast, treatment of adsorbed virions with DMSO showed changes in length and number of adsorbed virions when the concentration in suspension reached 80 vol.% in water. The adsorbed virions became shorter and distorted and the number of adsorbed virions decreased. The heights of the remains did not exceed 2-3 nm and the widths became much larger (100-200 nm). Other concentrations of DMSO were tried; with 60 vol.% of no considerable changes could be observed (see figure 6.12).

Tetrahydrofurane (THF) showed similar behaviour: With concentrations of up to 10 vol.% in water no considerable changes in length and number of attached virions were observed. Increasing concentration of THF lead to decreasing stability of TMV. Imaging with AFM became difficult in *contact mode*, and even in *non-contact mode* images yielded poor resolution. Apparently, remains of the virion particles attached easily to the tip, distorting the image (see figure 6.13). The virions showed decreased heights (4-6 nm) and increased widths (100-150 nm) after treatment with 10 vol.% THF. After treatment with 30 vol.% THF no TMV could be observed any more. A

Figure 6.11: AFM (NCM) image of TMV adsorbed on a silicon after incubation with n-methyl-pyrrolidone (topography mode).
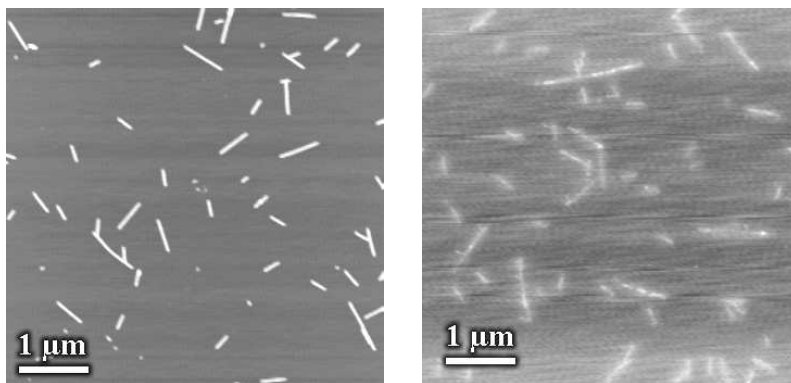
Figure 6.12: Left: AFM (NCM) image of TMV adsorbed on a silicon wafer after incubation with 60 vol.% DMSO in water for 10 min. (topography mode). Right: AFM (NCM) image of TMV adsorbed on a silicon wafer after incubation with 80 vol.% DMSO in water for 10 min. (topography mode).
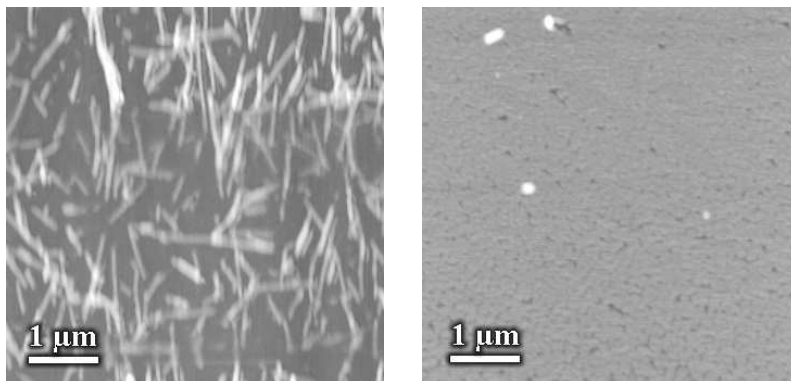
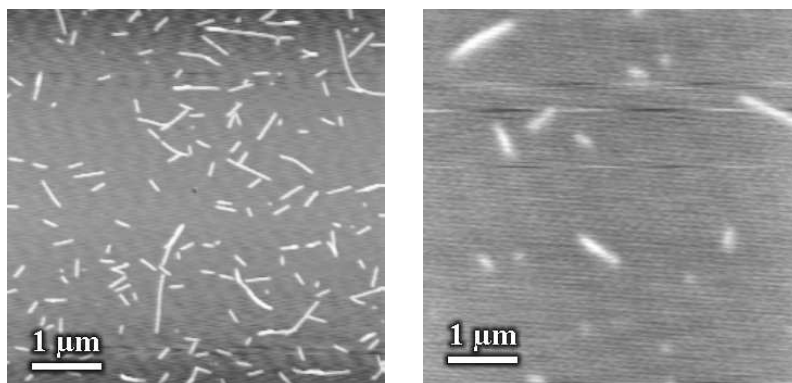**Figure 6.13:** Left: AFM (NCM) image of TMV adsorbed on a silicon wafer after incubation with 10% THF in water for 10 min. (topography mode). Right: AFM (NCM) image of TMV adsorbed on a silicon wafer after incubation with 30% THF in water for 10 min. (topography mode).

few particles on the silicon wafer (5-20 nm) are presumably due to some remaining protein aggregates, but they differ from TMV in length, width and height and they thus cannot be assigned to TMV particles.

As representative of an unpolar solvent toluene was selected. Since the solubility of toluene in water is very low (< 0.3 vol.%), no tests with different concentrations of toluene were done. Pure toluene was used instead. The results showed that toluene is destructive for the structural integrity of the virion. Some remaining features, reminding of virions, could be observed after 10 min. immersion with toluene, but the lengths and especially the heights show drastic changes as compared with the native virion (see figure 6.14). The remains of the virions showed heights of 2-4 nm. The widths were 100-200 nm.

The results have shown that for this particular case TMV is indeed resistant against the chemicals required for the lift-off technique, namely acetone and N-methylpyrrolidone. In addition the results show that most commonly used polar solvents can be used with TMV, at least in certain concentrations in water. Especially alcohols seem not to affect the virion, at least not short chain alcohols. THF as a slightly less polar solvent can be used with TMV, but only in smaller concentration in water (see figure 6.13), while toluene as unpolar solvent destroys the virion (see figure 6.14). This suggests that only solvents which are miscible with water are compatible with TMV. From X-ray diffraction studies it is known that the viral coat protein contains some tightly bound water molecules [125]. The water molecules together with the Ca^{2+} ions, situated deep

Figure 6.14: Left: AFM (NCM) image of TMV adsorbed on a silicon wafer prior to incubation with toluene (topography mode). Right: AFM (NCM) image of TMV adsorbed on a silicon wafer after incubation with toluene for 10 min. (topography mode).

inside the protein [119], are very important for the stability of the tubular structure. While electrostatic effects are responsible for the stabilization with Ca^{2+} ions, water molecules bridge different areas of the coat protein with hydrogen bonding. If we focus on the water molecules, the stability of the virion should be decreased if the water is displaced. Solvent molecules which are fully miscible with water should not change the stability of the virion since there is no strong driving force in those molecules to replace the water. If a replacement takes place, the molecules might even show similar stabilizing effects like water. The situation changes when water is to be replaced by unpolar molecules. In higher concentration (only concentrations close to 100 % are possible, since unpolar solvents are almost immiscible with water) those molecules tend to displace the water since interactions of unpolar groups of the virion with the unpolar solvent increase. The more water is displaced, the smaller is the interaction force between the coat proteins and the easier the virion disassembles. In addition the solvent molecules can penetrate the hydrophobic core of the coat protein. The interaction between the hydrophobic amino acids are in this case lowered, since the solvent interacts with them. In such a scenario the structural stability of the coat protein is decreased. An exception is DMSO. This solvent is polar, but still destroys the virion at high concentrations (see figure 6.12). Hindered aggregation of TMV could be observed in the AFM images when DMSO was added to the TMV suspension in low concentrations. The mechanism of disaggregation of TMV with DMSO is not yet clear.

6.1.5   Printing of TMV

Microcontact printing (μCP) is the ideal method for (sub-)micrometre structuring of a surface with the virions [80]. Although some self-assembly structuring of TMV, especially head-to-tail arrangement, can be observed, this is not very reliable and not reproducible in a controlled way, and the arrangements reach at best the micrometre range. μCP can help to improve the reliability and the length scale of the structuring. In ideal cases ordering up to millimetres should be reached. The performed experiments show only first results in this particular part of the project.

μCP was done by standard procedures with stamps made of (poly)dimethysiloxane (PDMS), formed on a master with smallest features of 400 nm in size (see chapter 3.3) [63, 80]. The substrates were mica and silicon wafer surfaces. The latter were pretreated by standard RCA cleaning method (see chapter 4.2.2) to obtain a hydrophilic termination of the substrate. Both substrates were treated with $MgCl_2$ before transfer of TMV with the stamp. The results show that patterned transfer of TMV with a PDMS stamp is possible.

First, hydrophilic stamps, pretreated with an oxygen plasma, were used. Within the contact areas no ordering of TMV could be obtained (see figure 6.15). TMV was in those areas randomly distributed, sometimes in more than a single layer.

The use of a hydrophilic stamp yields substrates with a nice pattern of transferred virions (see figure 6.15). However, inside those areas no ordering of TMV can be seen. The high affinity of the stamp to the virions forces them to adsorb on the stamp very fast, similar to the silicon wafer surface (indeed oxidized PDMS surfaces closely resemble silicon wafer surfaces). Once adsorbed, the driving force for the virions to diffuse on the substrate and to probably reach a higher structural order is much weaker than the interactions with the surface of the stamp, so they just remain at their places until the transfer. If TMV is transferred to substrates with similar affinity to TMV, one could assume that a competition of the substrate and the stamp in adsorption of the virion can take place. Indeed in some cases, if silicon wafer or mica surfaces are patterned, differences in heights within the transferred particles could be seen. In some cases features showed heights of 5 nm and less, whereas next to this particular feature a virion with the expected 13-15 nm could be found. This findings lead to the following scenario: If a virion in this short time scale (30-60 sec) can interact with many sites of the substrate to compete in interaction strength with the stamp, peeling off the stamp
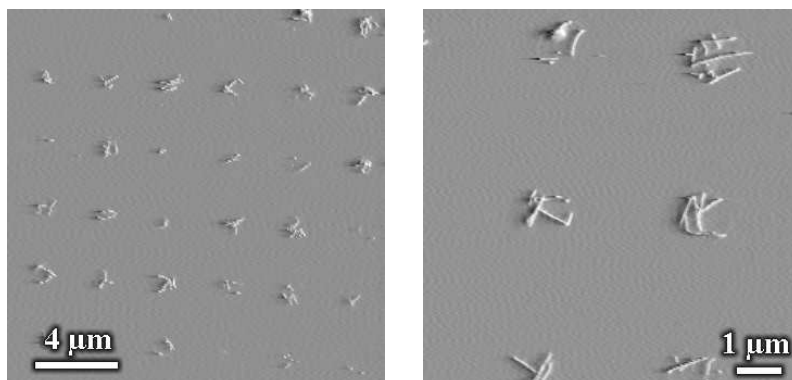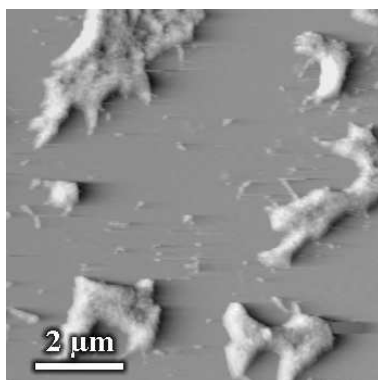
Figure 6.15: Left: AFM (C-AFM) image of TMV transferred onto mica with a hydrophilic stamp (error mode). The stamp had dotted features with micrometre sizes. Right: AFM (NCM) image of a smaller scan area of the left image (error mode).

can destroy the virion since some parts remain on the stamp and some stick to the substrate. This again means that the perfectly hydrophilized stamp is not ideal for transferring TMV.

Trying to transfer TMV with a hydrophobic stamp resulted in random aggregation of the virions (not linear). The resulting aggregates showed heights of several tens of nm (see figure 6.16). The effect is similar to the adsorption of TMV on hydrophobic substrates (see figure 6.1). Dewetting on the stamp forces the virions to aggregate in droplets. Once aggregated, the stamp can only transfer those droplet aggregates, resulting in a high concentration of viral particles on random spots without any recognition of the initial pattern of the stamp (see figure 6.16).

Using partially hydrophilic stamps (see chapter 4.3 for transfer of TMV under the same conditions yielded decreased density and increased ordering of virions in the contact areas (see figure 6.17). This effect was obtained only when the stamp properties were changed, but not when the concentration of TMV in suspension or the chemical properties of the substrates were changed. The hydrophilicity of the stamp was controlled by the duration of exposure of the stamp to the oxygen plasma. The left image shows the pattern transferred by the stamp. The lines in the image show increased height at the borders (10-15 nm) compared to the area between (2-7 nm). The right image shows a smaller scan area with vertically oriented TMV. The heights of the virions are 12-15 nm. Additionally some lines can be observed in the image. Those lines show heights of 2-4 nm and TMV is almost exclusively found on top of

Figure 6.16: AFM (C-AFM) image of TMV stamped on a Si wafer with a hydrophobic stamp (error mode). The transferred features are random aggregates of virions.
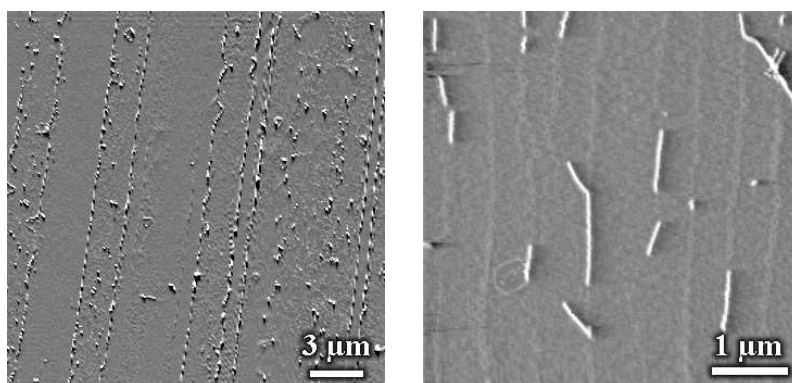
Figure 6.17: Left: AFM (C-AFM) image of TMV stamped on a Si-wafer with a partially hydrophilic stamp (error mode). The stamp had lined features. Right: AFM (NCM) image of a smaller scan area (error mode). The image shows line features with some attached virions on top.

these lines. The width of these lines corresponds to the widths of the virions (80-90 nm). The origin of the lines could not yet be distinguished.

The use of partially hydrophilic stamps resembles to be a possibility to avoid destruction of the virion and still transfer nice patterns. Some tests have been done where a hydrophobic stamp was exposed to an oxygen plasma for only very short times (1-2 sec). In this case stamp and TMV have some possible interaction sites, but few in number. This again may allow for enhanced diffusion of the virion in the solvent droplet, since it is not instantaneously adsorbed on the stamp. Dewetting phenomena of the droplet during drying force the virions to align along the edges of the stamp features, and the virions are as such transferred to the substrate. As a result the virions are

transferred in a very much smaller scale than the pattern of the stamp offers. In ideal cases linear arrangements of virions with several micrometres length and the width of a single adsorbed TMV can be built. Figure 6.17 shows a Si wafer surface after transfer of TMV with a partially hydrophilic stamp. The enhanced height of the linear features at the edges indicates an enhanced concentration of TMV particles in those areas. Still some particles can be found between those edges.

Ongoing experiments should improve the structuring and the reproducibility. The tests to arrange TMV by μCP are very promising. Although transfer with extremely hydrophilic and hydrophobic stamps did not yield the desired ordering on the substrates, experiments with intermediate hydrophilicity show that a structuring even in 1D becomes possible.

6.2   Summary

The results in this chapter have shown that TMV can be adsorbed on a variety of surfaces with different chemical and physical properties. The bonding strength of the virion with the surface depends strongly on the pH of the virion suspension and thus the electrostatic charge of the viral outer surface and the possibility of the viral coat proteins to chemically interact with the surface. Covalent bonding of TMV with carboxyl-terminated thiol monolayers on a gold surface was obtained in a fast reaction.

The resistance of TMV against some common organic solvents was investigated by immersion of adsorbed TMV on silicon wafer and imaging with AFM. The solvents often used for technological steps (e.g. lift-off technique in lithography), like acetone, ethanol and N-methylpyrrolidone, have no influence on the structural integrity of the adsorbed virion, while some other solvents, like toluene, THF and DMSO destroy the TMV. However, if those solvents are miscible with water, the destruction of the virion often depends on the concentration of the solvent.

μCP of TMV with a PDMS stamp is possible. Although the results are preliminary, tests with a partially hydrophilic stamp are promising. An improvement of the patterns is subject of future work.

Chapter 7

Conclusions and Outlook

TMV can reasonably be adsorbed on surfaces which offer binding sites for hydrogen bridging, electrostatic interactions or covalent bonding in terms of esterification. An adsorption results in a deformation of the virion in order to achieve an energy minimum by binding as many sites as possible. The deformation takes place only up to a certain degree because further deformation would need more energy than gained by binding additional accessible sites. The degree of deformation depends on the binding sites the virion can reach and on the amino acid sequence of the coat protein, since variations result in different stability and thus energy of the virion.

Substrates not capable of hydrophilic or covalent bonding show only weak interactions and are therefore difficult to analyze. Those substrates are not reasonable for further experiments, especially when contact with a liquid phase is involved, because it is very likely that the particles will detach from the surface.

The spectrum of substrates which can be used reaches from non-conductive to conductive and can be chosen according to the needs. The high stability of TMV offers a possibility to store substrates covered with TMV for a long time, since no degradation of the particles even on several weeks old samples, could be detected. This is of course only possible if storage is done under exclusion of biologically active molecules, e.g. ribosomes or RNAses, which can destroy the virion.

The metallization part of this work showed that metal attachment to the virion is possible in a very controlled way by electroless deposition. Several metals, including nickel and cobalt, can be attached either to the outer surface of the virion or to the inner channel. metal wires with 3 nm diameter and a high aspect ratio can be grown with a very simple protocol. Additionally, a shell of biomolecules can stabilize the metal wires

and protect them against environmental influences. Moreover the template for growing those metal wires is cheap and the resources (the virions) are practically infinite, since TMV can be replicated either naturally (in tobacco plantations) or in the laboratory without large effort.

Further experiments will improve the capabilities of metallization by either optimization of the metallization baths, or by changing the biochemical structure of the virion, i.e. the amino acid sequence. This should lead to a more defined metal deposition and so to an even larger efficiency of metal growth. With optimal modification of the viral coat protein even a simultaneous metal growth inside and outside the virion could become possible. This would lead to a nanoscaled capacitor.

An open question in the present stage is however whether the deposited metal wires show metallic properties like conductivity and magnetic properties similar to bulk metal or whether quantum effects already play a role. In order to examine this, it is first necessary to find out whether the deposited metal is continuous or is it a loose arrangement of clusters. Experiments in order to measure the electron transport capabilities of the metallized virion need to be done as well as measurement of magnetic properties of the deposited metal. Contacting by lithography using the lift-off technique is known from experiments with carbon nanotubes. Basically the same approach can be done with TMV. The experiments have shown that the virion is resistant against a number of different chemical solvents, among them acetone, which is used in the lift-off procedure. The only remaining problem in this case is the temperature resistance of the TMV. One step in the lift-off technique requires temperatures of up to 350°C in order to cure a polymer. First experiments with replacing this particular polymer with another one will be done in the near future.

Experiments with soft lithography of the virions showed that the transfer of such large biomolecules (300 nm, in aggregates up to several μm) onto a surface is possible. Since the chemistry of such molecules is very complex, simple models for diffusion of molecules on the stamp cannot be applied, as it is possible with smaller molecules, like dendrimers [14]. Nevertheless, one can create μm scale virus patterns on the surface, and further experiments will surely improve the results. Experiments with varying hydrophilicity of the stamp have shown that an arrangement of the virions in even smaller scale than offered by the stamp is possible. In contrast to handling complex and expensive sub-100 nm stamps, a linear arrangement of 18 nm wide biological structures should be enforced when a stamp with only μm features is employed.

Bibliography

[1] Agatow P., *Biochimia* **1941**, *6*, 269.

[2] Aranha H., Larson R., *Biopharm Supplement* **2000**, *40*, 30.

[3] Atkins P.W., *Physikalische Chemie*; VCH: Weinheim, **1987**.

[4] Banerjee N., Wang J.Y., Zaitlin M., *Virol.* **1995**, *207*, 234.

[5] Bawden F.C., Pirie N.W., Bernal J.D., Fankuchen I., *Nature* **1936**, *138*, 1051.

[6] Baker M.V., Landau J., *Aust. J. Chem.* **1995**, *48*, 1201.

[7] Barth J.V., *Surf. Sci. Rep.* **2000**, *40*, 75.

[8] Behm R.J., Garcia N., Rohrer H., eds. *Scanning Tunneling Microscopy and Related Methods*; NATO ASI Series E:184; Kluwer, Dordrecht, **1990**.

[9] Beijerinck M.W., *Verh. Kon. Akad. Wetesch.* **1898**, *5*, 3. 2225.

[10] Bhyravbhatla B., Watowich S.J., Caspar D.L.D., *Biophys. J.* **1998**, *74*, 604.

[11] Binnig G., Rohrer H., Gerber C., Weibel E., *Appl. Phys. Lett.* **1982**, *40*, 178.

[12] Binnig G., Rohrer H., *Sci. Am.* **1986**, *253*, 50.

[13] Binnig G., Quate C.F., Gerber C., *Phys. Rev. Lett.* **1986**, *56*, 930.

[14] Bittner A.M., Wu X.C., Kern K., *Adv. Funct. Mat.* **2002**, *12*, 432.

[15] Blundell T.L., Johnson L.N., *Protein crystallography*; Academic press: New York, London, San Francisco, **1976**.

[16] Bonafe C.F.S., Vital C.M.R., Telles R.C.B., Gonçalves M.C., Matsuura M.S.A., Pessine F.B.T., Freitas F.B.T., Freitas D.R.C., Vega J., *Biochemistry* **1998**, *37*, 11097.

[17] Branden C., Tooze J., *Introduction to protein structure, second edition*; Garland Publishing: New York, **1999**.

[18] Braun E., Eichen Y., Sivan U., Ben-Yoseph G., *Nature* **1998**, *391*, 775.

[19] Brunt E., Crabtree K., Dallwitz M.J., Gibbs A.J., Watson L., Zurcher E.J. (eds.), *Plant Viruses Online: Descriptions and Lists from the VIDE Database.* **1996**, URL: http://biology.anu.edu.au/Groups/MES/vide/.

[20] Butler P.J.G., *J. gen. Virol.* **1984**, *65*, 253.

[21] Chalisova N.N., Leonova O.G., Kochubei D.I., Yuz´ko M.I., *Russ. J. Inorg. Chem.* **1988**, *33(2)*, 409.

[22] Chang Y.S., Chou M.L., *J. Appl. Phys.* **1991**, *69(11)*, 7848.

[23] http://www.mdli.com; Software: MDL$^{©}$ Chime Ver. 2.6 SP4 **2002**

[24] Choi C.W., Park S.H., Choi J.K., Ryu K.H., Park W.M., *Acta Virol.* **2000**, *44*, 145.

[25] Culver J.N., Dawson W.O., Plonk K., Stubbs G., *Virol.* **1995**, *206*, 724.

[26] Dehm G., Ernst F., Mayer J., Möbus G., Müllejans H., Phillipp F., Scheu Ch., Rühle M., *Z. Metallkd.* **1996**, *87*, 11.

[27] Dinte B.P., Watson G.S., Dobson J.F., Myhra S., *Ultramicroscopy* **1996**, *63*, 115.

[28] Dodero G., De Michieli L., Cavalleri O., Rolandi R., Oliveri L., Daccà A., Parodi R., *Coll. Surf.* **2000**, *175*, 121.

[29] Doyle P.S., Bibette J., Bancaud A., Viovy J.-L., *Science* **2002**, *295*, 2237.

[30] Drygin Y.F., Bordunova O.A., Gallyamov M.O., Yaminsky I.V., *FEBS Letters* **1998**, *425*, 217.

[31] Duevel R.V., Corn R.M., *Anal. Chem.* **1992**, *64*, 337.

[32] Dujardin E., Peet C., Stubbs G., Culver J.N., Mann S., *Nanolett.* **2003**, *3*, 413.

[33] Edelstein A.S., Cammarata R.C., (eds.), *Nanomaterials: Synthesis, properties and applications*; Institute of physics publishing: Bristol, Philadelphia, **1996**.

[34] Eigler D., Schweizer E.K., *Nature* **2000**, *344*, 524.

[35] Falvo M.R., Washburn S., Superfine R., Finch M., Brooks F.P. Jr., Chi V., Taylor R.M. II, *Biophys. J.* **1997**, *72*, 1396.

[36] Finch J.T., *J. Mol. Biol.* **1972**, *66*, 291.

[37] Franklin R.E., Holmes K.C., *Acta Cryst.* **1958**, *11*, 213.

[38] Gallagher W.H., Lauffer M.A., *J. Mol. Biol.* **1983**, *170*, 905.

[39] Gallwitz U., King L., Perham R.N., *J. Mol. Biol.* **1974**, *87*, 257.

[40] Gambardella P., Blanc M., Bürgi L., Kuhnke K., Kern K., *Surf. Sci.* **2000**, *449*, 93.

[41] Gambardella P., Blanc M., Brune H., Kuhnke K., Kern K., *Phys. Rev. B* **2000**, *61(3)*, 2254.

[42] Gambardella P., Dallmeyer A., Maiti K., Malagoli M.C., Eberhardt W., Kern K., Carbone C., *Nature* **2002**, *416*, 301.

[43] Gierer A., Schramm G., *Nature* **1956**, *177*, 702.

[44] *Gmelins Handbuch der Anorganischen Chemie*; Verlag Chemie: Weinheim, 8. Auflage **1954**; Springer: Berlin, 8. Auflage **1975**; Springer: Berlin, 8. Auflage **1994**.

[45] Guckenberger R., Arce F.T., Hillebrand A., Hartmann T., *J. Vac. Sci. Techol. B* **1994**, *12(3)*, 1508.

[46] Han S.W., Joo S.W., Ha T.H., Kim Y., Kim K., *J. Phys. Chem. B* **2000**, *104*, 11987.

[47] Harris J.I., Knight C.A., *Nature* **1952**, *170*, 613.

[48] Heim M., Steigerwald R., Guckenberger R., *J. Struct. Biol.* **1997**, *119*, 212.

[49] Hofmann U., Weil K.G., *Plat. Surf. Fin.* **1992**, *March*, 60.

[50] Holleman A.F., Wiberg E., *Lehrbuch der anorganischen Chemie, 100. Auflage*; Walter de Gruyter: Berlin, New York, **1985**.

[51] Holmes F.O., *Botanical Gazette* **1929**, *87*, 39.

[52] Imai K., Yoshimura K., Tomitori M., Nishikawa O., Kokawa R., Yamamoto M., Kobayashi M., Ikai A., *Jpn. J. Appl. Phys.* **1993**, *32*, 2962.

[53] Israelachvili J., *Intermolecular and Surface Forces*; Academic Press: London, **1991**.

[54] Itakura K., Homma T., Osaka T., *Electrochim. Acta* **1999**, *44*, 3707.

[55] Jackman R.J., Brittain S.T., Adams A., Wu H., Prentiss M.G., Whitesides S., Whitesides G.M., *Langmuir* **1999**, *15*, 826.

[56] Jagannathan R., Krishnan M., *IBM J. Res. & Develop.* **1993**, *37(2)*, 117.

[57] Jusys Z., personal communication.

[58] Kasas S., Thomson N.H., Smith B.L., Hansma P.K., Miklossy J., Hansma H.G., *Int. J. Imag. Syst. Tech.* **1997**, *8*, 151.

[59] Kausche G.A., Pfankuch E., Ruska H., *Naturwissenschaften* **1939**, *27*, 292.

[60] Kausche G.A., Ruska H., *Kolloid Z.* **1939**, *89*, 21.

[61] Kausche G.A., Hahn F., *Z. Naturforsch. B* **1948**, *3*, 437.

[62] Kind H., Bittner A.M., Cavalleri O., Kern K., Greber T., *J. Phys. Chem. B* **1998**, *102*, 7582.

[63] Kind H., *Patterning of surfaces by locally catalyzed chemical reactions*; Dissertation at the Ecole polytechnique federale de Lausanne, **2000**.

[64] Kirsch R., Mertig M., Pompe W., Wahl R., Sadowski G., Böhm K.J., Unger E., *Thin Solid Films* **1997**, *305*, 248.

[65] Klug A., *Phil. Trans. R. Soc. Lond. B* **1999**, *354*, 531.

[66] Knez M., Sumser M., Bittner A.M., Wege Ch., Jeske H., Kooi S., Burghard M., Kern K., *J. Electroanalyt. Chem.* **2002**, *522*, 70.

[67] Kühnle A., Linderoth T.R., Hammer B., Besenbacher F., *Nature* **2002**, *415*, 891.

[68] Lebermann R., Finch J.T., Gilbert P.F.C., Witz J., Klug A., *J. Mol. Biol.* **1974**, *86*, 179.

[69] Lee S.-W., Mao C., Flynn C.E., Belcher, A.M., *Science* **2002**, *296*, 892.

[70] Lin K.-L., Chang Y.-L., Huang C.-C., Li F.-I, Hsu J.-C., *Appl. Surf. Sci.* **2001**, *181*, 166.

[71] Liu Z.H., Brown N.M.D., *Thin Solid Films* **1997**, *300*, 84.

[72] Loweth C.J., Caldwell W.B., Peng X., Alivisatos A.P., Schultz P.G., *Angew. Chem.* **1999**, *111(12)*, 1925.

[73] Mallory G.O., Hajdu J.B., *Electroless Plating: Fundamentals And Applications*; American Electroplaters and Surface Finishers Society: Orlando, **1990**.

[74] Mantovani J.G., Allison D.P., Warmack R.J., Ferrell T.L., Ford J.R., Manos R.E., Thompson J.R., Reddick B.B., Jacobson K.B., *J. Micros.* **1990**, *158*, 109.

[75] Martell A.E., (ed.), *Coordination chemistry, volume 2, ACS monograph 174*; American chemical society: Washington D.C., **1978**.

[76] Mayer A., *Landw. Vers. Sta.* **1886**, *32*, 451.

[77] Mertig M., Kirsch R., Pompe W., *Appl. Phys.* **1998**, *A66*, S723.

[78] Mertig M., Wahl R., Lehmann M., Simon P., Pompe, W., *Eur. Phys. J. D* **2001**, *16*, 317.

[79] Mertig M., Ciacchi L.C., Seidel R., Pompe, W., De Vita A., *Nanolett.* **2002**, *2(8)*, 841.

[80] Michel B., Bernard A., Bietsch A., Delamarche E., Geissler M., Juncker D., Kind H., Renault J.-P., Rothuizen H., Schmid H., Schmidt-Winkel P., Stutz R., Wolf H., *IBM J. Res. & Develop.* **2001**, *45(5)*, 697.

[81] Müller D.J., Amrein M., Engel A., *J. Struct. Biol.* **1997**, *119*, 172.

[82] Müller D.J., Engel A., Amrein M., *Biosensors & Bioelectronics* **1997**, *12*, 867.

[83] Mundry K.-W, personal communication.

[84] Namba K., Pattanayek R., Stubbs G., *J. Mol. Biol.* **1989**, *208*, 307.

[85] Nedoluzhko A., Douglas T., *J. Inorg. Biochem.* **2001**, *84*, 233.

[86] Nicolaïeff A., Lebeurier G., *Molec. gen. Genet.* **1979**, *171*, 327.

[87] Nishiguchi M., Motoyoshi F., Oshima N., *J. gen. Virol.* **1978**, *39*, 53.

[88] Okinaka Y., Hoshino M., *Gold Bulletin* **1998**, *31*, 3.

[89] O´shea S.J., Welland M.E., Wong T.M.H., *Ultramicroscopy* **1993**, *52*, 55.

[90] Paunovic M., Nguyen T., Mukherjee R., Sambucetti C., Romankiw L.T., *J. Electrochem. Soc.* **1995**, *142(5)*, 1495.

[91] Paunovic M., Schlesinger M., (eds.), *Fundamentals of electrochemical deposition*; Wiley Interscience: New York, Chichester, Weinheim, Brisbane, Singapore, Toronto, **1998**.

[92] Petsko G.A., *Acta Cryst.* **1975**, *A32*, 473.

[93] Petsko G.A., Phillips D.C., Williams R.J.P., Wilson I.A., *J. Mol. Biol.* **1978**, *120*, 345.

[94] Pfankuch E., Hagenguth K., *Biochemische Z.* **1942**, *313*, 1.

[95] Pfankuch E., Ruska H., *Z. Naturforsch. B* **1947**, *2(9-10)*, 358.

[96] Pourbaix M. in *Atlas of Electrochemical Equilibria*; National Association of Corrosion Engineers: Houston **1974**.

[97] Prusov Y.V., Makarov V.F., Flerov V.N., *Izv. Vuz. Khim. Kh. Tekh.* **1992**, *35*, 3.

[98] Ramani M., Haran B.S., White R.E., Popov B.N., *J. Electrochem. Soc.* **2001**, *148(4)*, A374.

[99] Reches M., Gazit E., *Science* **2003**, *300*, 625.

[100] Richter J., Seidel R., Kirsch R., Mertig M., Pompe W., Plaschke J., Schackert H.K., *Adv. Mat.* **2000**, *12(7)*, 507.

[101] Richter J., Mertig M., Pompe W., Mönch I., Schackert H.K., *Appl. Phys. Lett.* **2001**, *78*, 536.

[102] Schabert F., Hefti A., Goldie K., Stemmer A., Engel A., Meyer E., Overney R., Güntherodt H.J., *Ultramicroscopy* **1992**, *42-44*, 1118.

[103] Scheibel T., Parthasarathy R., Sawicki G., Lin X.-M., Jaeger H., Lindquist S.L., *Proc. Natl. Acad. Sci.* **2003**, *100(8)*, 4527.

[104] Schlesinger M., Paunovic M., (eds.), *Modern electroplating, fourth edition*; Wiley Interscience: New York, Chichester, Weinheim, Brisbane, Singapore, Toronto, **2001**.

[105] Shen T.C., Wang C., Abeln C., Tucker J.R., Lyding J.W., Avouris P., Walkup R.E., *Science* **1995**, *268*, 1590.

[106] Shenton W., Douglas T., Young M., Stubbs G., Mann S., *Adv. Mat.* **1999**, *11(3)*, 253.

[107] Sommerville J., Scheer U. (eds.), *Electron microscopy in molecular biology*; IRL Press: Oxford, Washington DC, **1987**.

[108] Stemmer A., Hefti A., Aebi U., Engel A., *Ultramicroscopy* **1989**, *30*, 263.

[109] Stubbs G., *Phil. Trans. R. Soc. Lond. B* **1999**, *354*, 551.

[110] Sumser M.P., *Das Tabakmosaikvirus (TMV) als Biotemplat für Anwendungen in der Nanotechnologie*; Diplomarbeit, Universität Stuttgart, Molekularbiologie, **2001**.

[111] Tarozaite R., Kurtinaitiene M., Dziuve A., Jusys Z., *Surf. Coat. Technol.* **1999**, *115*, 57.

[112] Takano H., Kenseth J.R., Wong S., O´Brien J.C., Porter M.D., *Chem. Rev.* **1999**, *99*, 2845.

[113] Thundat T., Zheng X.-Y., Sharp S.L., Allison D.P., Warmack R.J., Joy D.C., Ferrell T.L., *Scanning Microscopy* **1992**, *6*, 903.

[114] Van Regenmoertel M.H.V., Altschuh D., Zeder-Lutz G., *Biochimie* **1993**, *75*, 731.

[115] Van Regenmoertel M.H.V., *Phil. Trans. R. Soc. Lond. B* **1999**, *354*, 559.

[116] Von Heimendahl M., *Einführung in die Elektronenmikroskopie*; Vieweg: Braunschweig, **1970**.

[117] Wadu-Mesthrige K., Pati B., McClain W.M., Liu G.-Y., *Langmuir* **1996**, *12*, 3511.

[118] Wagner P., *FEBS Letters* **1998**, *430*, 112.

[119] Wang H., Planchart A., Stubbs G., *Biophys. J.* **1998**, *74*, 633.

[120] Watson J.D., *Biochim. Biophys. Acta* **1954**, *13*, 10.

[121] Wayner D.D.M., Wolkow R.A., *J. Chem. Soc. Perkin Trans.* **2001**, *2*, 23.

[122] Wetmur J.G.; Davidson N., *J. Mol. Biol.* **1986**, *31*, 349.

[123] Wilson T.M.A., Perham R.N., *Virol.* **1985**, *140*, 21.

[124] Wittmann H.G., *Virol.* **1960**, *12*, 609.

[125] http://pqs.ebi.ac.uk/pqs-bin/macmol.pl?filename=2tmv; Henrick K., Thornton J.M., *Trends Biochem. Sci.* **1998**, *23*, 358; Pattanayek R., Stubbs G., *J. Mol. Biol.* **1992**, *228*, 516; Namba K., Pattanayek R., Stubbs G., *J. Mol. Biol.* **1989**, *208*, 307.

[126] Zaitlin M., *Tobacco Mosaic Virus (Type Strain)*; A.A.B. Descriptions of Plant Viruses, **2000**, *8*, 370.

[127] Zenhausern F., Adrian M., ten Heggeler-Bordier B., Ardizzoni F., Descouts P., *J. Appl. Phys.* **1993**, *73*, 7232.

List of Publications

Journal Papers:

M. Knez, M.P. Sumser, A. Bittner, Ch. Wege, H. Jeske, S. Kooi, M. Burghard, K. Kern, "Electrochemical modification of individual nano-objects" *J. Electroanalyt. Chem.* **2002**, *522*, 70.

M. Knez, A.M. Bittner, F. Boes, Ch. Wege, H. Jeske, K. Kern "Biotemplate Synthesis of 3 nm Nickel and Cobalt Nanowires" *Nano Lett.* **2003**, *3(8)*, 1079.

M. Knez, M.P. Sumser, A.M. Bittner, Ch. Wege, H. Jeske, D.M.P. Hoffmann, K. Kuhnke, K. Kern "Binding the Tobacco Mosaic Virus to Inorganic Surfaces" *Langmuir* **2003**, *in press*.

M. Knez, M. P. Sumser, A. M. Bittner, Ch. Wege, H. Jeske, T. P. Martin and K. Kern "Spatially Selective Nucleation of Metal Clusters at the Tobacco Mosaic Virus" *Adv. Func. Mater.* **2003**, *in press*.

Talks:

"Approach to Nanoconductors by Using a Plant Virus as Template", *Scanning-Probe-Microscopies and Organic Materials 10 and Nanotechnology in Biology, Medicine and Pharmacy I*, Kaiserslautern, **09.10.2001**.

"Das Tabakmosaikvirus als Templat für Nanodrähte", *PhD-workshop in "Schwerpunktprogramm 1072 der DFG: Halbleiter- und Metallcluster als Bausteine für organisierte Strukturen"*, Blaubeuren **12.05.2002**.

"Biotemplated Growth of Nanowires", short oral contribution, *Gordon research conference "chemistry at interfaces"*, New London (CT), **16.07.2002**.

"Plant Virus Adsorption and Metallization", *Frontiers of science, workshop on nanoscale magnetism*, Ringberg (Tegernsee), **13.09.2002**.

Zusammenfassung

Das Tabakmosaikvirus (TMV) als Biologisches Templat für Nanostrukturierung

Das Tabakmosaikvirus (TMV) ist ein stabiler, zylindrischer Komplex bestehend aus einem helikalen RNA-Strang und 2130 Hüllproteinen. Diese spezielle Form macht das Virus zu einem interessanten Nanoobjekt, insbesondere für den Einsatz als Templat für chemische Reaktionen. In dieser Arbeit wurde das TMV als chemisch funktionalisiertes Templat für eine elektrostatische oder koordinative Anbindung von Metallen verwendet. Mit chemischer Reduktion oder stromloser Abscheidung von Metallen können Metallcluster mit einem Durchmesser von mehreren nm produziert und an das Virus gebunden werden, ohne seine Struktur zu zerstören. Während Goldcluster mit einem ascorbinsäurehaltigen Metallisierungsbad an der Aussenhülle und im Innenkanal des TMV produziert werden können, werden Silbercluster mit einem formaldehydhaltigen Protokoll ausschliesslich an der Aussenhülle des Virus gebildet. Nach einer Aktivierung des TMV mit Pd(II) oder Pt(II) kann Nickel oder Kobalt selektiv im Innenkanal abgeschieden werden. Dabei entsehen Cluster und Drähte mit einem Durchmesser von 3 nm, die bis zu 600 nm lang werden können. Nach einer Aktivierung mit Au(I) anstelle von Pd(II) oder Pt(II) kann Nickel oder Kobalt selektiv an der Aussenhülle des Virus abgeschieden werden.

Das Adsorptionsverhalten und die Oberflächenchemie des TMV auf definierten Metall- und Nichtleiteroberflächen wurde ebenfalls untersucht. Das TMV dient hierbei als supramolekulares Modellsystem mit bekannter Oberflächenstruktur. Die Ergebnisse zeigen, dass bei Ausbildung von starken Wechselwirkungen zwischen Substrat und molekularer Oberfläche die Beweglichkeit des Virus auf dem Substrat verhindert wird. Dadurch kann das TMV mit dem Rasterkraftmikroskop im Kontaktmodus abgebildet werden. Molekulare Monolagen auf einer Goldoberfläche, terminiert mit einem Säurechlorid, können verwendet werden, um das TMV kovalent anzubinden. Struk-

turierte Anbindung von TMV auf Siliziumwafer- und Glimmeroberflächen wurde mit Mikrokontaktdruck erreicht.

Schlüsselbegriffe: Tabakmosaikvirus, stromlose Abscheidung von Metallen, Adsorption auf anorganischen Substraten, Mikrokontaktdruck;

Danksagung

Mein besonderer Dank gilt an dieser Stelle:

Prof. Dr. Klaus Kern (MPI FKF), Prof. Dr. Holger Jeske (Universität Stuttgart) und Prof. Dr. Rolf-Jürgen Behm (Universität Ulm) für die interessante Aufgabenstellung, zahlreiche lehrreiche Diskussionen, die Finanzierung der Arbeit, die Möglichkeit der Nutzung der Räumlichkeiten und der Infrastruktur des MPI und Unterstützung bei allen sonstigen, für diese Arbeit relevanten Fragen. Dadurch bekam ich die Möglichkeit, meinen Wissenshorizont in der Chemie, aber auch in der Physik und der Biologie auszuweiten.

Dr. Alexander M. Bittner, dessen Ideen und Ratschläge für diese Arbeit von essentieller Bedeutung waren. Ebenfalls möchte ich ihm für sein Engagement danken, das die wissenschaftliche Arbeit und das generelle Arbeitsklima stets auf einem sehr hohen Niveau hielt.

Dr. Christina Wege, die bei wichtigen Fragen, insbesondere aus dem Bereich der Biologie, stets helfend zur Seite stand und die durch ihre Anregungen sehr zur Verwirklichung dieser Arbeit beigetragen hat.

Martin Sumser, Fabian Boes und Dirk Leinberger, die mich mit Ihren Diplom- bzw. Studienarbeiten tatkräftig unterstützt haben.

Dr. Fritz Phillipp und Marion Kelsch, die mir das TEM zur Verfügung stellten und mir bei Problemen stets weitergeholfen haben.

Dr. Hans-Ulrich Habermeier, Juliane Kahl und Birgit Lemke, die mich mit Proben für das AFM und STM versorgt haben.

Der gesamten Abteilung für Nanowissenschaften am MPI FKF für das ausserordentlich gute Arbeitsklima und Hilfestellung in allen Bereichen. Besonders hervorheben möchte ich hier Alpan Bek, Dr. Ralf Vogelgesang, Michael Vogelgesang, Dr. Roman Šordjan, Dr. Xiaochun Wu, Dr. Marko Burghard, Frank Stadler, Ulrich Schlecht, Kannan Balasubramanian und Sabine Birtel, die bei wissenschaftlichen, technischen

oder organisatorischen Fragen stets eine Lösung fanden.

Der IT-Servicegruppe, insbesondere Dr. Armin Burkhardt, Dr. Jörg Muster und Dr. Michael Wanitschek die in allen EDV-Fragen stets helfend zur Seite standen.

Der Deutschen Forschungsgemeinschaft (DFG) und der Max-Planck-Gesellschaft für die Finanzierung der Arbeit.

Curriculum Vitae

23.07.1971 Geburt in Augsburg, Deutschland.

1977-1979 Besuch der Elisen-Volksschule in Augsburg.

1979-1981 Besuch der Ante-Beretin Schule in Kastel Stari im damaligen
Jugoslawien (heute Kroatien).

1981-1982 Besuch der Hauptschule Kappeneck in Augsburg.

1982-1991 Besuch des Holbein-Gymnasiums in Augsburg und Abitur.

1991-1993 Studium der Elektrotechnik an der Fachhochschule in Augsburg.

1993-1998 Studium der Chemie an der Universität Ulm.

1998-1999 Diplomprüfung und Diplomarbeit bei Prof. Dr. H.-U. Siehl
an der Universität Ulm.

1999 Wissenschaftlicher Mitarbeiter bei Prof. Dr. H.-U. Siehl
an der Universität Ulm.

2000-2003 Anfertigung der vorliegenden Dissertation am
Max-Planck-Institut für Festkörperforschung in Stuttgart.

Erklärung

Hiermit versichere ich, dass ich die vorliegende Arbeit eigenständig und ohne fremde Hilfe und ausschliesslich mit den in der Dissertation angegebenen Hilfsmitteln erstellt habe.

Mato Knez